PROPERTIES OF GLUTAMATE UPTAKE IN SALAMANDER MÜLLER CELLS

Boris James Barbour

A thesis submitted for the degree of
Doctor of Philosophy
in the
University of London

Department of Physiology
University College London
November 1990

ProQuest Number: 10609976

All rights reserved

INFORMATION TO ALL USERS
The quality of this reproduction is dependent upon the quality of the copy submitted.

In the unlikely event that the author did not send a complete manuscript
and there are missing pages, these will be noted. Also, if material had to be removed,
a note will indicate the deletion.

ProQuest 10609976

Published by ProQuest LLC (2017). Copyright of the Dissertation is held by the Author.

All rights reserved.
This work is protected against unauthorized copying under Title 17, United States Code
Microform Edition © ProQuest LLC.

ProQuest LLC.
789 East Eisenhower Parkway
P.O. Box 1346
Ann Arbor, MI 48106 – 1346

Abstract

Glutamate is a major transmitter in the central nervous system. In order to understand its physiological and pathological actions it is necessary to investigate the properties of the uptake system which removes glutamate from the extracellular space. An important function of glutamate uptake is to maintain the extracellular glutamate concentration below neurotoxic levels.

High affinity, sodium-dependent, electrogenic glutamate uptake was measured using whole-cell patch-clamp recording in acutely isolated retinal glial (Müller) cells of the salamander.

The ionic dependence of the glutamate uptake current was investigated. Internal sodium and glutamate both inhibited the uptake current. It was activated by intracellular potassium and inhibited by extracellular potassium: therefore glutamate uptake involves counter-transport of potassium ions. Replacement of intracellular or extracellular chloride had no effect on the uptake current. The uptake current was maximal near pH 7.3.

Second messenger systems were manipulated in order to identify mechanisms regulating the uptake carrier. Variation of the intracellular calcium concentration or inclusion of cGMP, cAMP or GTP-γ-S in the patch pipette had little or no effect on the uptake current. Arachidonic acid induced a progressive and prolonged inhibition of the uptake current.

A fluorescence assay was used to measure glutamate uptake, independently of the uptake current. Manoeuvres which changed the uptake current had similar effects on uptake as measured by the fluorescence method. This confirmed that glutamate uptake into Müller cells occurs predominantly by the high affinity, sodium-dependent system and that the uptake current reflects accurately the rate of glutamate uptake into the cell.

Acknowledgements

I thank David Attwell, for excellent and generous supervision. Everybody in the lab has contributed to the friendly and stimulating environment: Monique Sarantis, Marek Szatkowski, Peter Mobbs, Karen Everett, Beverly Clark and Helen Brew. I thank Chris Magnus for help with some difficult experiments. It has been interesting and useful speaking with members of the Physiology and Pharmacology departments.

I was supported by a studentship from the Science and Engineering Research Council.

Contents

List of Figures 7

List of Tables 9

Chapter 1: Introduction

1.1 Evidence for a transmitter role for excitatory amino acids 10

1.2 Glutamate receptor function 16

1.3 Pathological roles of glutamate receptors 19

1.4 Transmitter uptake carriers 20

1.5 Previous studies of glutamate uptake 20

1.6 Studying glutamate uptake with patch-clamping 24

1.7 Investigations undertaken 28

Chapter 2: Methods

2.1 Cell preparation 29

2.2 Solutions and superfusion 30

2.3 Association of glutamate and divalent ions in solution 31

2.4 Experimental apparatus for electrical recording 33

2.5 Experimental apparatus for simultaneous electrical and fluorescence recording 34

2.6 Correction for junction potentials 35

2.7 Series resistance error 36

2.8 Voltage-clamp quality 36

2.9 Data analysis 43

Chapter 3: The ionic dependence of glutamate uptake

3.1 Introduction 58

3.2 Dependence on external sodium and related ions 58

3.3 Dependence on internal sodium 61

3.4 Inhibition by internal glutamate 64

3.5 Interaction of internal sodium and glutamate 67

3.6 Dependence on internal potassium and related ions 70

3.7 The effects of reducing $[K]_i$ on the affinity for $[glu]_o$ and $[Na]_o$, and on the voltage-dependence of glutamate uptake 78

3.8 Dependence on external potassium 84

3.9 Dependence on chloride 87

3.10 Dependence on external pH 90

Chapter 4: Modulation of glutamate uptake

4.1 Dependence on internal calcium 98

4.2 Effect of cGMP 98

4.3 Effect of cAMP 100

4.4 Effect of GTP-γ-S 102

4.5 Effect of phorbol ester 102

4.6 Effects of arachidonic acid 103

4.7 Possible mechanisms of action of arachidonic acid 106

4.8 Effects of other fatty acids 113

4.9 Kinetics of inhibition by arachidonic acid 116

Chapter 5: A fluorescence assay for glutamate uptake

5.1 Introduction 119

5.2 The glutamate-evoked fluorescence response 121

5.3 Sodium-dependence of the fluorescence response 124

5.4 Specificity for glutamate 127

5.5 Quantitation of the glutamate-evoked fluorescence response 128

5.6 Variation of the glutamate-evoked current and fluorescence with glutamate concentration 132

5.7 Relation of the fluorescence response to glutamate uptake 138

5.8 Voltage-dependence of the glutamate-evoked current and fluorescence change 142

5.9 Potassium-dependence of the glutamate-evoked fluorescence response 152

5.10 Removal of intracellular potassium 153

5.11 Raising the extracellular potassium concentration 157

Chapter 6: Discussion

6.1 Uptake current or channel? 163

6.2 Types of glutamate uptake 164

6.3 Mammalian and amphibian uptake systems are similar 168

6.4 Stoichiometry of uptake 168

6.5 Accumulative power of the carrier 174

6.6 Function of potassium counter-transport 175

6.7 Role of glutamate uptake at the synapse 176

6.8 Relevance of glutamate uptake to Long-Term Potentiation 177

6.9 Role of glutamate uptake in neurotoxicity 180

References 187

List of figures

Fig. 1.1	Müller cell picture	23
Fig. 1.2	Glutamate uptake current and stoichiometry of glutamate uptake	26
Fig. 2.1	Model of a Müller cell	38
Fig. 2.2	Capacity transient analysis	45
Fig. 2.3	Plot of uptake current vs. cell capacitance	48
Fig. 3.1	Dependence of the uptake current on external monovalent ions	60
Fig. 3.2	Inhibition of the uptake current by Na_i	63
Fig. 3.3	Interaction of glu_i and Na_i	66
Fig. 3.4	Removal of internal potassium abolishes the uptake current	69
Fig. 3.5	Dependence of the uptake current on $[K]_i$	72
Fig. 3.6	Comparison of the $[K]_i$-dependence of the uptake currents for L-glu and D-asp	75
Fig. 3.7	Replacement of internal potassium by rubidium and caesium	77
Fig. 3.8	Effect of reduction of $[K]_i$ on the apparent affinity for external glutamate and sodium	80
Fig. 3.9	Effect of lowering $[K]_i$ on the I-V relation for the uptake current	82
Fig. 3.10	Dependence on $[K]_o$	86
Fig. 3.11	Dependence on $[Cl]_o$ and $[Cl]_i$	89
Fig. 3.12	Changes of pH affect the glutamate-evoked current	92
Fig. 3.13	Dependence on external pH	97
Fig. 4.1	Arachidonic acid inhibits glutamate uptake	105

Fig. 4.2	Ouabain and inhibitors of arachidonic acid metabolism fail to prevent inhibition by arachidonic acid	108
Fig. 4.3	Arachidonic acid does not act via PKC on the uptake carrier	111
Fig. 4.4	Effects of other fatty acids	115
Fig. 4.5	Kinetics of arachidonic acid's inhibition of the uptake current	118
Fig. 5.1	Sodium-dependence of the glutamate-evoked fluorescence response	123
Fig. 5.2	Aspartate evokes no fluorescence response	126
Fig. 5.3	Quantification of the fluorescence response	131
Fig. 5.4	A lower glutamate concentration evokes a slower-rising fluorescence response	134
Fig. 5.5	Dependence of the glutamate-evoked fluorescence and current on $[glu]_o$	137
Fig. 5.6	Fluorescence-current relation from the glutamate dose-response data	140
Fig. 5.7	Depolarisation reduces the fluorescence response	144
Fig. 5.8	Voltage-dependence of the glutamate-evoked fluorescence and current	146
Fig. 5.9	Fluorescence-current relation for the voltage data	148
Fig. 5.10	Reduction of the fluorescence response by depolarisation and lowered $[glu]_o$ in one cell	151
Fig. 5.11	Removal of intracellular potassium reduces the fluorescence response	155
Fig. 5.12	Raising external potassium reduces the fluorescence response	159
Fig. 5.13	A fluorescence 'spike'	162
Fig. 6.1	The equilibrium $[glu]_o$ as a function of $[K]_o$	186

List of tables

Table 2.1	Extracellular solutions A-E	50
Table 2.2	Extracellular solutions F-I	51
Table 2.3	Extracellular solutions J & K	52
Table 2.4	Pipette filling solutions Z-W	53
Table 2.5	Pipette filling solutions V-T	54
Table 2.6	Pipette filling solution S	55
Table 2.7	Pipette filling solutions R-P	56
Table 2.8	Pipette filling soution O	57
Table 4.1	Effects of internal cGMP	99
Table 4.2	Effects of internal GTP-γ-S	101

Chapter 1

Introduction

There is a large body of evidence indicating that glutamate (or a closely related amino acid) is an important neurotransmitter in the central nervous system (CNS), subserving a wide variety of functions, from high-speed synaptic transmission to memory formation and brain development.

In this thesis I describe experiments characterising the properties of the glutamate uptake carrier which removes glutamate from the extracellular space. The experiments were carried out on isolated retinal glial cells (Müller cells) of the slamander. This introduction puts these experiments in context by (i) reviewing the evidence that glutamate is a neurotransmitter; (ii) describing the properties of the glutamate receptors in the CNS and their roles in physiological and pathological situations; (iii) by reviewing previous work on glutamate uptake and (iv) introducing the experiments in this thesis.

1.1 Evidence for a transmitter role for excitatory amino acids

A number of criteria must be satisfied in identifying a neurotransmitter:-

i) The transmitter candidate should undergo Ca^{2+}-dependent release on afferent stimulation.

ii) A population of synaptic vesicles should contain the transmitter candidate.

iii) Exogenously applied transmitter candidate should mimic the effects of the endogenous transmitter.

iv) Antagonists should affect normal transmission and the effects of exogenously applied transmitter similarly.

v) A mechanism should exist to remove the transmitter from the extracellular space.

I shall review briefly the evidence that glutamate or a related amino acid is the transmitter acting at 'excitatory amino acid' receptors, using the above criteria. Evidence will be drawn from many brain regions, but particular attention will be given to the retina, since retinal cells were used in the experiments described in this thesis. Compounds which are candidates for the endogenous transmitter are L-glutamate, L-aspartate and their sulphur-containing analogues: L-cysteate, L-homocysteate, L-cysteinesulphinate, L-homocysteinesulphinate and L-serine-O-sulphate. N-acetylaspartylglutamate (NAAG) and quinolinate will also be considered, as these endogenous compounds have been reported to act on excitatory amino acid receptors.

i) Calcium-dependent release

Calcium-dependent release of glutamate and aspartate from brain slices has been induced with field stimulation (White et al, 1977), potassium and veratridine (Nadler et al, 1977). Supporting the notion that this release is from nerve terminals, glutamate release from synaptosomes has been demonstrated (eg. Nicholls & Sihra, 1986).

The calcium-dependent release of other candidate transmitters has also been demonstrated. These include the sulphur-containing amino acids (Do et al, 1986) and NAAG (Pittaluga et al, 1988). Release of quinolinate has not been reported (Stone & Burton, 1988).

In the retina, Miller & Schwartz (1983) showed that five substances were released from photoreceptors in a calcium-dependent fashion by potassium depolarisation: glutamate, aspartate, N-acetylhistidine, putrescine and cadaverine. Interestingly, they also showed that glutamate, aspartate and N-acetylhistidine were released by depolarisaton in the absence of calcium. The suggestion was made that transmitter release at certain synapses might be calcium-independent and non-vesicular (Miller & Schwartz, 1983; Schwartz, 1986). It was proposed that depolarisation would reverse the direction of operation of the voltage-dependent carrier for glutamate which would then release glutamate. Although this is possible in principle, the physiological contribution of this mechanism is not clear. Contrasting results were obtained in isolated photoreceptors, where the release of glutamate was largely blocked by calcium channel blockers such as cadmium, cobalt and magnesium and was thus probably calcium-dependent (Ayoub et al, 1989).

ii) Transmitter-containing vesicles

The isolation of a population of synaptic vesicles able to accumulate glutamate has been demonstrated (Naito & Ueda, 1985; Maycox et al, 1988, 1990). Uptake of glutamate into the vesicles requires ATP and is stimulated by low concentrations (eg. 4mM) of chloride (Naito & Ueda, 1985, Maycox et al, 1988, 1990). Glutamate is concentrated in the vesicles by a glutamate transporter distinct from that present in the plasma membrane of glial cells and neurones, the properties of which are described in section 1.5. In particular, the vesicular glutamate transporter is characterised as sodium-independent and chloride-dependent. Interestingly, L-aspartate and L-homocysteate are poor substrates for this carrier (Naito & Ueda, 1985), so vesicles are probably unable to accumulate these amino acids, making a transmitter role for either aspartate or homocysteate seem unlikely. Vesicular uptake of other sulphur-containing amino acids, NAAG or quinolinate has not been investigated.

iii) Identity of action with endogenous transmitter

The postsynaptic currents at 'glutamatergic' synapses have a reversal potential near to 0mV and are carried largely by sodium and potassium ions (eg. Hablitz &

Langmoen, 1982). They are controlled by a number of receptors. These have been classified, using selective agonists, into NMDA (N-methyl-D-aspartate), AMPA (α-amino-3-hydroxy-5-methyl-isoxazole-4-propionate)/kaninate (formerly quisqualate/kainate) and APB (2-amino-4-phosphonobutyrate) receptors (Watkins & Evans, 1981; Monaghan et al, 1989; see section 1.2). The first two receptor types open ion channels permeable to sodium and potassium (Mayer & Westbrook, 1984) and also calcium in the case of NMDA receptors (MacDermott et al, 1986). The APB receptor closes cation channels in one class of retinal bipolar cell (Slaughter & Miller, 1981; Attwell et al, 1987; Nawy & Jahr, 1990).

Glutamate is able to mimic all of these effects and activate all of the above receptors. Aspartate is completely selective for NMDA receptors (Patneau & Mayer, 1990), so it cannot be the only endogenous transmitter at the many synapses where there is a non-NMDA receptor-mediated component of the synaptic current. Consistent with the selective action of aspartate, this amino acid had no effect on isolated retinal bipolar cells that responded to glutamate (Attwell et al, 1987); bipolar cells in situ express only non-NMDA receptors (Slaughter & Miller, 1983).

The sulphur-containing amino acids are active at both NMDA and non-NMDA receptors, but with higher EC_{50} values than those for glutamate (in some cases much higher) (Patneau & Mayer, 1990).

Evidence that NAAG had the same effect as the endogenous transmitter in the lateral olfactory tract (LOT) (ffrench-Mullen et al, 1985) has been subsequently ascribed to potassium in the iontophoretic solution used to apply NAAG (Whittemore & Koerner, 1989). Interpretation of experiments in which NAAG is applied to intact tissue is complicated by the presence of a peptidase which breaks down NAAG, producing glutamate (Robinson et al, 1987). When applied to isolated cells, NAAG is a weak agonist at NMDA receptors only (Westbrook et al, 1986). Quinolinate is a very poor agonist at both NMDA and non-NMDA receptors (Patneau & Mayer, 1990).

iv) Effects of antagonists

A range of competitive and non-competitive glutamate antagonists have been developed which interact with either NMDA or AMPA/kainate receptors. Active at the NMDA receptor are competitive antagonists such as APV (2-amino-5-phosphonovalerate), CPP [3-(2-carboxypiperazin-4-yl)propyl-1-phosphate] (reviewed by Watkins et al, 1990) and non-competitive antagonists such as MK-801 and phencyclidine (PCP) (reviewed by Lodge & Johnson, 1990). An effective and relatively selective blocker of AMPA/kainate receptors is CNQX (6-cyano-7-nitro-quinoxaline-2,3-dione) (Honoré et al, 1988). In addition, it is possible to inhibit or unmask NMDA receptor-mediated responses by exploiting their voltage-dependent block by magnesium (Nowak et al, 1984). Glycine is a co-agonist at the NMDA receptor (Johnson & Ascher, 1987) and NMDA responses can also be blocked by antagonists at this site, eg. 7-chloro-kynurenate. CNQX and APV together are able to abolish most 'glutamatergic' synaptic currents (eg. Davies & Collingridge, 1989).

The excitatory actions of the sulphur-containing amino acids in brain slices are attenuated by APV (Mewett et al, 1983). CNQX was not tested in the study. The current evoked by NAAG in isolated cells was abolished by APV (Westbrook et al, 1986).

v) Removal of transmitter

In order for a synapse to function repeatedly, the released transmitter must be inactivated or removed from the extracellular space. At the vertebrate neuromuscular junction and other cholinergic synapses, released acetylcholine is broken down by the enzyme acetylcholinesterase. For many other transmitters, such as noradrenaline, GABA and glycine (see section 1.4) there are carrier proteins which transport the transmitter from the extracellular space into cells. The demonstration of an uptake system for glutamate and aspartate (Logan & Snyder, 1972; Balcar & Johnston, 1972) was an important piece of evidence that these compounds might have transmitter roles.

L-cysteate and L-cysteinesulphinate are taken up by the same mechanism as glutamate and aspartate (Wilson & Pastuszko, 1986). L-homocysteate is reported (Cox et al, 1977) to be taken up by the same 'low-affinity system' as glutamate (which is probably high affinity glutamate uptake: see section 6.2 which explains how high affinity uptake in brain slices can appear to be 'low affinity'). At high concentrations L-homocysteate is able to evoke a small uptake current in Müller cells (Muriel Bouvier, Barbara Miller & David Attwell, personal communication), suggesting that it is slowly transported by the high affinity glutamate uptake carrier. NAAG is broken down by a peptidase, but liberates glutamate in the process (Robinson et al, 1987). No breakdown of quinolinate has been demonstrated and it does not appear to be taken up (Stone & Burton, 1988).

Summary

Of the transmitter candidates, the most convincing evidence has been accumulated in support of glutamate as an endogenous transmitter. It is released by a number of stimuli in a calcium-dependent fashion, is accumulated by synaptic vesicles, is a good agonist at all of the receptor types, its actions can be blocked by the same antagonists which inhibit the actions of the endogenous transmitter and there is a very efficient uptake system to remove it from the extracellular space.

Aspartate is less likely to act as a transmitter: it is not taken up into synaptic vesicles and it is not an agonist at the non-NMDA receptors which are activated at most 'glutamatergic' synapses. Members of the family of sulphur containing amino acids can activate both NMDA and non-NMDA receptors, although they all have higher EC_{50} values than glutamate. They are taken up and their calcium-dependent release has been demonstrated. Their presence in synaptic vesicles has not been shown, however, and homocysteate, at least, is not taken up into the vesicles. There is little evidence supporting NAAG as a transmitter; it is a weak NMDA receptor agonist only. Quinolinate is very unlikely to have a transmitter role.

1.2 Glutamate receptor function

AMPA/kainate receptor

Recently a family of glutamate receptors has been cloned and expressed (Hollmann et al, 1989; Boulter et al, 1990; Keinänen et al, 1990; Sommer et al, 1990) which respond to both AMPA and kainate with currents like those evoked by these compounds in neurones: a rapidly desensitising response to AMPA and a sustained response to kainate (eg. Patneau & Mayer, 1990). This suggests that AMPA and kainate receptors may be one and the same. A report of apparently selective responses to kainate in a C-fibre preparation (Agrawal & Evans, 1986) has been used as evidence that distinct kainate receptors do exist. Recently, however, Heuttner (1990) has shown that isolated DRG neurons do respond to AMPA and quisqualate as well as to kainate. The reason that AMPA and quisqualate were apparently inactive in the preparation of Agrawal & Evans (1986) was that these agonists evoked a very rapidly and completely desensitising response, while kainate evoked a sustained response.

AMPA receptors mediate 'fast' transmission at most glutamatergic synapses. For example, at the mossy fibre-granule cell synapse in the cerebellum, the fast, CNQX-sensitive component of the synaptic current has a (10-90%)

rise time of less than 200μs and a decay time constant of about 1ms (Angus Silver, Stephen Traynelis & Stuart Cull-Candy, personal communication). Such synaptic currents could, in principle, mediate transmission at hundreds of Hertz (depending on the kinetics of the sodium and potassium currents generating pre- and post-synaptic action potentials).

NMDA receptor

The voltage-dependent block of NMDA channels by magnesium (Nowak et al, 1984; Mayer et al, 1984) means that glutamate and postsynaptic depolarisation are required for full activation, providing a mechanism for signalling conjunctive presynaptic and postsynaptic activity. The time course of the NMDA receptor-mediated synaptic current (eg. Lester et al, 1990) is much slower (ie. >100ms) than that of the AMPA receptor-mediated responses (see above), so NMDA receptor/channels could integrate inputs over periods containing many AMPA-mediated events. The calcium permeability of the open channel (MacDermott et al, 1986) enables it to influence any processes controlled by $[Ca^{2+}]_i$.

Of particular interest is the involvement of NMDA receptors in long-term potentiation, or LTP, in the mammalian hippocampus (CA1 region and dentate gyrus). LTP is a long-lasting increase of gain at glutamatergic synapses; it is thought to be triggered by the the calcium influx produced by activation of NMDA receptors (see section 6.8). This form of synaptic plasticity could plausibly underlie some learning processes.

Some glutamatergic synapses do not appear to have NMDA receptors (Miller & Slaughter, 1983) and at others the NMDA receptor current does not contribute to the synaptic current except under conditions, like during tetanic stimulation, which produce postsynaptic depolarisation (Davies & Collingridge, 1989). There are synapses, however, at which NMDA receptor-mediated currents contribute to normal transmission (Jones & Baughman, 1988).

APB (L-AP4) receptor

This receptor type mediates transmission between photoreceptors and depolarising (ON-) bipolar cells in the retina (Slaughter & Miller, 1981). Its activation leads to the closure of channels (Attwell et al, 1987) via a second messenger cascade involving a G-protein and cGMP (Nawy & Jahr, 1990). This arrangement accounts for the high synaptic gain of photoreceptor-depolarising bipolar cell transmission compared to the gain of photoreceptor transmission to hyperpolarising bipolar cells and horizontal cells (Falk, 1989).

An APB receptor causing presynaptic inhibition has also been reported in the hippocampus (Koerner & Cotman, 1981; Cotman et al, 1986) and at synapses between cultured hippocampal cells (Forsythe & Clements, 1990). Nothing is known about the mechanism of action of this receptor.

'Metabotropic' receptor

Glutamate, acting at these receptors, is capable of causing the release of calcium from intracellular stores via a G-protein, phospholipase C and IP_3 cascade (Sugiyama et al, 1987). The receptor is also activated by quisqualate, but not AMPA. A selective agonist is *trans*-ACPD (*trans*-1-amino-cyclopentyl-1,3-dicarboxylate) (Monaghan et al, 1989). Cultured astrocytes express this receptor (Cornell-Bell et al, 1990). In these cells glutamate induced propagating (and sometimes repetitive) calcium waves which were transmitted to neighbouring cells, presumably via gap junctions. A function for this receptor and the calcium mobilisation it produces has yet to be elucidated.

Glutamate-gated chloride channels

Glutamate opens chloride-selective channels in locust muscle (Cull-Candy, 1976), Helix neurones (Szczepaniak & Cottrell, 1973) and in cone photoreceptors (Sarantis et al, 1988). The cone receptor is apparently presynaptic and is also activated by kainate. The current evoked by activation of this receptor has the unusual property of being sodium-dependent, although sodium ions are not conducted by the channel. A presynaptic receptor is likely to modulate transmitter release, but such a role has yet to be demonstrated in the retina.

1.3 Pathological roles of glutamate receptors

Glutamate can be neurotoxic (Choi et al, 1987; Meldrum & Garthwaite, 1990). It is likely that this common transmitter is involved in neurodegenerative processes, in particular in anoxic/ischaemic and epileptic damage. The same mechanisms may underlie both pathologies, because in each there is an increased release of glutamate (see section 6.9). Thus, the pattern of hippocampal damage following excitatory amino acid application is similar to that in epileptic damage (Sloviter & Dempster, 1985). In vitro, much of the damage caused by glutamate, which activates NMDA receptors to admit a lethal calcium influx, is prevented by NMDA antagonists (Choi, 1987; Choi et al, 1988). NMDA antagonists also reduce ischaemic/anoxic degeneration in intact tissues (eg. Ozyurt et al, 1988). Other glutamate receptors, particularly the metabotropic receptor which releases intracellular calcium, may also be involved in neurotoxic processes (Garthwaite & Garthwaite, 1989; Sheardown et al, 1990).

1.4 Transmitter uptake carriers

Many transmitters appear to be removed from the extracellular space by uptake into cells. This is achieved by specific carrier systems for noradrenaline, GABA, glycine, serotonin, dopamine and glutamate. These carrier mechanisms are all sodium co-transporters: they utilise the existing electrochemical gradient for sodium to derive the free energy required to accumulate the transmitter inside cells. By co-transporting two or more sodium ions with each amino acid molecule, such carriers are able to maintain large $[\text{transmitter}]_{in}/[\text{transmitter}]_{out}$ gradients.

The various neurotransmitter carriers are distinct in that they are specific for the particular transmitter transported, but also in that they have different stoichiometries. In addition to the transmitter and sodium ions, chloride, potassium and hydrogen ions can also be transported. For example, GABA is probably co-transported with two sodium ions and a chloride ion, while the favoured stoichiometry for serotonin uptake is serotonin,Na^+,Cl^-/K^+ (where a comma indicates co-transport and a slash counter-transport). The properties of these carriers are reviewed in detail by Kanner & Schuldiner (1987).

1.5 Previous studies of glutamate uptake

Glutamate uptake has been extensively studied using biochemical techniques, mostly radiotracing. A variety of preparations have been used, including: brain slices, cultured cells and suspensions of synaptosomes or resealed synaptosomal ghosts. These studies have shown clearly that the glutamate uptake carrier is a sodium co-transporter, with probably two or more sodium ions being taken up with each glutamate molecule (see section 6.4).

Several reports have shown that internal potassium stimulates glutamate uptake (Kanner & Sharon, 1978a & b; Burckhardt et al, 1980; Schneider & Sacktor, 1980, Kanner

& Schuldiner, 1987) and some of the experimenters have concluded from this result that the glutamate uptake carrier counter-transports potassium ions out of the cell as it takes up glutamate and sodium ions. Care must be exercised in reaching this conclusion, however, because potassium could also stimulate uptake in the following manner. Loading synaptosomes with potassium will generate an inside-negative membrane potential (being derived from cell membranes they have a relatively large potassium conductance). As glutamate uptake is electrogenic (transporting a net positive charge into the cell) it will be potentiated by such a membrane potential (Murer et al, 1980; Brew & Attwell, 1987), so internal potassium could activate uptake in this way without being transported by the carrier.

The only experiments which address this problem are those of Kanner and co-workers (Kanner & Sharon, 1978a, b; Kanner & Marva, 1982; Kanner & Schuldiner, 1987) who show that internal potassium is absolutely required for glutamate uptake, even in the presence of external thiocyanate ions which are expected to generate an inside-negative membrane potential in the absence of potassium. This is a qualitative result showing that internal potassium is required for operation of the glutamate uptake carrier. Using synaptosomal suspensions, however, it is not feasible to quantify the direct and indirect effects of potassium on glutamate uptake. The use of whole-cell patch-clamping, where the cell is voltage clamped, to study glutamate uptake enables a precise evaluation of the effects of potassium to be made (see section 1.6 below).

The radiotracing experiments on the effects of potassium were performed using synaptosomes, which are of neuronal origin. Glial cells appear to be the major sites of expression of the glutamate uptake carrier, as most exogenous glutamate applied to intact retinae (White & Neal, 1976; Ehinger, 1977) or brain slices (McLennan, 1976) is accumulated by the glial cells.

Fig. 1.1 An acutely isolated salamander Müller cell. Cells such as these were used for all the experiments in this thesis. They were prepared by papain dissociation of salamander retinae (see methods).

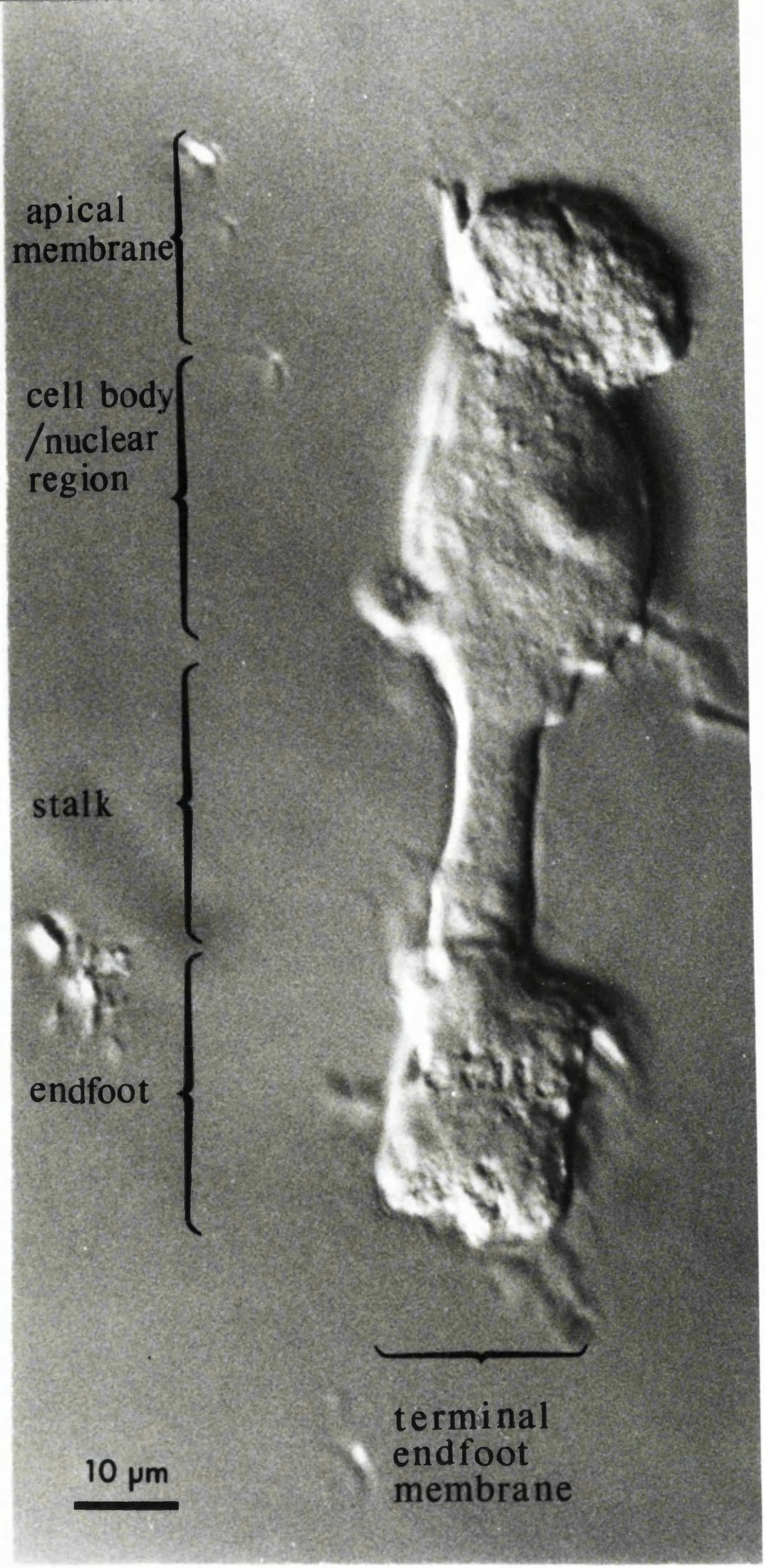
apical membrane
cell body /nuclear region
stalk
endfoot
terminal endfoot membrane
10 µm

It is therefore of interest to know whether the uptake mechanism in glial cells is also potassium-dependent.

Sodium-dependent, high-affinity glutamate uptake is not the only mechanism transporting glutamate into cells. 'Chloride-dependent' (Pin et al, 1984) and 'low affinity' (Logan & Snyder, 1972) uptake systems have also been described. It is not clear what contribution these systems make, whether they are found in glial cells, or indeed whether they are not artefactual (see section 6.2).

Little is known concerning the regulation or modulation of the glutamate uptake carrier.

1.6 Studying glutamate uptake with patch-clamping

Figure 1.1 shows a picture of an isolated retinal glial (Müller) cell from the salamander, such as was used in the experiments presented in this thesis. Brew & Attwell (1987) showed that high-affinity, sodium-dependent glutamate uptake in salamander Müller cells is electrogenic. An example of the uptake current measured in a whole-cell patch-clamped Müller cell is shown in Fig. 1.2A. Bath application of 30μM glutamate evokes an inward current, consistent with the electrogenic uptake of glutamate. Fig. 1.2B shows the likely stoichiometry of glutamate uptake: glutamate uptake generates a net inward current because each glutamate anion is taken up with an excess of positively charged ions (see section 6.4). Results obtained by Brew & Attwell (1987) and in this thesis (see section 6.1) show that the glutamate-evoked current is indeed due to electrogenic uptake and is not detectably contaminated with current flowing through glutamate-gated channels. Glutamate gated channels have been described in cultured glia (Usowicz et al, 1989), but are not expressed in acutely isolated Müller cells.

The whole-cell clamped Müller cell is the basic preparation which has been used in all of the experiments in this thesis. Use of this preparation allows the study

Fig. 1.2 **A** The glutamate uptake current. Bath application of 30μM glutamate to a whole-cell patch-clamped Müller cell (see Fig. 1.1) evokes an inward current under voltage-clamp. The inward current is due to electrogenic glutamate uptake and is not due to activation of glutamate-gated channels (see section 6.1). The holding potential was -43mV, external solution B and pipette solution Y. This holding potential and these solutions are frequently used throughout this thesis. **B** The likely stoichiometry of glutamate uptake in salamander Müller cells (see section 6.4).

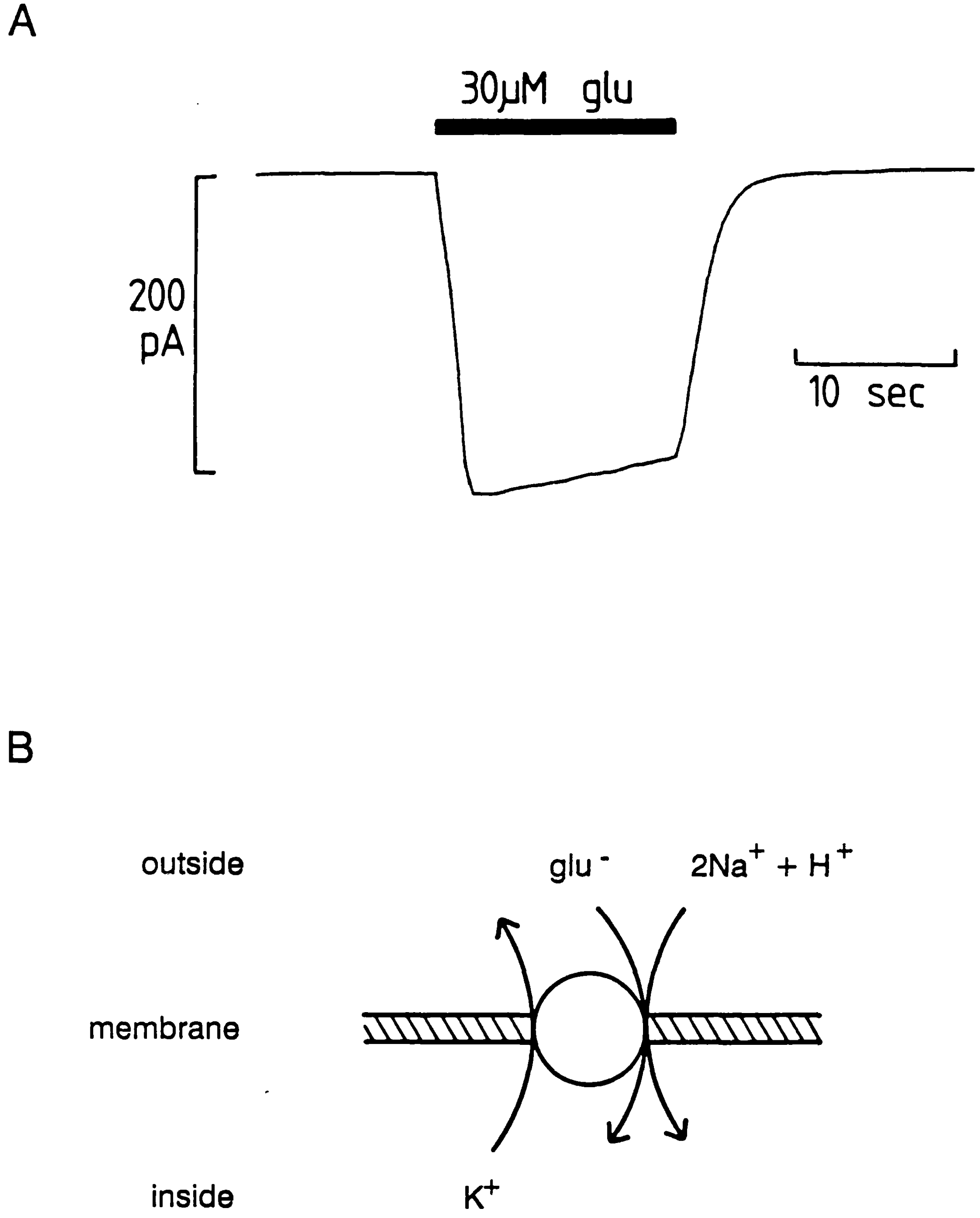
A
30μM glu
200 pA
10 sec
B
outside
glu⁻
2Na⁺ + H⁺
membrane
inside
K⁺

of glutamate uptake, by monitoring the current it produces, in a single cell with a high time resolution. It offers a number of significant advantages over biochemical methods. The most important of these is that the membrane potential of the cell is controlled independently. Not only does this mean that changes of the ionic composition of the intracellular and extracellular solutions have no effect on the membrane potential, but also that the membrane potential can be changed at will. This is particularly important when studying the effects of potassium (chapter 3), but, in principle, changes of any permeant ion could also affect the membrane potential were it not clamped.

Because the patch-clamped cell is held in position by the patch-pipette, it is possible to make repeated and rapid changes of external solution. The dialysis of the cell interior by the solution filling the pipette ensures a relatively constant intracellular composition: ionic gradients are not depleted by time or by operation of the uptake carrier. It is also easy to study the effects of changing the intracellular solution by comparing responses between (groups of) cells recorded with the different pipette-filling solutions. As well as using this method to investigate the role of internal ions in the uptake process (chapter 3), various compounds which influence intracellular second messenger systems can also introduced into the cell in this way (see chapter 4).

I have also developed a fluorescence method of detecting glutamate uptake into a single cell which complements the electrical recording technique (see chapter 5). After glutamate is taken up, at least some of it is metabolised by the enzyme glutamate dehydrogenase to α-ketoglutarate. This reaction can be followed in a single cell, because in the reaction the co-factor NAD is reduced to NADH, which is fluorescent. This method will detect glutamate entry by any pathway (eg. electroneutral uptake, as a weak acid or base), while the electrical technique is only useful for electrogenic uptake.

1.7 Investigations undertaken

Using whole-cell recording from Müller cells, a detailed investigation of the ionic dependence of the glutamate uptake current was performed, with the aim of determining which ions are involved in the transport reaction. The results are presented in chapter 3. The principal finding is that the glutamate uptake carrier counter-transports a potassium ion as each glutamate anion is taken up.

In chapter 4, the same technique is applied to survey second messenger systems in an attempt to identify putative regulatory mechanisms of the uptake carrier. As the preliminary results showed that arachidonic acid exerted a powerful inhibitory effect on uptake, the mechanism of its action was studied in detail.

The fluorescence technique for measuring glutamate uptake is used in chapter 5, in conjunction with the electrical method, to show that high affinity, sodium-dependent glutamate uptake is the only significant process transporting glutamate into Müller cells. It is also used to confirm that manipulations which reduce the uptake current also reduce the rate of glutamate influx, an assumption underlying the interpretation of the results of chapter 3 (and Brew & Attwell, 1987).

Chapter 2

Methods

In this section I will describe how electrical and fluorescence recordings were made from single isolated Müller (retinal glial) cells.

2.1 Cell preparation

The isolated Müller cells used in all experiments were obtained from larval tiger salamanders (Ambystoma tigrinum), 20-30cm long.

The animals were decapitated and their eyes enucleated. Excess tissue was trimmed from each eyeball under a dissecting microscope. By cutting the sclera just anterior to the ora serrata, each eyeball was divided into two: the eyecup containing the retina was separated from the cornea and lens (which were discarded). The eyecups were stored in solution A (see section 2.2 or table 2.1) at 5°C in the dark and used within 48 hours. Before use, an eyecup was bisected and half a neural retina gently detached from the pigment epithelium and sclera using fine forceps.

Half retinae were transferred to the dissociation solution, containing (mM): NaCl 66; KCl 3.7; $NaHCO_3$ 25; NaH_2PO_4 10; Na pyruvate 1; DL-cysteine HCl (Sigma) 10 and 10-20 units of papain (Sigma P3125). The retina was then immediately incubated for 20-30 minutes at 30-35°C.

After incubation, the retina was rinsed by dropping it through solution A (about 3ml, 3-4 times). It was then triturated by drawing it in and out of a narrowed Pasteur pipette (tip diameter about 0.5mm) 2-5 times in 1ml of solution A.

In most experiments the resulting cell suspension was plated directly into the recording chamber. Alternatively, 0.1-0.2ml aliquots of the suspension were plated onto 13mm diameter glass coverslips. One coverslip at a time was placed in the recording chamber and each was discarded once recordings had been made from one cell on it. The latter procedure was used for experiments in which a particular drug could be applied once only to a cell. This occurred when the drug was suspected of having an irreversible effect: using bath application, the first application of the drug would render recordings from any other cells in the chamber invalid.

Cells were allowed at least 5 minutes to settle before recording began. Typically, cells from a single dissociation would remain viable for 3 hours.

Müller cells were easily identified by their characteristic morphology (see Fig. 1.1).

2.2 Solutions and superfusion

All extracellular solutions were bath applied. Different solutions were led through polythene tubing under gravity feed to a common bath inlet. Solutions were selected by opening and closing stopcocks in the solution lines. Perfusion was continuous during recording: solution was removed from the recording chamber by a vacuum pump sucking through a small tube. In most experiments cells which had been whole-cell patch-clamped were lifted off the bottom of the recording chamber and moved close to the solution inlet, ensuring a rapid and complete solution change around the cell (in 1-10 seconds). For the experiments in which fluorescence measurements were made the cells were not moved, but a movable inlet was located near the cell. L-glutamate and analogues were added from a 100mM or 10mM stock to the perfusion solution.

Arachidonic acid was made up as a 10mM stock in water then aliquots were frozen under nitrogen or argon. When required, the aliquots were thawed, sonicated, the stock pipetted and the final solution sonicated. Other fatty acids (and occasionally arachidonic acid) were made up in

DMSO stock, but otherwise were prepared by the same procedure.

Other drugs were dissolved as described in the appropriate results sections. Where a vehicle was used, this was also added to the control solution. The pH of the extracellular solutions was titrated to 7.3 with NaOH, or occasionally KOH (as stated). The extracellular solutions used are given in tables 2.1-2.3. The standard external solution was B.

The various solutions used to fill the patch-pipettes for whole-cell recordings are given in tables 2.4-2.8, the most commonly used being solution Y. The pH of the intracellular solutions was adjusted to 7.0 with KOH, or occasionally NaOH (as stated). The free calcium concentration for the patch-pipette solutions, calculated using the equilibrium constants for calcium binding to EGTA given by Martell and Smith (1974), allowing for magnesium binding and pH, was 1.2×10^{-7}M. All experiments were carried out at room temperature (20-25°C).

2.3 Association of glutamate and divalent ions in solution

In solution glutamate (and aspartate) form soluble complexes with divalent ions. The extent of this association in the solutions used is sufficient to significantly reduce the free concentration of the amino acid. The association is of the form

$$\text{metal}^{2+} + \text{amino acid} \rightleftharpoons \text{metal.amino acid}$$

The equilibrium constants (units M^{-1}), calculated from the quotient

$$K_{metal} = [\text{metal-amino acid}]/[\text{metal}^{2+}][\text{amino-acid}],$$

are given in Martell and Smith (1974). For glutamate $\log(K_{Mg}) = 1.9$, $\log(K_{Ca}) = 1.43$ and $\log(K_{Ba}) = 1.28$ and for aspartate (same order) 2.43, 1.6 and 1.14. The concentrations of divalents used were (mM): Mg^{2+} 0.5, Ca^{2+} 3 and Ba^{2+} 6 (magnesium and calcium are normal extracellular constituents, the barium was added to block the Müller cell's potassium conductance).

The free amino acid concentration, G_f is related to the total added concentrations of amino acid, G_T, and the divalents, $[\text{metal}]_T$, by

$$G_T = G_f \left\{ 1 + \frac{K_{Mg}[Mg]_T}{1 + G_f K_{Mg}} + \frac{K_{Ca}[Ca]_T}{1 + G_f K_{Ca}} + \frac{K_{Ba}[Ba]_T}{1 + G_f K_{Ba}} \right\} \quad (2.1)$$

The exact algebraic solution for G_f is cumbersome, but a close approximation is obtained by neglecting the terms $G_f K_{metal}$ in the denominators of the right hand side. With concentrations of added glutamate or aspartate $\leq 100\mu M$, the error this introduces is <0.3% of the G_f value obtained. With 1mM added amino acid, this error limit becomes 2.7%, but is unimportant because the amino acid binding site of the uptake carrier is at least 98% saturated at this concentration. Equation (2.1) then becomes:

$$G_f = \frac{G_T}{1 + K_{Mg}[Mg]_T + K_{Ca}[Ca]_T + K_{Ba}[Ba]_T} \quad (2.2)$$

Substitution of the concentrations of the divalents used into this approximate solution gives

$$[glu]_{free}/[glu]_{total} = 0.81$$
$$[asp]_{free}/[asp]_{total} = 0.75.$$

In the absence of barium these ratios for glutamate and aspartate are 0.89 and 0.82 respectively. Thus addition of barium reduces the effective concentration of either amino acid by about 9%.

Adding 6mM $BaCl_2$ to the external solution reduced the uptake current evoked by 30μM glutamate by 4.7 ± 1.1% (SEM, n=5) (Attwell & Brew, personal communication). Assuming a K_m (in barium) of 20μM for activation of the uptake current by glutamate, a 9% reduction of free glutamate caused by barium would be expected to reduce the glutamate-evoked current by 3.6%. It is concluded that barium has a negligible effect, if any, on the uptake current.

Concentrations of glutamate and aspartate given in this thesis have not been corrected by these formulae: none of the conclusions reached are critically dependent on the exact amino acid concentration. Furthermore, as G_f is proportional to G_T in equation (2.2), the association of amino acid and divalents will not affect the shape of the glutamate dose-response curve for activation of the uptake current, just artefactually reduce the apparent affinity for glutamate.

2.4 Experimental apparatus for electrical recording

The recording chamber (bath) was located on the fixed stage of an Ergaval microscope through which the cells and electrode could be viewed. The electrode holder and headstage were mounted on a hydraulic micromanipulator (Narashige) which was itself mounted on a coarse micromanipulator (Prior).

Electrical recordings were made using the whole-cell patch-clamp technique (Hamill et al, 1981).

Patch-pipettes were pulled on a BBCH puller (Mecanex, Geneva) from pyrex glass with a microfilament insertion (Clark Electromedical, GC150TF10). Typically, when filled with solution Y, the electrodes had a resistance of 1MΩ in solution B.

Pipettes filled with internal medium were inserted into a perspex electrode holder (Clark Electromedical), also filled with internal medium. (In cases where the pipette filling solution contained expensive drugs, or was a zero chloride solution, the holder and most of the electrode shaft were filled with a standard, chloride containing solution: eg. solution Y). Electrical connection with the pipette filling solution was made by a silver/silver chloride pellet in the back of the holder.

The indifferent electrode was a silver/silver chloride pellet immersed in the bath solution. During the measurement of junction potentials, and during experiments in which the external chloride was varied, this was connected to the solution by a 4M NaCl agar bridge. The electrode/solution junction potential of the agar bridge is expected to vary negligibly with the solutions used.

All electrical recording was carried out under voltage-clamp, with the current being measured as the voltage drop across the 500MΩ resistor of a current-to-voltage converter (List Electronics, L/M EPC-7). Current and voltage were recorded on magnetic tape.

2.5 Experimental apparatus for simultaneous electrical and fluorescence measurements

The apparatus for the electrical recordings was similar in principle to that described in the section above, but with the following differences in detail. The bath electrode was routinely a 3M KCl agar bridge and a chlorided silver wire was used to make electrical connection with the pipette filling solution. The current and pipette voltage were monitored using a different patch-clamp amplifier: Axopatch 1-C (Axon Instruments).

The fluorescence experiments were done as follows. The cells were plated onto a borosilicate glass cover slip (25x25mm) held in the recording chamber, mounted on an inverted microscope (Nikon Diaphot, fitted with a 40x 1.3NA oil-immersion lens). The fluorescence of a single cell was measured using an epifluorescence system. The cells were illuminated with UV light from a 150W xenon arc lamp (Ealing Optics, XBO150), after it had been passed through an iris/diaphragm which varied the intensity of the illuminating light, a narrow band interference filter

(360 ± 5nm, Ealing Optics), a fluid filled light guide (Micro Instruments, Oxford) and a dichroic mirror (430nm). Emitted light was collected through the dichroic mirror, filtered by a 470nm barrier filter and a 500 ± 40nm broad band filter (Nikon) and projected onto a photomultiplier (Thorn EMI, 9924B). An iris and pivoted mirror allowed the image of a cell to be positioned so that only light from that cell reached the photomultiplier. The photocurrent and membrane current were stored on magnetic tape.

2.6 Correction for junction potentials

Whenever two different solutions meet, a diffusion potential forms across the interface. The magnitude of this potential depends upon the charges, mobilities and concentrations of the ions in each solution. Such a potential is generated between the extracellular and pipette filling solutions when the pipette is in solution, before patching onto the cell. It will be abolished when, after going whole-cell, the cell interior is dialysed by the pipette solution. The experimental protocol was to zero the current with the electrode in solution. Thus, when the junction potential across the pipette tip had been abolished by dialysis of the cytoplasm, the apparent membrane potential was in error by the magnitude of the original extracellular/pipette solution junction potential.

The magnitude of this junction potential was measured by the method of Fenwick et al (1982). Using a 4M NaCl agar bridge as the bath electrode, the zero-current potential of a filled pipette in solution was recorded by switching the patch-clamp amplifier to current-clamp. The junction potential desired was obtained by observing the change of potential as the bath solution was changed from extracellular, to pipette filling solution. The potentials thus obtained were specific for the solution pairs used and are listed under the pipette solution recipes in tables 2.4-2.8. Holding potentials cited have been corrected for the voltage error by subtracting the junction potential listed. For example, for a cell nominally held at a potential of -40mV, where the pipette was filled with solution Y and the junction potential had been offset in solution B, the true holding potential would have been -43mV.

2.7 Series resistance error

In the recording circuit, flow of current through a resistance in series with the cell membrane causes a potential drop across that resistance. Most of this resistance is due to the resistance of the electrode tip and cell cytoplasm. The potential drop across the series resistance causes the true membrane potential to differ from the apparent holding potential. It was not possible to use the series resistance compensation circuitry of the patch-clamp amplifier, because the Müller cell capacitance was too large to be cancelled (typically 300pF). However, knowing the series resistance (see section 2.9), it is possible to calculate the voltage error. Because the currents and series resistances in these experiments were relatively small, the voltage errors were small enough to be neglected. This is illustrated by the following worst case calculation. The largest current ever flowing (ie. the holding current at negative potentials plus the glutamate-evoked current) was about 800pA. Thus, for a worst case series resistance of 5MΩ, the largest voltage error would be only 4mV.

2.8 Voltage-clamp quality

In order to assess the uniformity of voltage-clamp in Müller cells, I will represent the isolated Müller cell as a cylinder of diameter 9μm and length 100μm (see Fig 2.1).

__Fig. 2.1.__ The Müller cell model used in section 2.8 to assess the uniformity of the voltage-clamp. Physically, a cylinder of the dimensions shown; electrically, a finite one-dimensional cable. At one end (left) it terminates in an open circuit and is voltage-clamped to V_0 (the location of the whole-cell patch-clamp electrode). The other end terminates in a resistor to ground, R_{end}. r_m and r_i represent the membrane and axial resistances, normalised to length, of the cable.

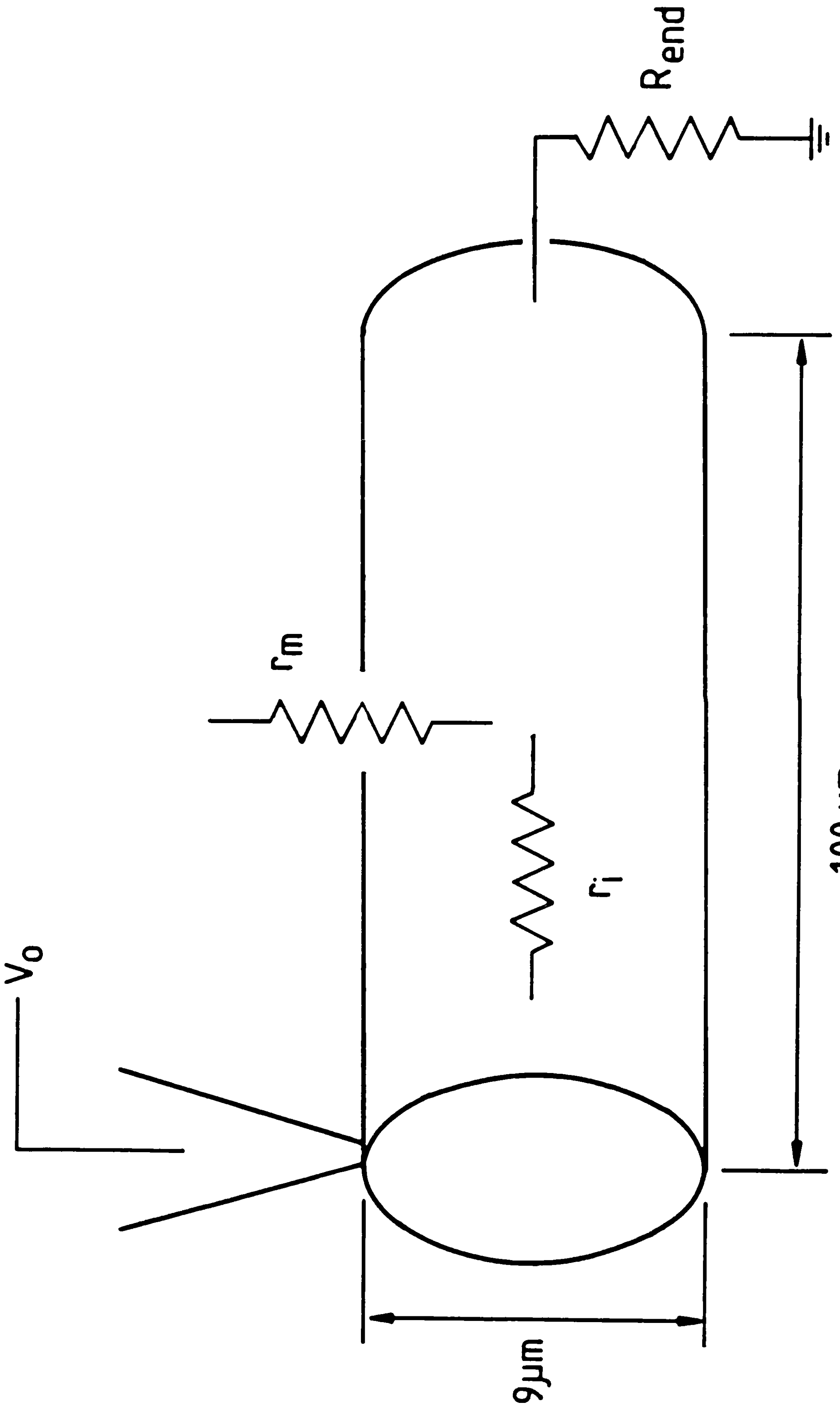

V_o
r_m
r_i
R_{end}
100 µm
9µm

In order to assess the worst case, I shall assume that the Müller cell was patch-clamped at one end (rather than in the middle). Electrically, this model can be represented by a one-dimensional cable, voltage clamped at one end and terminating in a resistor to ground at the other.

The behaviour of a one-dimensional cable is defined by the cable equation.

$$\lambda^2 \frac{\partial^2 V}{\partial x^2} = \tau_m \frac{\partial V}{\partial t} + V \tag{2.3}$$

where V = voltage

x = distance

t = time

r_m = membrane resistance per unit length

r_i = cytoplasmic resistance per unit length

λ = space constant = $\sqrt{(r_m/r_i)}$

c_m = membrane capacitance per unit length

$\tau_m = r_m c_m$

For voltage-clamping the glutamate uptake current it is necessary only to consider the steady-state voltage profile. Because there are no time-dependent changes, eqn (2.3) reduces to

$$\lambda^2 \frac{d^2 V}{dx^2} - V = 0 \tag{2.4}$$

The general solution for this eqn is

$$V = Ae^{x/\lambda} + Be^{-x/\lambda} \tag{2.5}$$

where A and B are arbitrary constants to be determined by the boundary conditions.

From the electrical model of the Müller cell (Fig. 2.1) one boundary condition is readily obtained: at $x = 0$, V is clamped to V_0. Thus

$$V_0 = A + B \tag{2.6}$$

The other boundary condition is obtained by considering the termination by the resistor to ground, R_{end}. The axial current at the termination $(x = L)$ must satisfy the equation

$$i_a = (V)_{x=L} \,/\, R_{end}. \tag{2.7}$$

Now $$\left(\frac{dV}{dx}\right)_{x=L} = -r_i i_a \tag{2.8}$$

therefore,

$$\left(\frac{dV}{dx}\right)_{x=L} = \frac{-r_i (V)_{x=L}}{R_{end}} \tag{2.9}$$

Substituting eqn (2.5) and its derivative into eqn (2.9) and rearranging, we get

$$A = Be^{-2L/\lambda}\frac{\{R_{end} - \lambda r_i\}}{\{R_{end} + \lambda r_i\}} \tag{2.10}$$

By using eqns (2.6) and (2.10) to find A and B we arrive at an exact solution of eqn (2.3) which is specific for the values of r_m, r_i, R_{end} and cable length, L

$$V(x) = V_0\left(\frac{K-1}{K}\right)e^{x/\lambda} + V_0\left(\frac{1}{1+K}\right)e^{-x/\lambda} \tag{2.11}$$

where

$$K = 1 + [e^{-2L/\lambda}\{R_{end}-\lambda r_i\}/\{R_{end}+\lambda r_i\}] \tag{2.12}$$

Müller cells have a low input resistance, about 10MΩ, due almost exclusively to a large potassium conductance. The potassium conductance is very asymmetrically distributed, with 94% located in the terminal endfoot membrane and only 6% spread over the rest of the cell (Newman, 1984). Most of the experiments were carried out with 6mM barium in the superfusion solution to block the potassium channels (Newman, 1985). This was to minimise current noise and reduce the potassium currents flowing when the voltage was changed, which would cause large series resistance errors. In barium, Müller cells had a very high input resistance, typically 200-500MΩ. Application of glutamate causes a conductance increase, because the uptake current is voltage-dependent. Glutamate uptake is distributed fairly evenly over the cell, except for the endfoot membrane where there is less (Brew and Attwell, 1987).

I will consider the voltage profile expected in two basic cases: with the potassium conductance unblocked (no barium) and with the potassium conductance blocked by barium. In each case I will show what effect the application of glutamate will have.

Case 1: potassium conductance unblocked.

The input resistance of an isolated Müller cell is approximately 10MΩ (input conductance 10^{-7}S) in the absence of barium. Of this conductance, 94% (equivalent to 10.6MΩ), is in the endfoot and the remaining 6% (= 167MΩ) is distributed over the rest of the cell. Multiplying this resistance by the surface area of the cylinder (excluding one end-face) gives the specific membrane resistance

$$Rm = 167M\Omega \times 2.891 \times 10^{-9}m^2 = 0.482\Omega m^2$$

The resistivity of cytoplasm, R_i, is assumed to be 2Ωm. r_m and r_i are related to R_m and R_i as follows

$$r_m = R_m/(2\pi \times 4.5 \times 10^{-6}m) = 17k\Omega m$$
$$r_i = R_i/(\pi\ (4.5 \times 10^{-6})^2) = 3.14 \times 10^{10}\Omega m^{-1}$$

thus the space constant under these conditions is

$$\lambda = \sqrt{}(r_m/r_i) = 736\mu m$$

The resistance to ground is simply the endfoot resistance: $R_{end} = 10.6M\Omega$. Using eqns (2.6) and (2.10) to find A and B gives $A = -0.395V_0$, $B = 1.395V_0$ and the following function for the voltage

$$V = V_0\{-0.395\exp(x/7.36x10^{-6}) + 1.395\exp(-x/7.36x10^{-6})\}$$

When $x = 100\mu m$ (ie. with the patch electrode attached at the end opposite the low resistance endfoot), $V = 0.765V_0$. Thus, the maximum voltage drop along the Müller cell under these conditions will be 23.5%.

Adding glutamate will increase the conductance of the non-endfoot membrane. The glutamate evoked conductance is approximately ohmic negative to -20mV (Brew and Attwell, 1987). The largest glutamate-evoked current at -40mV (the normal experimental holding potential) was about 400pA, giving a conductance of 10^{-8}S. Combining this with 6% of the potassium conductance gives a new R_m of $0.181\Omega m^2$ and a new r_m of $6.39k\Omega m$. Working through the same calculations with this new value (the others being unchanged) yields a voltage drop of 24.5%, so application of glutamate changes the voltage non-uniformity by a small fraction only.

Case 2: potassium conductance blocked by barium.

In the presence of barium the input resistance of a Müller cell is 200MΩ or greater. I will assume that this is uniformly distributed over the cell membrane. The product of the input resistance and the total surface area of the cylinder gives the following estimate of R_m

$$R_m = 200M\Omega \times 2.95 \times 10^{-9}m^2 = 0.591\Omega m^2$$

and hence $r_m = 20.9k\Omega m$. R_{end} becomes 9.3GΩ. Following the same procedure as before, the voltage drop over the length of the cell is about 0.8%. Addition of glutamate, evoking the same magnitude and distribution of conductance change as above, increases the voltage drop to 2.3%.

In summary, in the presence of barium the voltage non-uniformities expected are trivial. In the absence of barium the voltage non-uniformity is significant, amounting to some 25% at the endfoot, but the voltage profile is only negligibly altered by the application of glutamate. Only a few experiments were performed without barium and the conclusions of these do not depend on a uniform voltage profile, requiring only an unchanging profile for validity.

2.9 Data analysis

Most of the parameters required (eg. peak glutamate-evoked current, rate of change of fluorescence) could be measured directly from chart recordings. Three parameters, the input resistance, series resistance and membrane capacitance were obtained from analysis of the current response to 10 or 20mV voltage-clamp steps. The steps were applied at the beginning of recording from each cell and whenever else required. The current transients (a typical transient is shown in Fig. 2.2A) were later analysed with the aid of a computer program. The data were played back into a PDP/11 (DEC) via an analogue to digital converter (Cambridge Electronic Design, CED 502).

The cell membrane in series with the pipette resistance can be represented by the circuit shown in Fig. 2.2B. The current flow through this circuit in response to a voltage step has the form of an exponential decay

Fig. 2.2. Capacity transient analysis. **A.** Current flowing in a whole-cell clamped Müller cell in response to a 20mV step depolarisation from -83mV. I_b and I_∞ are the steady-state currents before and during the step, respectively. **B.** Circuit equivalent to a whole-cell clamped cell. R_s is the series resistance, R_m the membrane resistance and C_m the membrane capacitance. V is the holding potential. **C.** Semilogarithmic plot of $I-I_\infty$ vs t, time after voltage step imposition, produced by computer analysis of the transient in A. The regression line was fitted by the analysis program. The triangular symbol marks τ, the time constant of the current relaxation. For the transient shown (which was typical), the parameters obtained were: $R_s = 2M\Omega$, $R_m = 425M\Omega$ and $C_m = 257pF$.

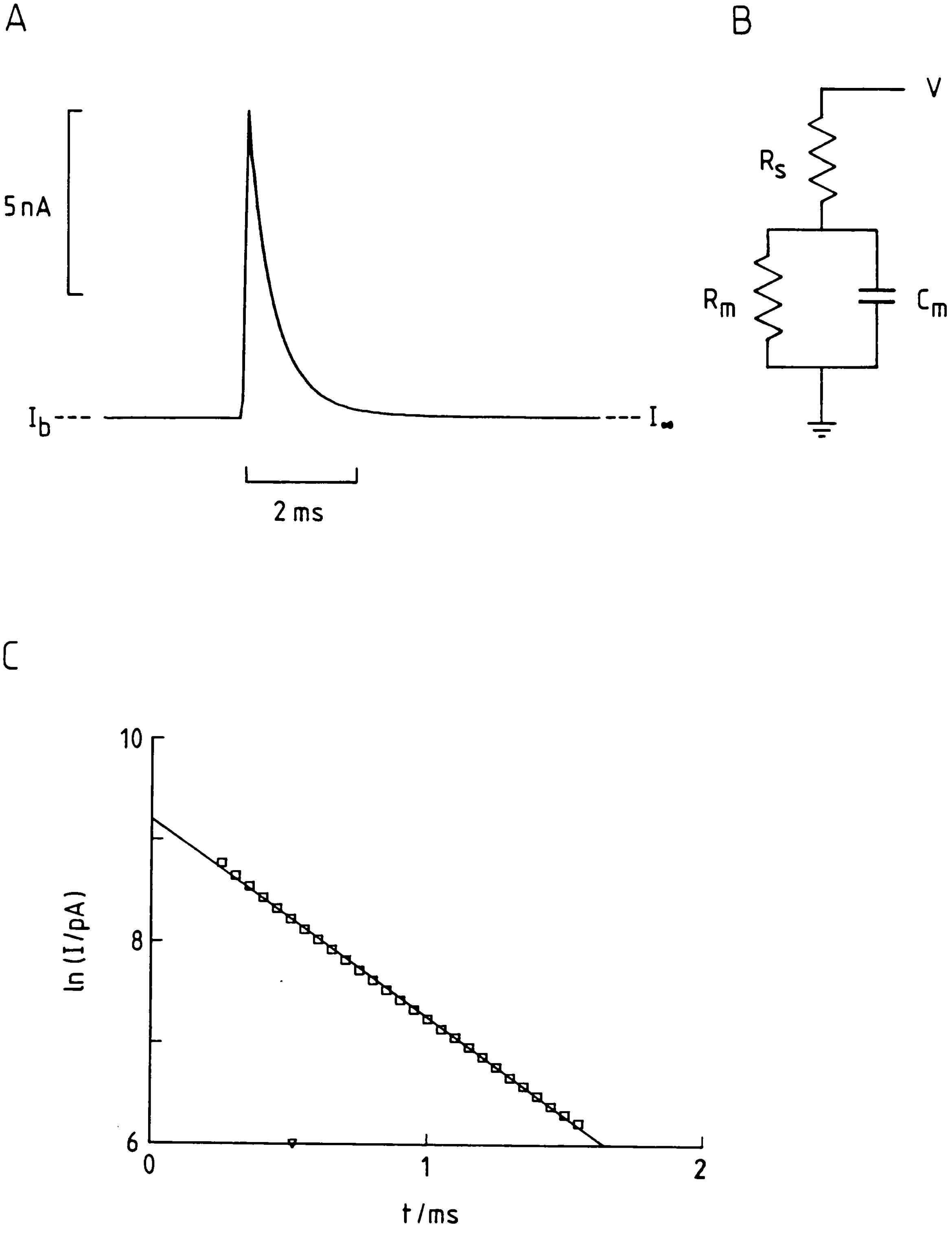
A
5nA
Ib
I∞
2 ms
B
V
Rs
Rm
Cm
C
10
8
6
0
1
2
ln(I/pA)
t/ms

$$I(t) = V\{1 + (R_m/R_s)e^{-t/\tau}\}/(R_m + R_s)$$

where V = magnitude of the voltage step
R_m = input resistance
R_s = series resistance
$\tau = C_mR_mR_s/(R_m+R_s)$
$t = 0$ at the onset of the voltage step.

The program allowed, by positioning of cursors, the input of the baseline current before the pulse (I_b), I_∞ (the steady-state current at the end of the pulse) and the best estimate of t_0 - taken as the time at which the current first started to rise.

$I-I_\infty$ was plotted against time on a semilogarithmic plot (as in Fig. 2.2C). The (typical) good fit to a single exponential confirms that the equivalent circuit in Fig. 2.2B is a good approximation. Rs was obtained from

$$R_s = V/I_0$$

where I_0 is the extrapolated current ($I-I_b$) at t=0. R_m was obtained from

$$R_m = \{V/(I_\infty-I_b)\} - R_s$$

and the capacitance from the time constant of the current relaxation

$$C_m = \tau(R_m+R_s)/R_mR_s.$$

Variation of surface area between cells will cause variation in the magnitude of the uptake current. Such variation will complicate comparison of current magnitudes from different cells. To reduce this variation, current magnitudes were often normalised by cell capacitance. Fig. 2.3 shows a plot of uptake current magnitude as a function of cell capacitance and demonstrates a clear correlation

Fig. 2.3. The glutamate uptake current is correlated with cell surface area. A plot of the magnitude of the inward current evoked by 30μM glutamate at -43mV as a function of cell capacitance (assumed to be proportional to membrane area). Each point represents one cell; there are 44 in total. The straight line is a least-squares best fit, constrained to pass through the origin: without this constraint the best-fit straight line was only slightly different, intersecting the capacitance axis at 12pF. External solution D, pipette solution W with 95mM [K] (y=95).

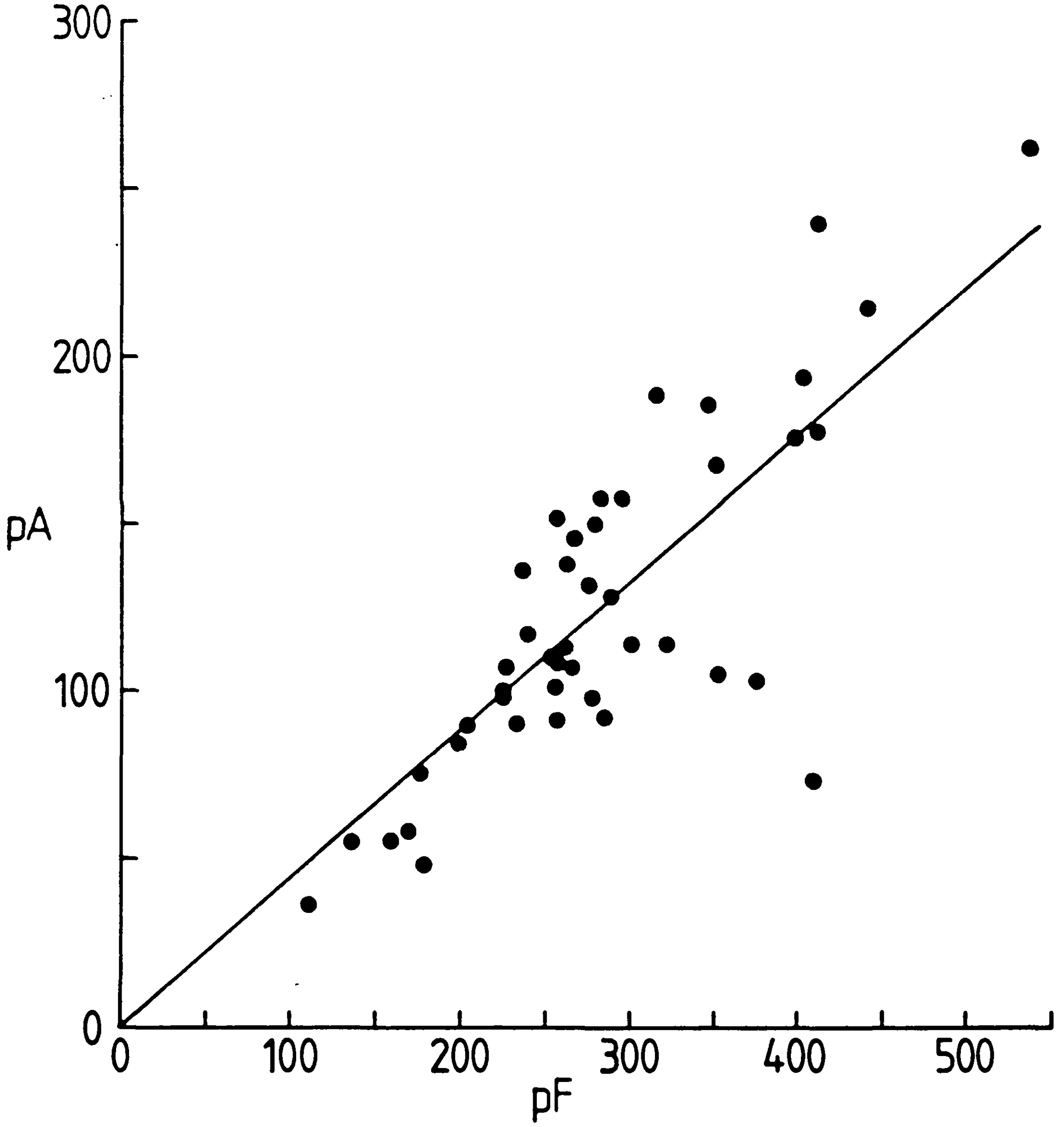
300
200
100
0
pA
0
100
200
300
400
500
pF

between these two parameters, justifying the normalisation procedure. The fractional variation (standard deviation/mean) of the normalised currents is about half that of the un-normalised current magnitudes.

Results in this thesis are presented as the mean ± standard error of the mean (SEM), unless otherwise stated. In a number of experiments the ratio of the mean of two small samples was compared with other similarly obtained ratios. In these cases, the ratio is given with the standard deviation (SD), calculated by the following formula.

$$\sigma = \frac{x_1}{x_2}\sqrt{\left(\frac{\sigma_1^2}{x_1^2} + \frac{\sigma_2^2}{x_2^2}\right)}$$

where x_1 and σ_1 are the mean and standard deviation of one of the samples.

Table 2.1

Extracellular solutions A-E

Solution use

A	storage and washing
B	standard external solution
C	vary $[Na]_o$
D	zero $[K]_o$
E	vary $[K]_o$

	Solution				
	A	**B**	**C**	**D**	**E**
NaCl	105	105	x	105	50
KCl	2.5	2.5	2.5	0	y
choline Cl	0	0	105-x	0	57-y
HEPES	5	5	5	5	5
$CaCl_2$	3	3	3	3	3
$MgCl_2$	0.5	0.5	0.5	0.5	0.5
D-glucose	15	15	15	15	15
$BaCl_2$	0	6	6	6	6
NaOH	2	2	2	2	2

All concentrations are in mM and the pH of all solutions was 7.3.

Table 2.2

Extracellular solutions F-I

For replacement of Na_o by different monovalent cations

	Solution			
	F	**G**	**H**	**I**
monovalent Cl	NaCl 105	LiCl 105	KCl 105	CsCl 105
$MgCl_2$	0.5	0.5	0.5	0.5
$CaCl_2$	3	3	3	3
HEPES	5	5	5	5
D-glucose	15	15	15	15
$BaCl_2$	6	6	6	6
KOH	2	2	2	2

All concentrations are in mM and the pH of the solutions was 7.3.

Table 2.3

Extracellular solutions J & K

Solution use

J Cl_o replaced by gluconate
K   change $[K]_o$ at low $[Na]_o$

	Solution		
	J		**K**
Na gluconate	105	NaCl	25
K gluconate	2.5	KCl	57 or 2.5
		choline Cl	25 or 79.5
HEPES	5	HEPES	5
$Mg(gluconate)_2$	0.5	$MgCl_2$	0.5
$Ca(gluconate)_2$	3	$CaCl_2$	3
$Ba(gluconate)_2$	6	$BaCl_2$	6
D-glucose	15	D-glucose	15
NaOH	0.8	NaOH	2

All concentrations are in mM and the solution pH was 7.3.

Table 2.4

Pipette filling solutions Z-W

Solution use

Z,Y	standard internal solutions
X	vary $[Na]_i$
W	vary $[K]_i$

	Solution			
	Z	**Y**	**X**	**W**
KCl	80	95	-	y
K acetate	15	-	-	-
NaCl	5	5	x	-
choline Cl	-	-	100-x	100-y
K_2EGTA	5	5	5	-
Na_2EGTA	-	-	-	5
Na_2ATP	5	5	-	-
MgATP	-	-	5	5
HEPES	5	5	5	5
$MgCl_2$	7	7	7	7
$CaCl_2$	1	1	1	1
	KOH 16	KOH 14	KOH 14	NaOH 14
junction potential	-3mV	-3mV	+1mV (x=0) -1mV (x=100)	+1mV (y=0) -3mV (y=100)
with sol^n	B	B	B	D

All concentrations are in mM and the pH of all solutions was 7.0.

Table 2.5

Pipette filling solutions V-T

Solution use

V Cl_i replaced by gluconate

U,T replacement of some Cl_i by glutamate at varying $[Na]_i$

		Solution		
	V		**U**	**T**
K gluconate	95	KCl	55	0
		K glutamate	0	55
Na gluconate	5	NaCl	x	x
		choline Cl	40-x	40-x
K_2EGTA	5	K_2EGTA	5	5
HEPES	5	HEPES	5	5
Na_2ATP	5	MgATP	5	5
$Mg(gluconate)_2$	7	$MgCl_2$	7	7
$Ca(gluconate)_2$	1	$CaCl_2$	1	1
KOH		KOH	13	13
junction potential	-7mV		-2mV	-5mV
with sol^n	B		B	B

All concentrations are in mM and the pH of all solutions was 7.0.

Table 2.6

Pipette filling solution S

For replacement of K_i by Rb or Cs

	S
KCl or RbCl or CsCl	95
Na_2EGTA	5
HEPES	5
MgATP	5
$MgCl_2$	2
$CaCl_2$	1
NaOH	11
junction potential	-3mV
with sol^n	D

All concentrations are in mM and the solution pH was 7.0.

Table 2.7

Pipette filling solutions R-P

For fluorescence measurements

R	standard internal solution for fluorescence measurements
Q	90mM $[K]_i$
P	zero $[K]_i$

	Solution		
	R	**Q**	**P**
KCl	85	90	0
choline Cl	-	0	90
NaCl	5	-	-
K_2EGTA	5	-	-
Na_2EGTA	-	5	5
Na_2ATP	5	-	-
MgATP	-	5	5
HEPES	5	5	5
$MgCl_2$	7	2	2
$CaCl_2$	1	1	1
NAD	5	5	5
malonate	0.1	0.1	0.1
2-deoxyglucose	20	20	20
KOH	17	16	16
junction potential	-3mV	-3mV	+1mV
with sol^n	B	D	D

All concentrations are in mM and the pH of all solutions was 7.0.

Table 2.8

Pipette filling solution O

$[Ca^{2+}]_i$ buffered to different values

		O	
free $[Ca^{2+}]$	10^{-8}M	10^{-7}M	10^{-6}M
NaCl	5	5	5
$CaCl_2$	0.39	3.35	13.4
$MgCl_2$	9.15	8.75	7.4
HEPES	5	5	5
MgATP	5	5	5
$K_{2.5}$EGTA	20	20	20
KOH	11.3	18.3	38.5
KCl	54.9	48.8	30.0
total [K]	115.8	116.7	118.1
total [Cl]	79.0	78.0	76.6
junction potential (soln B)		-4mV	

Unless otherwise stated, concentrations are in mM; the pH of the solution was 7.0.

Chapter 3

The ionic dependence of glutamate uptake

3.1 Introduction

This chapter describes investigations of the ionic dependence of glutamate uptake. The effects of changes of the extracellular and intracellular concentrations of a variety of ions were studied. A particular aim of the experiments was to determine which ions are translocated by the glutamate uptake carrier, in order to help determine the stoichiometry of the uptake process. Glutamate uptake was measured as the inward membrane current evoked by glutamate in whole-cell clamped isolated Müller cells (see Introduction, section 1.6, and Methods).

3.2 Dependence on external sodium and related ions

Brew & Attwell (1987) reported that complete replacement of external sodium by choline abolished the glutamate-evoked current. In Fig. 3.1A-C are shown experiments in which the external sodium was completely replaced by various monovalent cations: lithium, potassium and caesium (extracellular solutions F, G, H and I; intracellular solution Y). The glutamate-evoked current was much smaller in these solutions than with sodium present. The relative amplitudes (mean ± SEM) of the currents evoked at -43mV by 30μM glutamate in the presence of the different cations were $I_{Na} : I_{Li} : I_{K} : I_{Cs} : I_{choline} = 1 : 0.011 \pm 0.002$ (n=4): 0.008 ± 0.008 (n=4): 0 (n=3): 0 (n=7). Thus, as has been found for the uptake of radiolabeled glutamate into synaptosomes (Kanner & Sharon, 1978a), activation of the uptake current in glial cells by external cations is highly selective for external sodium.

Fig. 3.1 Dependence of glutamate uptake on external monovalent cations. **A** Membrane current of a Müller cell at -43mV during repeated application of 30μM glutamate in the superfusate (timing shown by black bars at bottom), and while sodium ions in the external solution were completely replaced by lithium (top bar). **B** Similar experiment to that in **A**, but with external Na replaced by K. Raising the external potassium concentration generates a large inward current, presumably through the small fraction of potassium channels that remain unblocked by 6mM barium (although the slow onset of this current is not understood). **C** Similar experiment to that in **A** but with Na replaced by Cs. Lithium, potassium and caesium support very little uptake current. **D** The dependence of uptake current (produced by 30μM glutamate at -43mV) on external sodium concentration (sodium replaced by choline). Data (mean ± SEM) from 3, 5, 11 & 5 cells in 10, 20, 30 & 50mM $[Na]_o$, normalised to the response in 107mM $[Na]_o$. Continuous curve through the points is the cube of a Michaelis-Menten relation, ie. $V_{max}\{[Na]_o/([Na]_o+K)\}^3$, with V_{max}=1.77, K=22.5mM. Dashed curve is a Hill plot with the form $V_{max}\{[Na]_o\}^2/(\{[Na]_o\}^2+K^2)$, where V_{max}=1.218 and K=50mM.

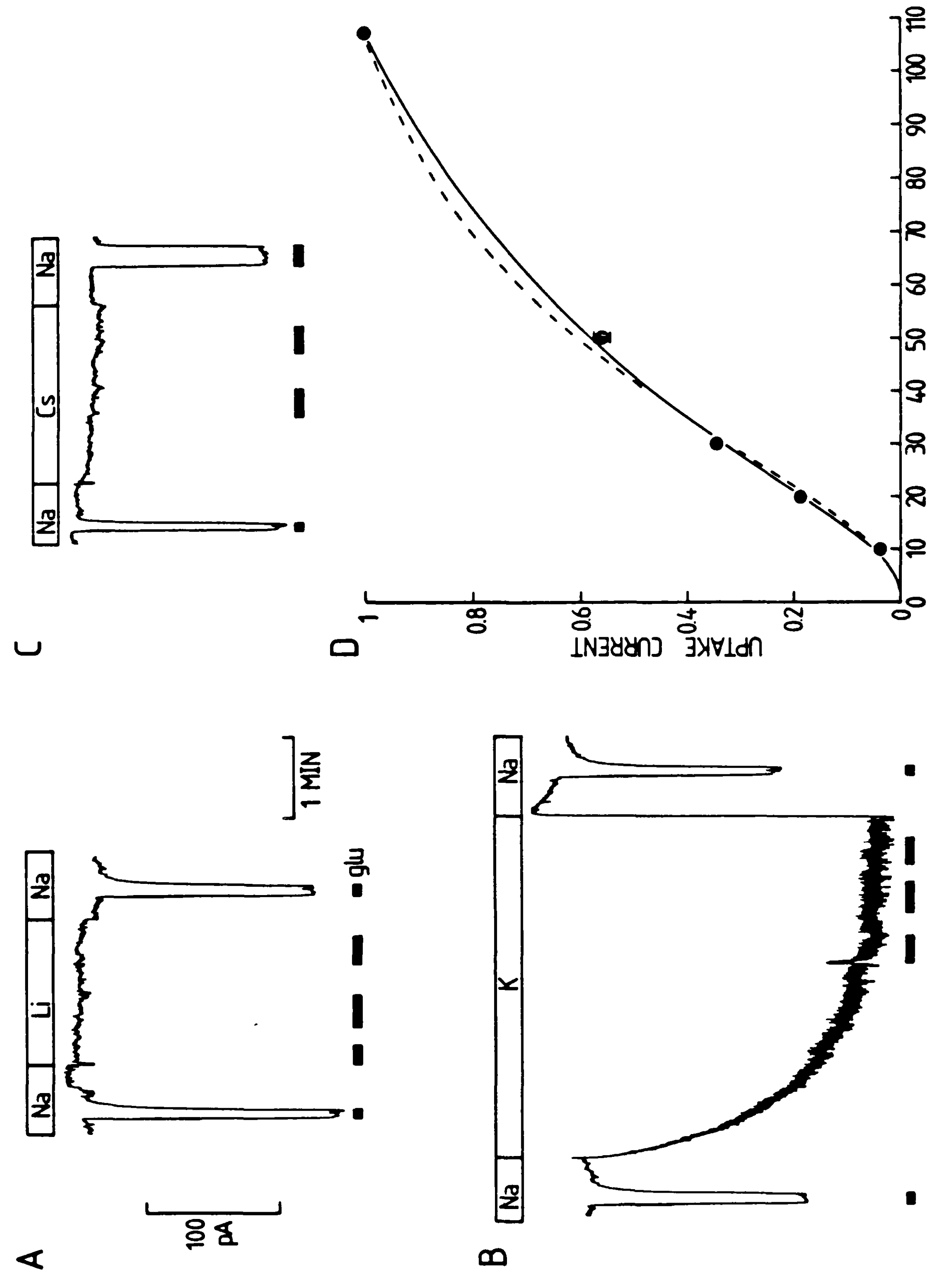
A
100 pA
1 MIN
Na
Li
Na
glu
B
Na
K
Na
C
Na
Cs
Na
D
UPTAKE CURRENT
0
0.2
0.4
0.6
0.8
1
$[Na]_o$ mM
0
10
20
30
40
50
60
70
80
90
100
110

The dependence of the current on external sodium concentration (sodium replaced by choline; external solution C; 30μM glutamate; -43mV) is plotted in Fig. 3.1D. At low external sodium concentrations the current depends on $[Na]_o$ in a sigmoid manner, suggesting that more than one Na^+ ion is transported by each carrier 'cycle'. The data could roughly be fitted by a power of a Michaelis-Menten relation, or by the Hill equation (see Fig. 3.1D legend), but the glutamate-evoked currents recorded below 10mM $[Na]_o$ were too small to determine accurately whether the current is proportional to the 2nd, 3rd or a higher power of $[Na]_o$.

3.3 Dependence on internal sodium

Since the glutamate uptake carrier transports sodium into the cell (Stallcup et al, 1979; Baetge et al, 1979), one would expect that raising the sodium concentration inside the cell (by filling the patch pipette used for whole-cell recording with a high sodium concentration solution) would decrease the current evoked by glutamate. Figure 3.2A shows that this is indeed the case. It shows the dependence of the uptake current on the internal (pipette) sodium concentration. Raising the internal sodium inhibits the uptake current. For these experiments a range of pipette solutions with different [Na] were used (solution X with [Na] = x = 0, 15, 40, 60 or 100mM; [K] was 25mM in this solution). For each value of sodium concentration in the patch pipette, the response to 30μM glutamate at -40mV (external solution B) was measured in 5 cells. After normalising by cell capacitance (see Methods), the mean current/capacitance thus obtained was then divided by the mean current/capacitance obtained in 5 cells studied with 0mM $[Na]_{pipette}$ on the same day. When the sodium concentration in the pipette was large, the glutamate response was smaller, with a reduction to one half occurring at approximately $[Na]_{pipette}$ = 60mM.

__Fig. 3.2__ Inhibition of glutamate uptake by internal (patch pipette) sodium. **A** Increasing the internal sodium concentration (replacing choline) decreases the glutamate-evoked current in cells clamped to -40mV. Data shown are mean ± SD for 5 cells at each value of $[Na]_{pipette}$ relative to 5 cells studied with 0mM $[Na]_{pipette}$. **B** Specimen I-V relations for the current induced by 30μM glutamate in one cell studied with 0mM $[Na]_{pipette}$ and in another with 100mM $[Na]_{pipette}$. Data are normalized by the capacitance of each cell (423pF and 360pF for the 0mM and 100mM $[Na]_{pipette}$ cells respectively).

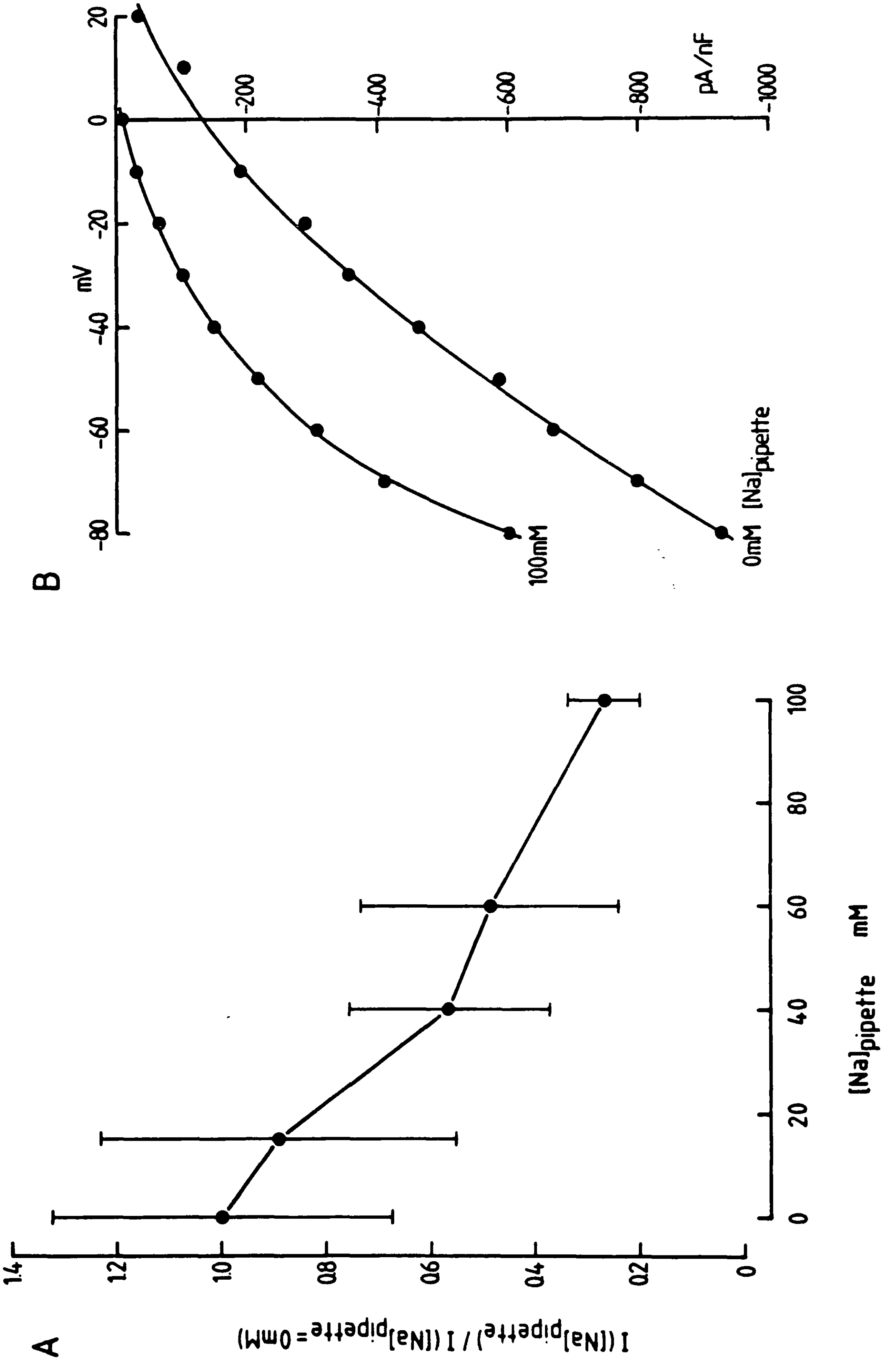
A
I ([Na]pipette) / I ([Na]pipette = 0mM)
1.4
1.2
1.0
0.8
0.6
0.4
0.2
0
0
20
40
60
80
100
[Na]pipette mM
B
mV
-80
-60
-40
-20
0
20
pA/nF
-200
-400
-600
-800
-1000
100mM
0mM [Na]pipette

Raising internal sodium also alters the voltage-dependence of the glutamate-evoked current (Fig. 3.2B). High $[Na]_i$ produces a greater fractional suppression of uptake at depolarised potentials than at hyperpolarised potentials. A similar change in the shape of the I-V relation is observed when uptake is reduced by lowering the external sodium concentration (Brew & Attwell, 1987).

3.4 Inhibition by internal glutamate

A high concentration of glutamate inside the cell would be expected to reduce the current due to glutamate uptake: in this situation the uptake carrier will remain longer in the conformation to which glutamate is bound at the internal face, so return of the carrier to the outer membrane surface will be slowed. The effects of raising internal glutamate are also a check that the glutamate-evoked current is not due to glutamate-gated channels, as the internal glutamate concentration should not influence a current flowing through channels.

Figure 3.3A (lower panel) shows that when the sodium concentration in the patch pipette is 40mM, replacing 55mM KCl in the patch pipette by 55mM K-glutamate decreases by about 70% the current evoked by 30μM external glutamate at -44mV, consistent with a reduction of glutamate uptake as predicted above (the responses shown are from two cells and are typical of the mean responses from two groups of cells recorded with pipette solutions U and T with [Na] = x = 40mM; external solution B). Removal of internal chloride has no effect on the uptake current (see section 3.9), so the decrease of current seen is due to the addition of glutamate inside the cell. This result is confirmation that the glutamate-evoked current in Müller cells is due to electrogenic glutamate uptake and not due to glutamate-gated channels (see also Discussion, section 6.1).

Fig. 3.3 Inhibition of the glutamate-evoked current by intracellular glutamate depends on the internal sodium concentration. **A** Specimen records from 4 different Müller cells showing the effect on the current evoked at -44mV by 30μM glutamate (black bars) of raising the concentration of glutamate in the patch pipette (and hence presumably in the cell) from 0 (left pair of records) to 55mM (right pair of records), for a patch pipette sodium concentration of 2.5mM (top records) and 40mM (bottom records). Currents have been normalized by cell capacitance. **B** Dependence on pipette sodium concentration (abscissa) of the suppressive effect of internal glutamate. The ordinate is the ratio (mean ± SD) of the current evoked by 30μM glutamate when the pipette contained 55mM glutamate to that evoked with no glutamate in the pipette, ie. comparing the size of the left and right hand records in **A**. The smooth curve was fitted by eye and has the form of a modified Hill equation, $y = 95 - 70x^3 / \{x^3 + K^3\}$, where $x = [Na]_i$ and K = 10.4mM.

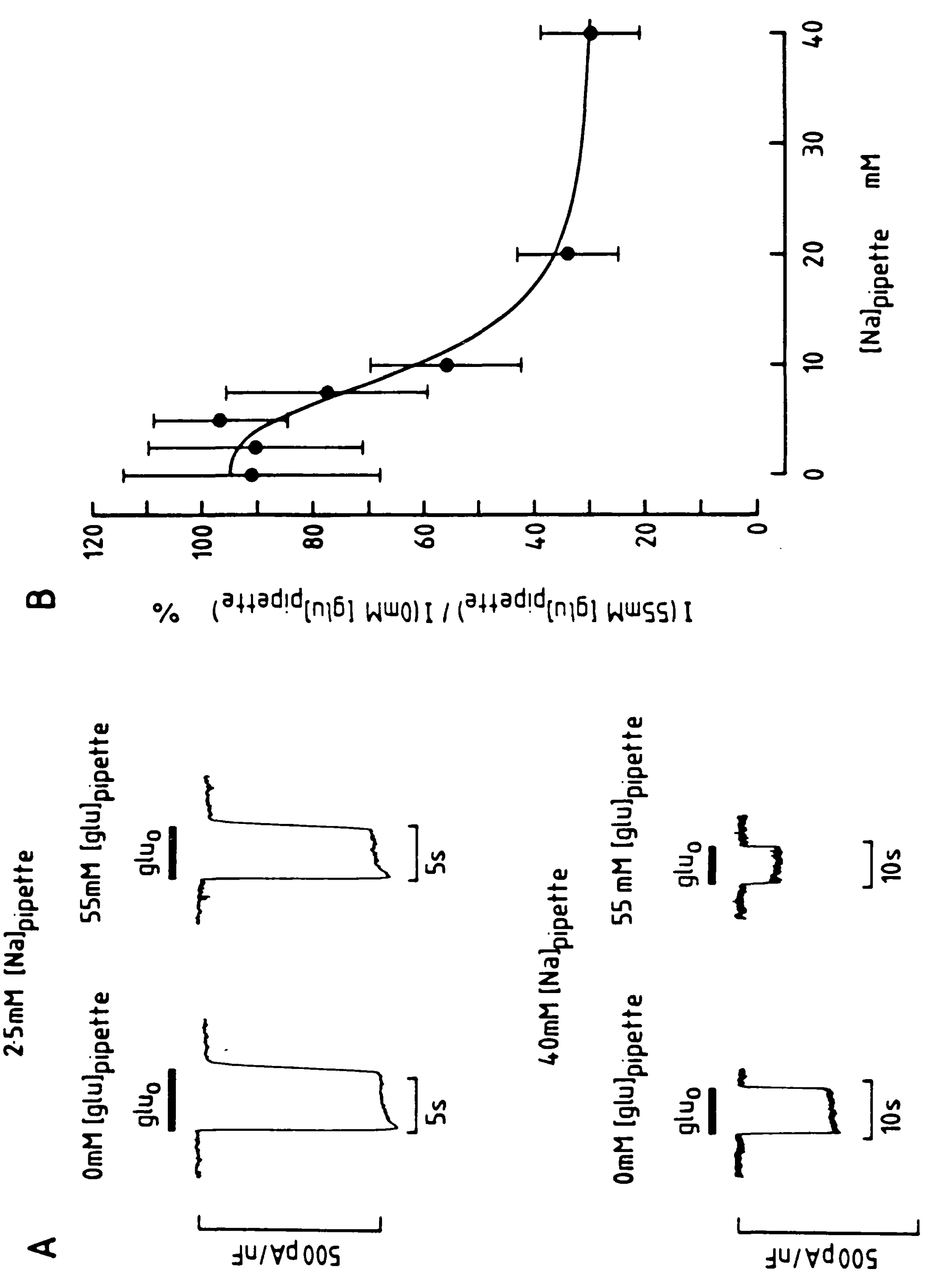
A
2·5mM [Na]pipette
0mM [glu]pipette
55mM [glu]pipette
gluo
5s
500pA/nF
40mM [Na]pipette
0mM [glu]pipette
55 mM [glu]pipette
gluo
10s
500pA/nF
B
I (55mM [glu]pipette) / I (0mM [glu]pipette) %
0
20
40
60
80
100
120
0
10
20
30
40
[Na]pipette mM

3.5 Interaction of internal sodium and glutamate

Changing the internal sodium concentration was found to have a dramatic effect on the suppression of the glutamate-evoked current by internal glutamate. Fig. 3.3A (bottom) compared the glutamate responses of two cells studied with or without 55mM glutamate in the pipette when $[Na]_{pipette}$ was 40mM. In contrast, at the top of Fig. 3.3A the same experiment is shown for two cells with only 2.5mM [Na] in the patch pipette (same solutions, but with $[Na]_{pipette} = x = 2.5mM$). In this situation, internal glutamate has almost no suppressive effect. Figure 3.3B shows the mean response with 55mM glutamate in the pipette relative to that with no glutamate in the pipette, as a function of $[Na]_{pipette}$ (solutions U and T with x = 0 to 40mM). The suppressive effect of internal glutamate increases in a sigmoid manner with $[Na]_{pipette}$, so that below 5mM $[Na]_{pipette}$ there is almost no suppression, but at higher $[Na]_{pipette}$ internal glutamate does reduce the response, reaching a maximum suppression of about 70% (i.e. $I\{55mM\ [glu]_{pipette}\}/I\{0mM\ [glu]_{pipette}\} = 0.3$) when $[Na]_{pipette} = 40mM$.

This interaction of the suppressive effects of internal sodium and glutamate would be very difficult to explain if the glutamate-evoked current were due to channels, but could be explained as a result of both sodium and glutamate being transported by the uptake carrier. One simple explanation of the result follows.

Assume that there is a strict order of unbinding of glutamate and sodium at the internal face of the carrier: glutamate unbinds before the sodium ions do. Assume further, that the sodium ions unbind rapidly and that the unbinding of the sodium ions changes the carrier conformation so that glutamate can no longer bind at the internal face. For internal glutamate to bind to the carrier and prevent its 'cycling' would require carriers with sodium bound at the internal face: this would only occur when the internal sodium concentration was high.

Fig. 3.4 The glutamate-evoked current declines with zero potassium in the pipette. Responses to 20μM glutamate get progressively smaller with time after going to whole-cell recording mode. Extrapolation of the glutamate-evoked current backwards in time suggests that much of the current decay occurs in the first 40s after patch rupture. Holding potential -39mV; pipette solution W with [K] = y = 0; external solution D.

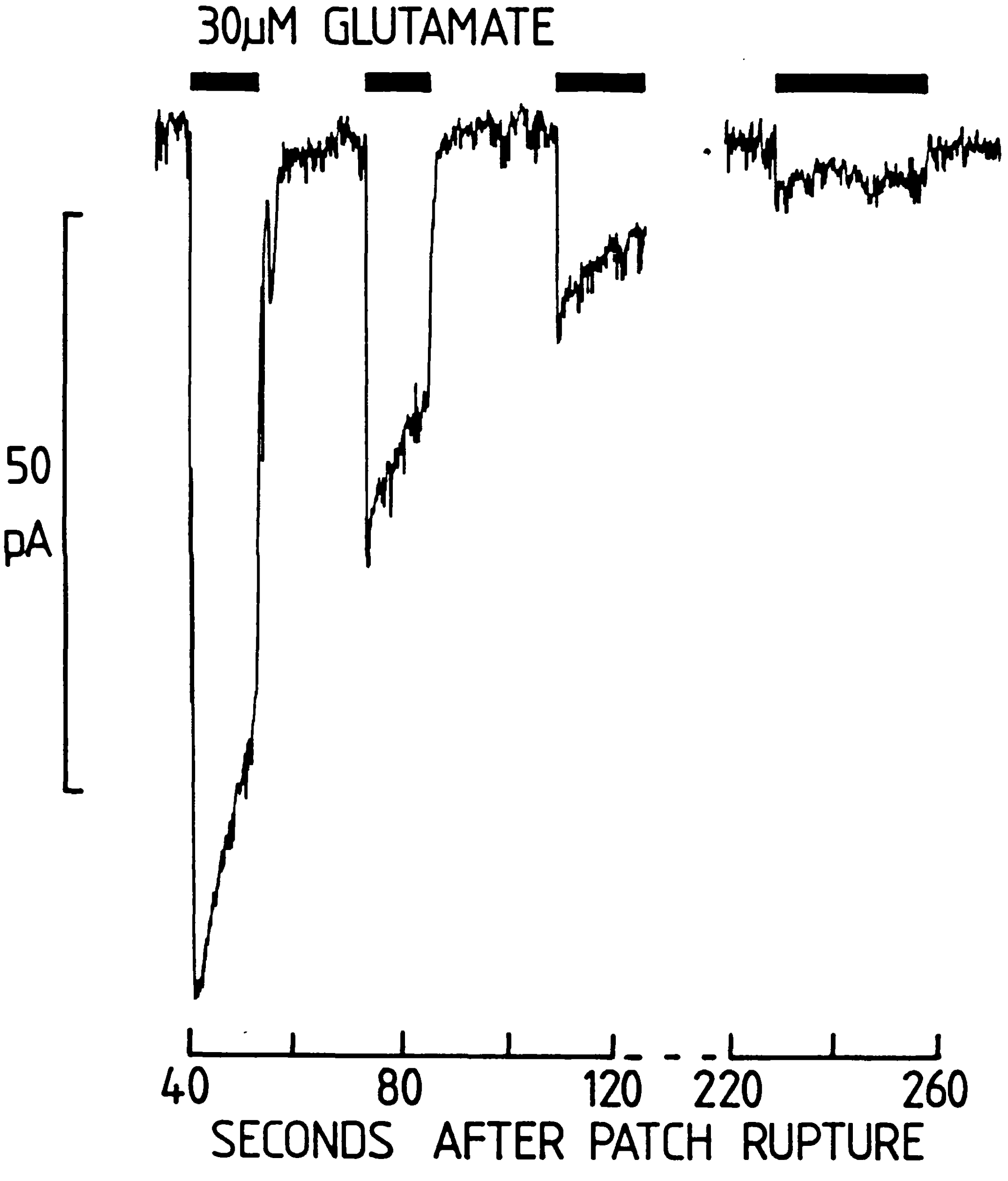
30μM GLUTAMATE
50
pA
40
80
120
220
260
SECONDS AFTER PATCH RUPTURE

3.6 Dependence on internal potassium and related ions

To determine the dependence of the uptake current on the internal potassium concentration, recordings were made from cells with pipettes containing potassium concentrations ranging from 95mM down to 0mM (potassium replaced by choline; solution W with y = 95 to 0). Potassium was omitted from the external solution (D), to prevent any potassium influx across the cell membrane from raising the intracellular concentration at low $[K]_{pipette}$. When $[K]_{pipette}$ was zero the glutamate-evoked current decreased to almost zero in the first few minutes following transition to whole-cell recording, presumably as the cell interior was dialysed by the pipette solution. This is seen in Fig. 3.4 which shows the responses to glutamate (20μM) of a cell whole-cell clamped with no potassium in the pipette. The timecourse of this decline was typical, with the response reaching a steady level after 3-4 minutes. Similar results were observed when pipette potassium was completely replaced with isotonic sucrose. This decline did not occur when $[K]_{pipette}$ was high, suggesting that intracellular potassium activates glutamate uptake in these cells.

Typical steady-state responses to 30μM glutamate with varying $[K]_{pipette}$ are shown in Fig. 3.5A. The current magnitudes have been normalised by cell capacitance. Although the glutamate-evoked current was small with no potassium in the patch pipette, it was still significantly greater than zero, either because the intracellular [K] had not been reduced to zero, or because some electrogenic uptake is possible in the absence of potassium. The dependence of the glutamate-evoked current on pipette potassium concentration approximately fits a Michaelis-Menten curve with an apparent K_m of 15mM (Fig. 3.5B), implying that the uptake carrier is activated by the binding of one potassium ion.

Fig. 3.5 Dependence of the glutamate-evoked current on $[K]_{pipette}$. **A** The currents (normalised by cell capacitance) evoked by 30μM glutamate in 4 cells voltage-clamped at -41mV with patch-pipettes containing solution W in which [K] = x = 0, 5, 20, 95mM. External solution D. **B** Mean current amplitudes (± SEM) from experiments like those in **A** plotted as a function of $[K]_{pipette}$. The figure by each point is the number of cells. The smooth line is a Michaelis-Menten curve with a K_m of 15mM.

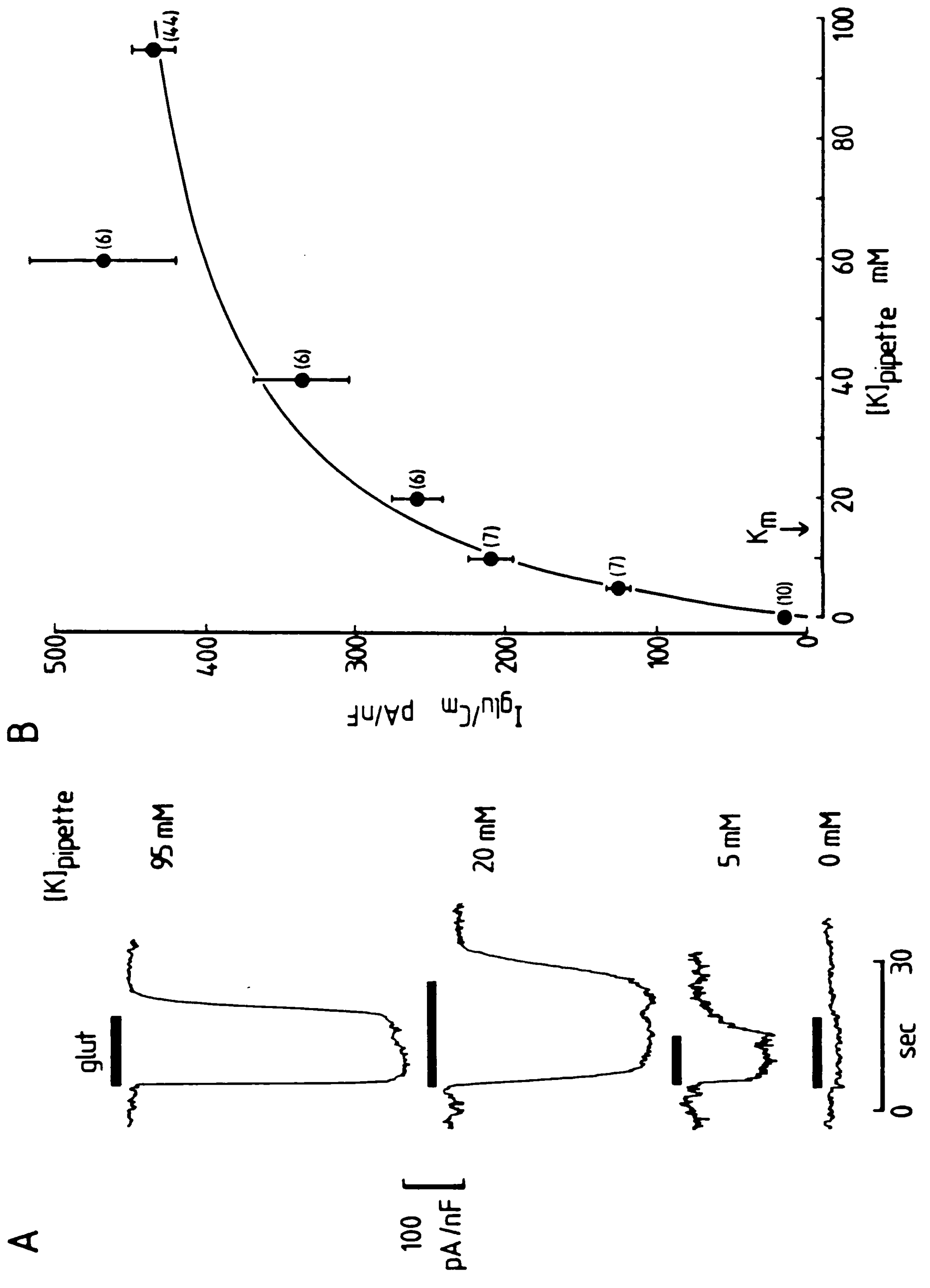
A
100 pA/nF
glut
[K]pipette
95 mM
20 mM
5 mM
0 mM
0 sec 30
B
I_{glu}/C_m pA/nF
0
100
200
300
400
500
(10)
(7)
(7)
(6)
(6)
(6)
(44)
K_m
0
20
40
60
80
100
$[K]_{pipette}$ mM

In similar experiments testing the $[K]_i$-dependence of the uptake current in salamander Müller cells, Schwartz & Tachibana (1990) showed data in which lowering $[K]_i$ from 90 to 9mM hardly altered the current evoked by D-aspartate (which is taken up by the same electrogenic carrier as L-glutamate). They concluded that glutamate uptake was not dependent on intracellular potassium. The results in Fig. 3.6 partially account for the apparent contradiction between the Schwartz & Tachibana results and those in Fig. 3.5. Fig. 3.6A was obtained by the same protocol as Fig. 3.5, except that 200μM L-glutamate and 200μM D-aspartate were used to probe the uptake current. The data show that the D-asp-evoked current is potassium-dependent. The D-asp-evoked current with 0 $[K]_{pipette}$ was 12% of that with 95mM $[K]_{pipette}$. The difference is significant ($P << 0.001$).

Fig. 3.6 shows two striking differences between the currents evoked by D-asp and L-glu. Firstly, the maximum D-asp-evoked current is much smaller than that for L-glu: the ratio (D-asp/L-glu) of the currents evoked by 200μM [amino acid] (an almost saturating dose) was 0.25 at 95mM $[K]_i$ and 0.21 when extrapolated to saturating $[K]_i$. Secondly, there is a marked difference in the $[K]_i$ required to activate $I_{L\text{-}glu}$ and $I_{D\text{-}asp}$. This is clearly seen in Fig. 3.6B, in which the data from Fig. 3.6A are replotted, normalised to their respective Michaelis-Menten maxima (see Fig. 3.6B legend). The apparent K_m values, obtained from the best-fit Michaelis-Menten curves, are 25.3mM for L-glu and 5.4mM for D-asp. This difference of affinity partially accounts for the apparent lack of $[K]_i$-dependence of the $I_{D\text{-}asp}$ observed by Schwartz & Tachibana (see Discussion, section 6.4).

Activation of the glutamate-evoked current by other internal cations was studied using the same external solution (D), and internal solution S in which 95mM KCl was replaced by 95mM CsCl, RbCl or 100mM choline-Cl (solution W with $y = 0$). Caesium and rubidium were found to be effective activators of the uptake current (Fig. 3.7).

Fig. 3.6 Comparison of the $[K]_i$-dependence of the currents evoked by L-glutamate and D-aspartate. **A** Plot of the mean (± SD) current (normalised by capacitance) evoked at -41mV by 200μM L-glu (filled circles) and 200μM D-aspartate (open circles) as a function of $[K]_{pipette}$. The number of cells studied was n=4 (5mM & 40mM [K]), 5 (0 & 10mM [K]) or 9 (95mM [K]). External solution D; pipette solution W with x = 0, 5, 10, 40 and 95. The two sets of data are fitted by Michaelis-Menten curves (best-fit parameters obtained from Eadie-Hoftsee transformations of the data) with K_m = 25.3mM, $(I/C)_{max}$ = 0.995pA/pF for L-glu and K_m = 5.4mM, $(I/C)_{max}$ = 0.205pA/pF for D-asp. **B** Data from **A** replotted after normalisation to the respective $(I/C)_{max}$ values for L-glu and D-asp, obtained from the best-fit Michaelis-Menten equations.

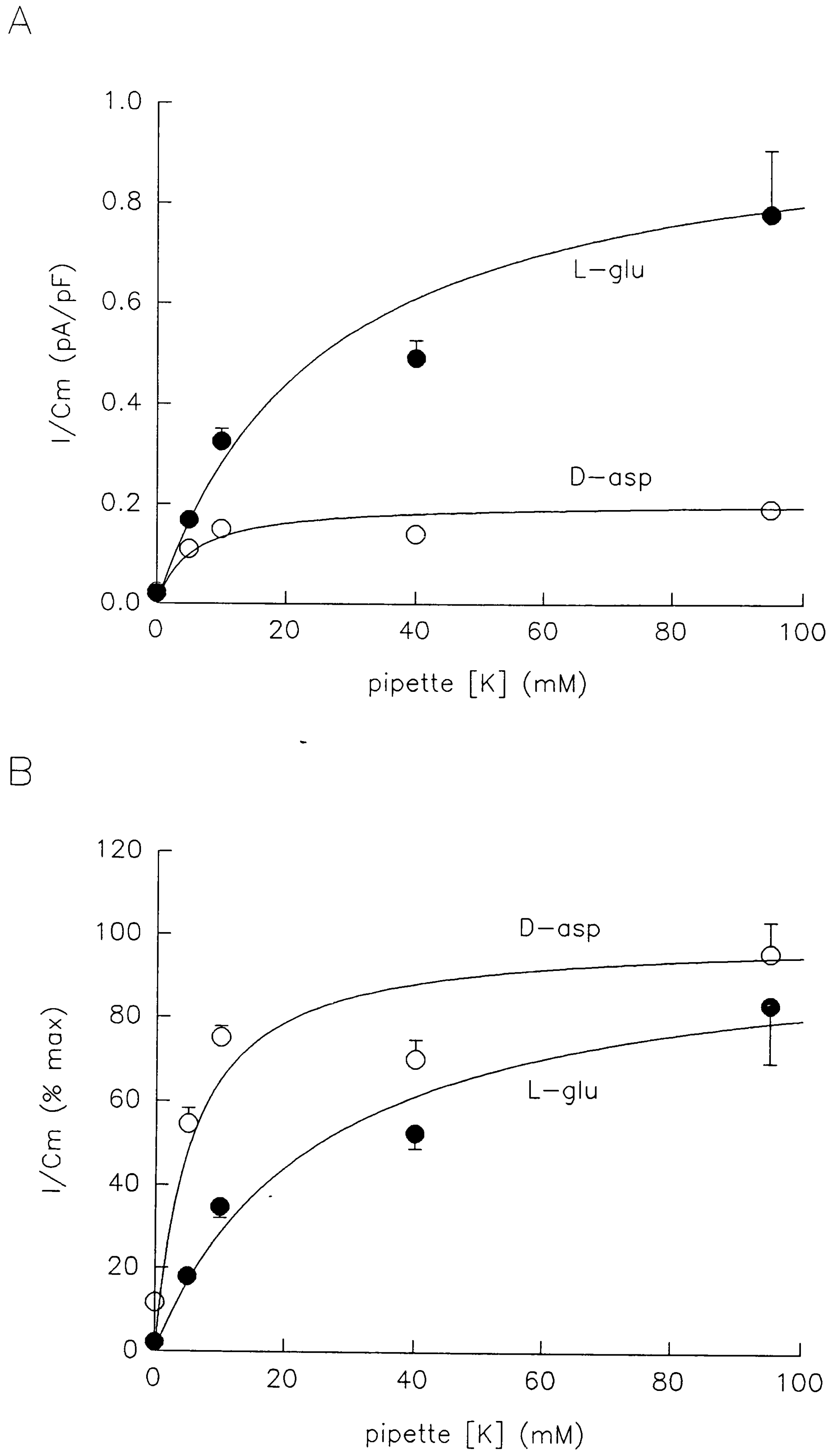
A
1.0
0.8
0.6
0.4
0.2
0.0
I/Cm (pA/pF)
L−glu
D−asp
0
20
40
60
80
100
pipette [K] (mM)
B
120
100
80
60
40
20
0
I/Cm (% max)
D−asp
L−glu
0
20
40
60
80
100
pipette [K] (mM)

Fig. 3.7 Specimen records showing that with all the internal (patch pipette) potassium replaced by rubidium (top) or caesium (bottom), 30μM glutamate (black bars) still produces a substantial uptake current at -43mV. External solution D and internal solution S.

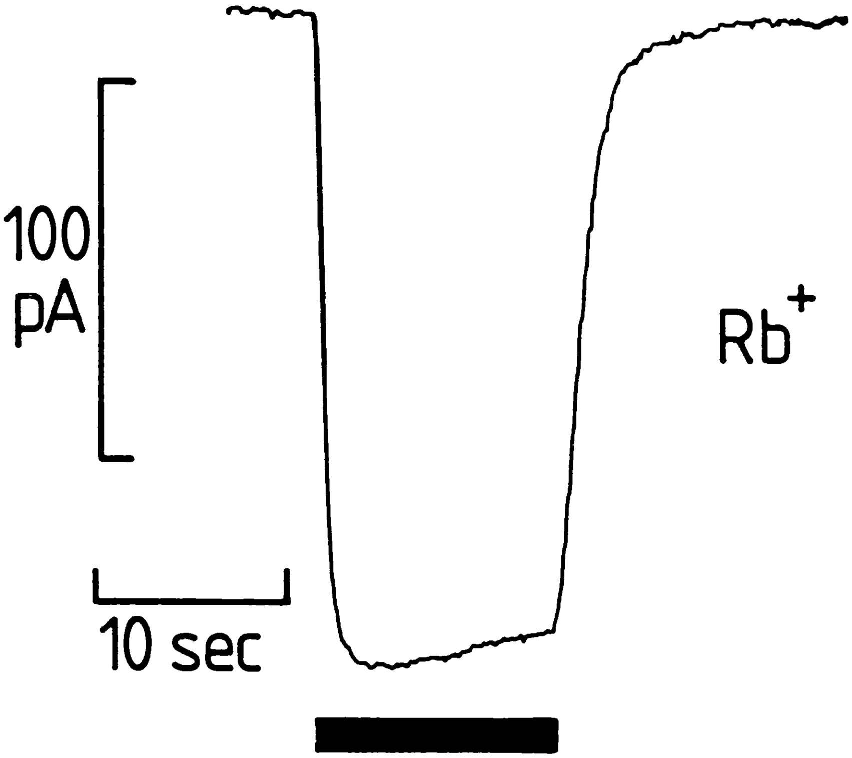
100
pA
10 sec
Rb$^+$

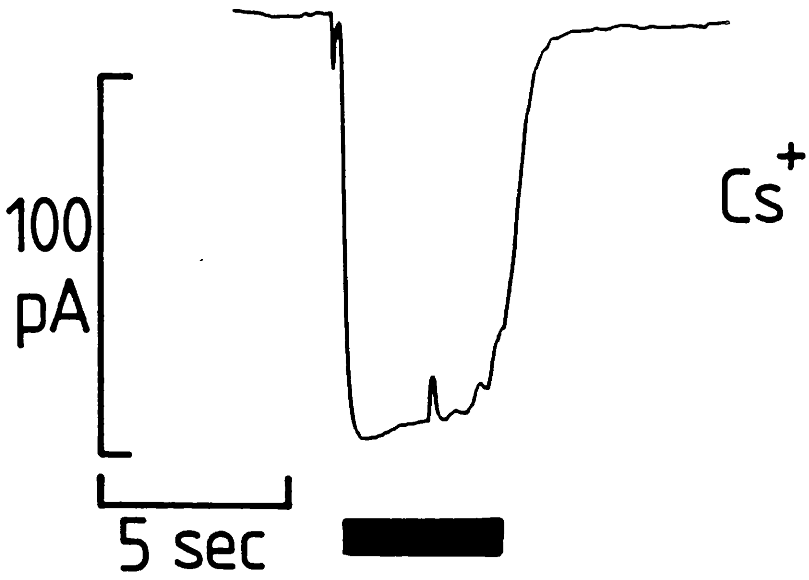
100
pA
5 sec
Cs$^+$

At -43mV, 30μM glutamate produced currents (normalised by cell capacitance) with the different cations of relative magnitudes (mean ± SD) $I_K : I_{Rb} : I_{Cs} : I_{choline} = 1 : 0.86 \pm 0.14$ (n=4) : 0.66 ± 0.17 (n=4) : 0.04 ± 0.03 (n=10).

These results show that internal potassium has a direct effect on the uptake carrier (ie. not mediated by a change of potential since this was held constant). There are two alternative mechanisms which could mediate the effect. One possibility is that potassium is indeed transported out of the cell by the glutamate carrier. Another possibility, however, is that potassium binds to the internal face of the carrier and allosterically modifies its properties without being transported. If the latter possibility were the case, there are a number of properties which could be modified to reduce the uptake current. A reduced affinity of the carrier for glutamate or sodium, would decrease the uptake current, as could a change in the voltage-dependence of uptake. These hypotheses are tested below. A final possibility, that the decreased uptake current reflects a reduction of the ratio of charge transported to glutamate transported, is tested in chapter 5.

3.7 The effects of reducing $[K]_i$ on the affinity for $[glu]_o$ and $[Na]_o$, and on the voltage-dependence of glutamate uptake

Glutamate dose-response curves for the current evoked by glutamate at -41mV are shown in Fig. 3.8A for 7 cells with 95mM $[K]_{pipette}$ (filled symbols) and 8 cells with 5mM $[K]_{pipette}$ (open symbols). The data are plotted normalised to the current evoked by 1mM glutamate. Both sets of data were fitted with Michaelis-Menten curves and a comparison of the parameters for 95mM $[K]_{pipette}$ (the apparent K_m for glutamate was 8.3μM) and 5mM $[K]_{pipette}$ (apparent K_m 5μM) reveals that lowering the internal potassium concentration increases the apparent affinity for glutamate, so this cannot underlie the decreased magnitude of the uptake current.

Fig. 3.8 Lowering the internal potassium concentration does not decrease the carrier's affinity for external glutamate or sodium. **A** Dose-response curves (mean ± SEM) for the current evoked by glutamate at -41mV, for 7 cells studied with 95mM $[K]_{pipette}$ (filled symbols) and 8 cells with 5mM $[K]_{pipette}$ (open symbols). The Michaelis-Menten curves are normalised to the current produced by 1mM glutamate. For 95 and 5mM $[K]_{pipette}$ the apparent K_m was 8.3 and 5μM respectively. Pipette solution W with $[K]_{pipette}$ = y = 95 and 5mM; external solution D. **B** Dependence of the current evoked by 30μM glutamate at -41mV on the external sodium concentration (Na replaced by choline), when $[K]_{pipette}$ was 95mM (filled symbols) and 5mM (open symbols). Averaged data (± SEM, number of cells shown by each point), normalised to the current obtained when $[Na]_o$ = 107mM. Pipette solutions as in **A**; external solution C, but with the 2.5mM KCl omitted.

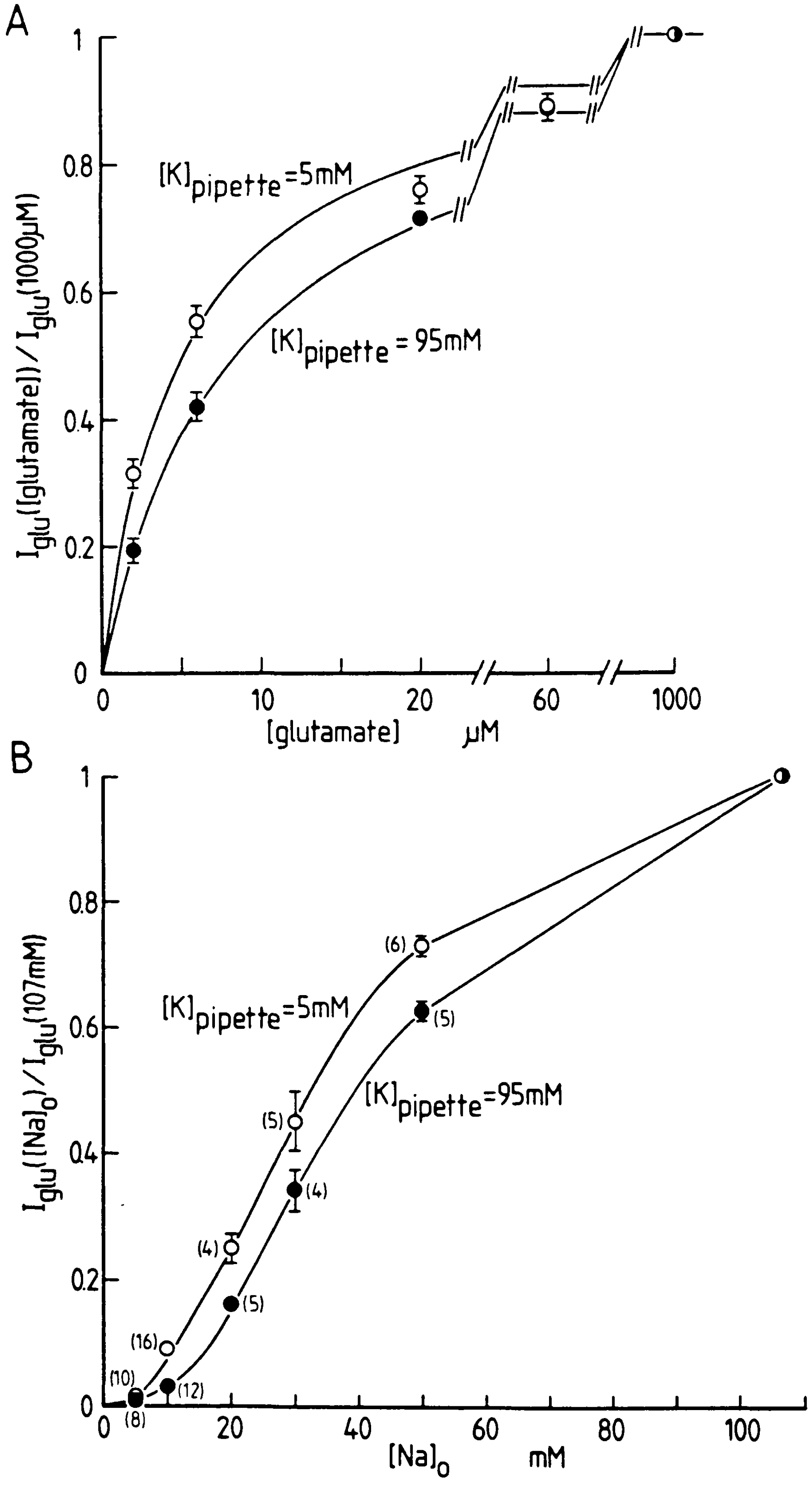
A
[K]$_{pipette}$=5mM
[K]$_{pipette}$ = 95mM
I_{glu}([glutamate]) / I_{glu}(1000µM)
1
0.8
0.6
0.4
0.2
0
0
10
20
60
1000
[glutamate] µM
B
[K]$_{pipette}$=5mM
[K]$_{pipette}$=95mM
I_{glu}([Na]$_o$) / I_{glu}(107mM)
(6)
(5)
(5)
(4)
(4)
(5)
(16)
(10)
(12)
(8)
1
0.8
0.6
0.4
0.2
0
0
20
40
60
80
100
[Na]$_o$ mM

Fig 3.9 Specimen I-V relations for the current evoked by 30μM glutamate in one cell with 95mM $[K]_{pipette}$ and another with 5mM $[K]_{pipette}$. Data normalised by cell capacitance (315 and 243pF, respectively). External solution D; pipette solution W with [K] = y = 95 and 5mM respectively.

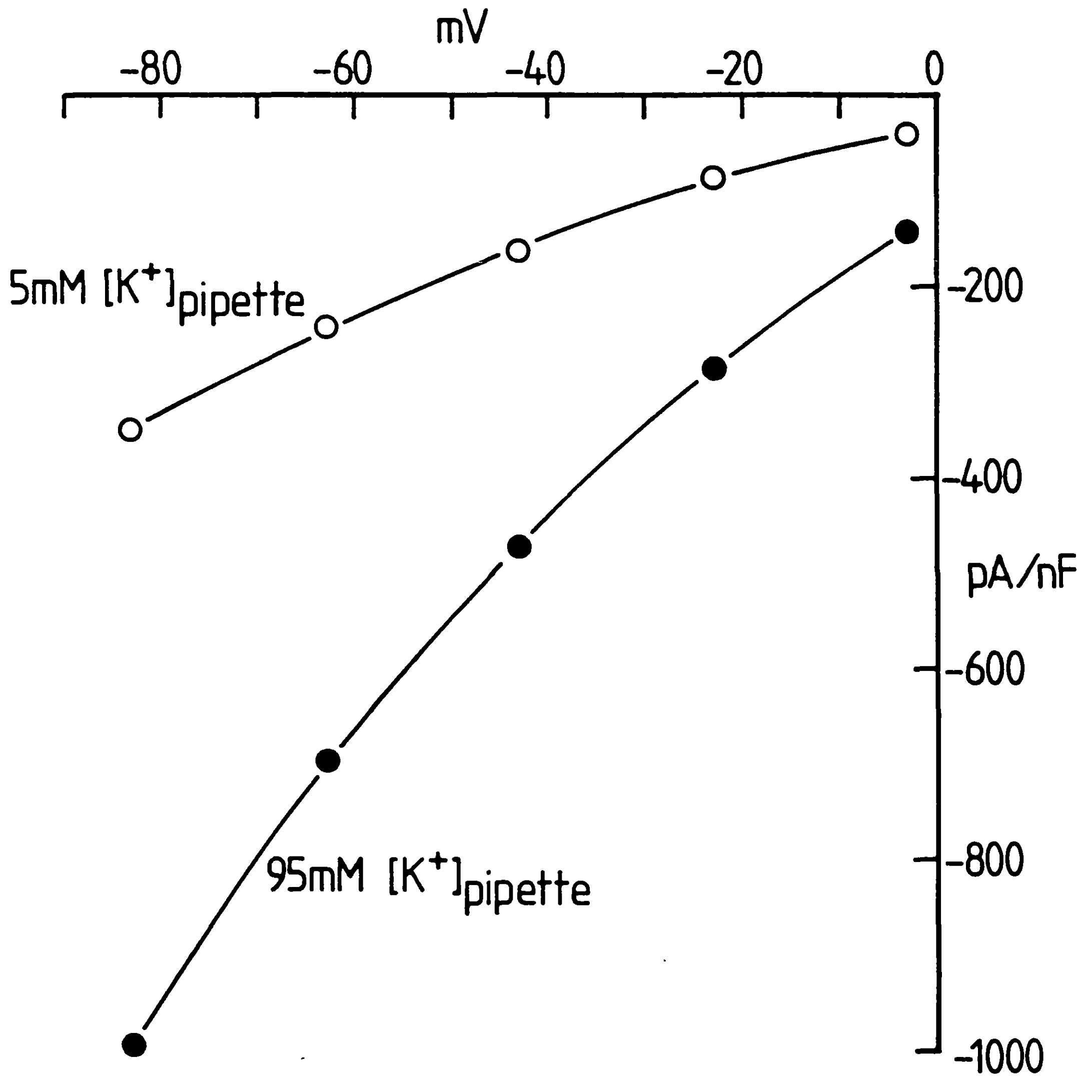
mV
-80
-60
-40
-20
0
5mM [K+]pipette
95mM [K+]pipette
-200
-400
pA/nF
-600
-800
-1000

In similar experiments the sodium-dependence of the uptake current was determined for the same pipette potassium concentrations (Fig. 3.8B). The results have been normalised by the currents evoked in 107mM $[Na]_o$. For 95 and 5mM $[K]_{pipette}$ the uptake current was half of its magnitude at 107mM $[Na]_o$ when $[Na]_o$ was 40 and 32mM respectively. Thus, as was the case for glutamate, there is a slight rise of the apparent affinity for sodium as the internal potassium is lowered. This excludes a reduced sodium affinity as a mechanism for the decreased uptake current magnitude at low $[K]_{pipette}$.

The small increases of affinity for sodium and glutamate caused by lowered $[K]_i$ are, in fact, expected if potassium is transported out of the cell by the carrier. At low concentrations of external substrate (sodium or glutamate) the rate of uptake will be limited by binding of external substrate and relatively unaffected by $[K]_i$. At high concentrations of external substrate (when binding of external substrate is not rate-limiting), K_i-binding will limit the rate of uptake. This will affect the shape of the dose-response curve for glutamate or sodium; the apparent affinity for $[K]_i$ will be higher when the concentration of external substrate is low.

Lowering $[K]_{pipette}$ had only a small effect on the voltage-dependence of the current evoked by 30μM glutamate (Fig. 3.9), the current being reduced by a slightly greater fraction at positive than at negative voltages.

The above evidence provides no support for the hypothesis that lowering internal potassium reduces the uptake current by allosterically modifying the carrier's properties. However, not all of the possible allosteric mechanisms have been investigated; for example, a dramatic increase of the carrier's affinity for internal sodium might produce the observed inhibition of the uptake current. So these experiments do not conclusively rule out the allosteric mechanism.

The two possible mechanisms, allosteric activation by internal potassium and counter-transport of potassium, can be distinguished in another way: by testing the effects of raising the external potassium concentration. If internal potassium acts by allosterically activating the carrier then the rate of uptake should be unaffected by changes of external potassium. If, however, the carrier does transport potassium out of the cell then a rise of external potassium would be expected to reduce the rate of uptake.

3.8 Dependence on external potassium

The effects on the uptake current of raising the external potassium concentration from 2.5mM to 57mM (potassium replacing choline, solution E with y = 2.5 and 57mM) are shown in Fig. 3.10A. 30μM glutamate applied at -43mV with 57mM $[K]_o$ evokes a smaller current than that obtained with 2.5mM $[K]_o$. Thus the uptake current is inhibited by raising $[K]_o$; the mean reduction of the uptake current was 40.4 ± 5.8 % (SEM, n=5). Changing to the high potassium solution caused an inward current of 220pA which presumably flows through potassium channels, although the slow onset is not understood. The form of the dependence of the uptake current on $[K]_o$ is shown in Fig. 3.10B. The smooth curve is of the form $K_m/([K]_o + K_m)$ with K_m = 100mM.

Control experiments were performed to check whether competition of external potassium for the external sodium or glutamate binding sites could account for the inhibition. With a near-saturating glutamate concentration (1mM, V_H = -43mV), the current in 57mM $[K]_o$ was 65.2% (± 2.1% SEM, n=5) of its size in 2.5mM $[K]_o$, similar to the value for 30μM glutamate in Fig. 3.10B (59.6 ± 5.8%). This rules out the possibility that high $[K]_o$ reduces the uptake current by greatly reducing the affinity of the carrier for glutamate. Lowering $[Na]_o$ from 52 to 27mM (in solution E, replaced by choline) reduced the current evoked by 30μM glutamate at -43mV by 62.6% (± 1.9% SEM, n=12) in 2.5mM $[K]_o$ and by 61.2% (± 2.5%) in 57mM $[K]_o$.

Fig. 3.10 External potassium inhibits electrogenic glutamate uptake. **A** Current evoked by 30μM glutamate (black bars) at -43mV in a cell that was initially in a solution (E) containing 2.5mM K (y = 2.5), then in a solution containing 57mM K (y = 57), then again in 2.5mM K. **B** Dependence on $[K]_o$ of the glutamate-evoked current from experiments like that in **A**. Mean data (± SEM) from 5 cells for $[K]_o$ = 0, 10, 57mM and 6 cells for $[K]_o$ = 25mM, normalised to the current measured on the same cell with 2.5mM $[K]_o$ (the value of which was set to 0.98 so that the mean value obtained for 0mM $[K]_o$ was unity). Pipette solution Y, external solution E with [K] = y = 0, 2.5, 10, 25 and 57mM.

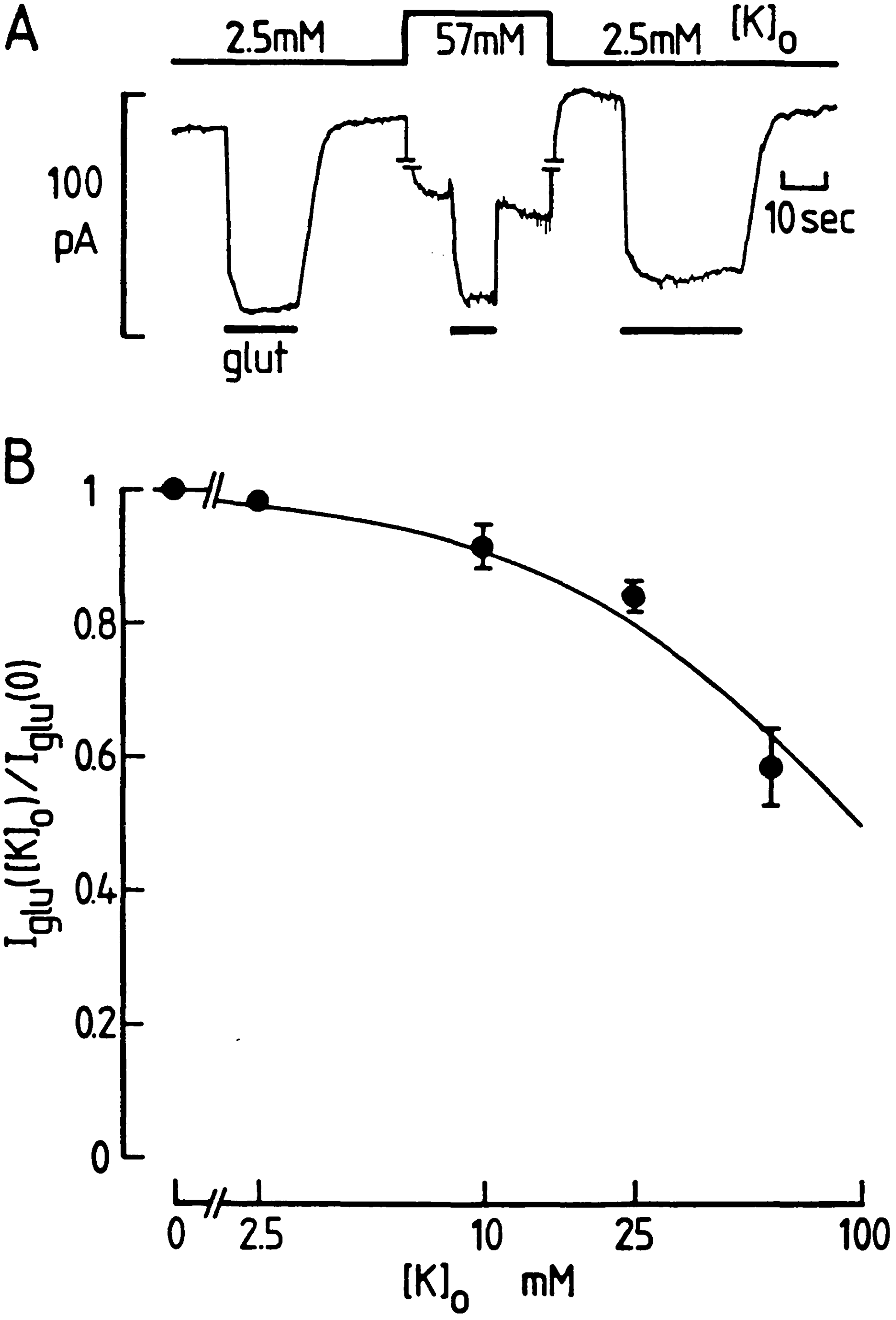
A
2.5mM
57mM
2.5mM
[K]o
100 pA
10 sec
glut
B
1
0.8
0.6
0.4
0.2
0
Iglu([K]o)/Iglu(0)
0
2.5
10
25
100
[K]o mM

This result excludes the possibility that potassium inhibits uptake by competing for the sodium binding sites, because in this situation the carrier would have a lower affinity for sodium and removing sodium would cause a greater fractional reduction of the uptake current in high $[K]_o$.

The simplest explanation of the activation by internal potassium and inhibition by external potassium of the uptake current is that potassium is indeed transported out of the cell by the carrier as glutamate is taken up.

3.9 Dependence on chloride

The main anion, both intracellularly and extracellularly, in most of these experiments, was chloride. Any chloride-dependence of the glutamate-evoked current is of interest, because a chloride-dependent glutamate uptake system has previously been reported (Pin, Bockaert & Recasens, 1984; Waniewski & Martin, 1984). Also, other transmitter uptake carriers co-transport chloride ions (Kanner & Schuldiner, 1987). Figure 3.11A & B show an experiment in which the dependence of the glutamate-evoked current on external chloride was tested. All the chloride in the external solution was replaced by the much larger gluconate anion (solutions B and J). This had no effect (7 cells) on the magnitude of the glutamate-evoked current at -43mV (Fig. 3.11A), nor on the voltage-dependence of the current (Fig. 3.11B).

To test the dependence of the glutamate-evoked current on intracellular chloride, cells were recorded from sequentially, alternating between 6 cells with a chloride-containing pipette solution (Y) and 7 cells with a gluconate-containing pipette solution (V). On average at -40mV 30μM glutamate evoked a current (per unit capacitance) of 0.59 ± 0.02 (SEM) pA/pF with chloride inside and 0.52 ± 0.05 pA/pF with gluconate inside, ie not significantly different ($P>0.2$).

Fig. 3.11 Effect on the glutamate-evoked current of changing the extra- and intracellular chloride concentration. **A** Membrane current of a Müller cell at -43mV for which the external chloride was completely replaced by gluconate (top bar, external solution B to J), while glutamate was repeatedly applied (bottom black bars). Chloride removal had no effect on the magnitude of the glutamate-evoked current. **B** Magnitude of the current evoked by 30μM glutamate in another cell at different voltages, with either chloride or gluconate as the main external anion. Over the voltage range studied, chloride removal had no effect on the shape of the I-V relation. **C** Currents produced by 30μM glutamate at various voltages in two different Müller cells with chloride and gluconate as the main pipette anion (pipette solutions Y and V). Currents from the two cells were normalized by cell capacitance (265pF for the cell studied with Cl^-_i and 230pF for the cell studied with $gluconate^-_i$).

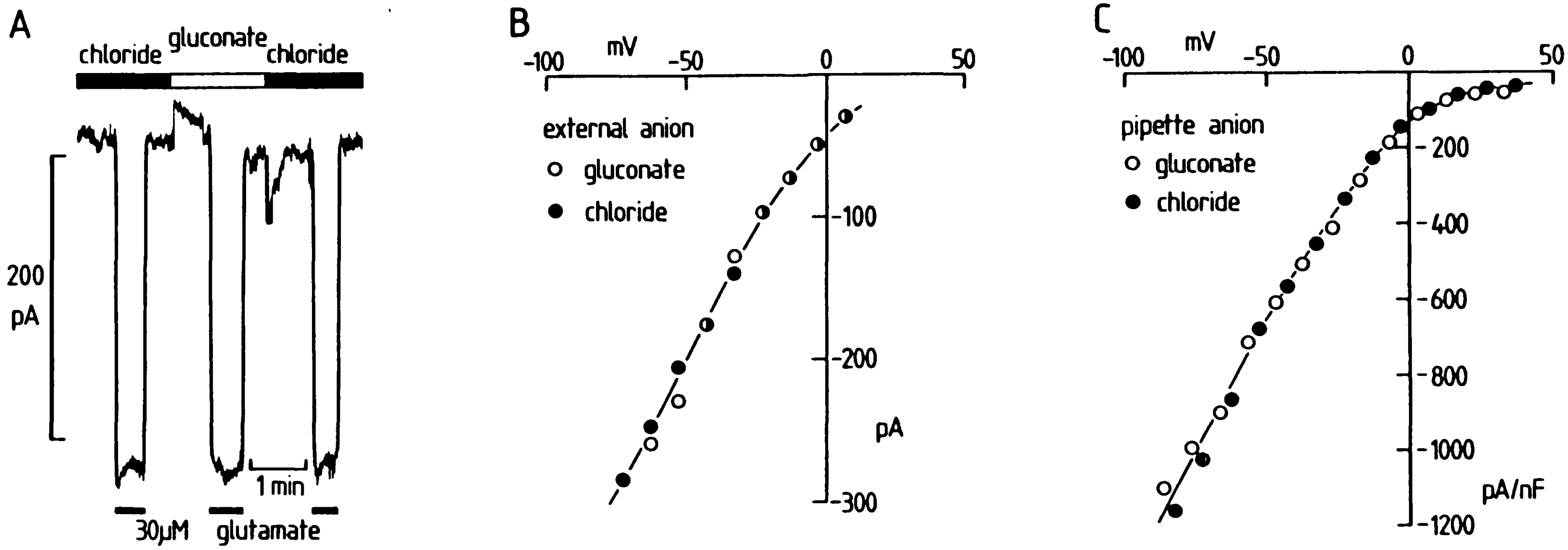
A
chloride
gluconate
chloride
200 pA
1 min
30μM glutamate
B
mV
-100
-50
0
50
external anion
gluconate
chloride
-100
-200
-300
pA
C
mV
-100
-50
0
50
pipette anion
gluconate
chloride
-200
-400
-600
-800
-1000
-1200
pA/nF

Replacing internal chloride by gluconate had no effect on the voltage-dependence of the glutamate-evoked current (Fig. 3.11C). These results show that the sodium-dependent carrier expressed in Müller cells can be unequivocally distinguished from the 'chloride-dependent' system described in other tissues, in that the Na-dependent system here does not transport or require chloride.

3.10 Dependence on external pH

It is of interest to determine the dependence of glutamate uptake on external pH, because this may give information as to whether or not protons are co-transported with glutamate. Strong evidence for this has been obtained in the kidney (Nelson et al, 1983) and it has also been suggested to occur in synaptosomes and glia (Erecinska et al, 1983, 1986).

How uptake varies with external pH was investigated in experiments such as those illustrated in figure 3.12, where 30μM glutamate was applied at -43mV in solutions buffered to different pH values (external solution B, with pH buffer as described below). Either raising or lowering the pH from 7.3 reduced the magnitude of the glutamate-evoked current. The control solution was buffered with 5 or 10mM HEPES ($pK_a = 7.5$) adjusted to pH 7.3 and the test solutions were buffered with 10mM MES ($pK_a = 6.1$), 10mM TAPS ($pK_a = 8.4$), 5 or 10mM HEPES. The pH of samples of solution collected from the perfusion inlet of the recording bath before and after the experiment was measured, and the average of these two values (which never differed by more than 0.1 pH units) was taken. Adjusting the pH of the solutions added varying amounts of NaOH. The resulting variations of sodium concentration, 105-112mM, would be expected to change the uptake current by less than 4%, according to the equations used to fit the external sodium-dependence of the uptake current in Fig. 3.1D.

Fig. 3.12 The glutamate-evoked current is pH-sensitive. Changing the external pH from 7.3 (HEPES-buffered) to 5.1 (MES-buffered) (top panel) or to 9.0 (TAPS-buffered) (bottom panel) reduces the magnitude of the current evoked by 30μM glutamate at -43mV. External solution B with 5 or 10mM HEPES or 10mM MES or TAPS; pipette solution Z.

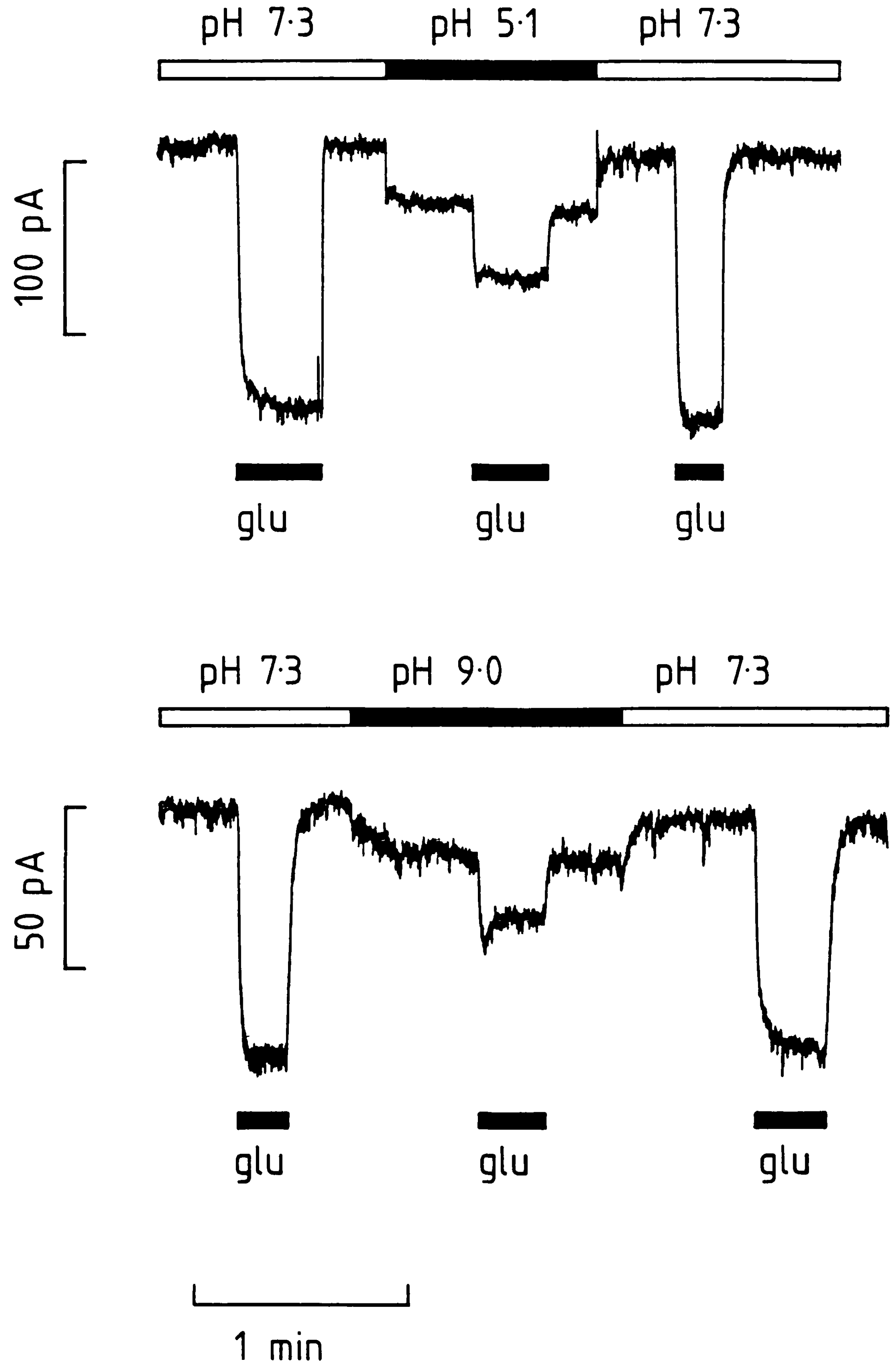
pH 7·3
pH 5·1
pH 7·3
100 pA
glu
glu
glu
pH 7·3
pH 9·0
pH 7·3
50 pA
glu
glu
glu
1 min

To check that neither MES nor TAPS directly affected glutamate uptake, the uptake current in a HEPES-buffered solution was compared to that of a MES-, or TAPS-buffered solution at the same pH. The mean glutamate-evoked currents at pH 6.7 in solutions buffered with 10mM HEPES or MES were 84 ± 4% (SEM, n=8) and 84 ± 2% (n=8), respectively, of the controls at pH 7.3 (no significant difference, $P > 0.9$). At pH 7.9, 10mM HEPES and TAPS were also compared, the mean current magnitudes being 68 ± 4% (n=8) and 75 ± 2%, respectively, of the controls at pH 7.3 (no significant difference, $P > 0.1$).

Changing the pH sometimes evoked a shift in the baseline current, as can be seen from Fig. 3.12. The mechanism of these shifts were not investigated.

The two specimen traces in Fig. 3.12A show that changes of pH away from 7.3 inhibit the uptake current. The mean uptake current magnitudes (± SEM), normalised to the current magnitude in pH 7.3 solution, are plotted in Fig. 3.13 as a function of the external pH, showing that the uptake current has a pH optimum at around pH 7.3. There are a number of possible mechanisms which could account for the observed pH-dependence of the uptake current.

The first is that it reflects changes in the ionisation state of free glutamate. Glutamate has three titratable groups: an α-COOH group ($pK_a = 2.13$), an α-NH_3^+ group ($pK_a = 9.95$) and a γ-COOH group on the side-chain ($pK_a = 4.32$). Rearrangement of the Henderson-Hasselbalch equation

$$pH = pK + \log\{[A^-]/[HA]\} \qquad (3.1)$$

to find how the proportions of the dissociated and undissociated forms of each acid (or base) group vary with pH gives

$$[HA]/\{[HA]+[A^-]\} = 1/\{1+10^{(pH-pK)}\} \qquad (3.2)$$

and

$$[A^-]/\{[HA]+[A^-]\} = 1/\{1+10^{(pK-pH)}\} \tag{3.3}$$

It is widely assumed that the transported form of glutamate is that on which all three ionisable groups are charged, because over 99% of the glutamate is in this form at physiological pH. This can be calculated from a product of three terms (one for each ionisable group) using eqns. (3.1) and (3.2)

$$[glu^{+--}]/[glu]_{tot} = \frac{1}{\{1+10^{(pH-9.95)}\}\{1+10^{(2.13-pH)}\}\{1+10^{(4.32-pH)}\}} \tag{3.4}$$

For pH = 7.3 this fraction takes the value 99.7%. At pH 5 and 9, the value falls only to 82.6% and 89.9% respectively, which would inhibit uptake by at most 17% at pH 5 (the observed inhibition is 74% at pH 5.1). This is the maximum effect that the changed glutamate concentration could have and this assumes a linear glutamate dose-response relation at 30μM glutamate. If the carrier has the same affinity for glutamate as at pH 7.3 (a K_m of about 20μM), then a 17% decrease of the glutamate concentration from 30μM would reduce the uptake current by only 8%. Thus, titration of the charged groups on the free glutamate molecule can only account for a small part of the inhibition at extremes of pH.

Changes of pH could alter the rate of glutamate uptake by surface charge effects, as the uptake current is voltage-sensitive, but they would be unlikely to give rise to a biphasic pH-dependence or cause such a profound inhibition of uptake, since varying the external calcium concentration between 2×10^{-8}M and 10mM (in the absence of external barium), which should also alter the surface charge, has no apparent effect on the magnitude or voltage-dependence of the uptake current (Attwell & Brew, personal communication). It is also conceivable that alterations of the external pH change the internal pH (although this was nominally buffered to pH 7.0 with 5mM HEPES), and that the apparent pH_0-dependence reflects the unknown dependence of the uptake current on internal pH.

There remain two mechanisms which could account for the form of the pH-dependence. One is titration of groups necessary for the normal function of the uptake carrier, the other is transport of protons by the carrier. These two possibilities cannot be distinguished using the data presented here. Thus, although the activation of the uptake current on changing from high to physiological pH is consistent with the carrier co-transporting protons and glutamate, it could equally well reflect titration of a group which must be protonated for carrier activity. The expected forms of the pH-dependence of uptake arising from these alternative mechanisms are identical.

The curves in Fig. 3.13 have been calculated on the assumption that the pH-dependence reflects titration of two groups: one which must be protonated for the carrier to work (roughly accounting for the alkaline part of the graph) and one which, when protonated, either completely (curve marked by arrows) or partially (unmarked curve) prevents the carrier from working (see Fig. 3.13 legend). The curve marked with arrows assumes pK_a values of 6 and 8.4 while the unmarked curve assumes 6.5 and 8.3. The scatter of the data precludes accurate curve fitting, but the pK_a values of the titratable groups should lie close to the pH ranges 6.5 ± 1 and 8 ± 1 if such a model were to account for the pH-dependence of the uptake current. The side chains of free histidine and cysteine have pK_a values of 6.00 and 8.33 respectively, so these might be the titrated groups. Note, however, that if this were the case, then it would be the uncharged forms of these side-chain groups which would be required for normal carrier function.

Fig. 3.13 The glutamate-evoked current has a pH optimum. The mean (± SEM, n ≥ 5) magnitude of the glutamate-evoked current, normalised to the current obtained at pH 7.3, as a function of the external pH. Data from experiments like in Fig. 3.12. The curve marked by arrows has the form

$$y = \frac{\{1 + 10^{-1.2}\}^2}{\{1 + 10^{(pH - 8.4)}\}\{1 + 10^{(6.0 - pH)}\}}$$

The unmarked curve has the form

$$y = \{1 + 10^{-0.9}\}^2 \left[0.25 + \frac{0.75}{\{1 + 10^{(pH - 8.3)}\}}\right]\left[\frac{1}{\{1 + 10^{(6.5 - pH)}\}}\right]$$

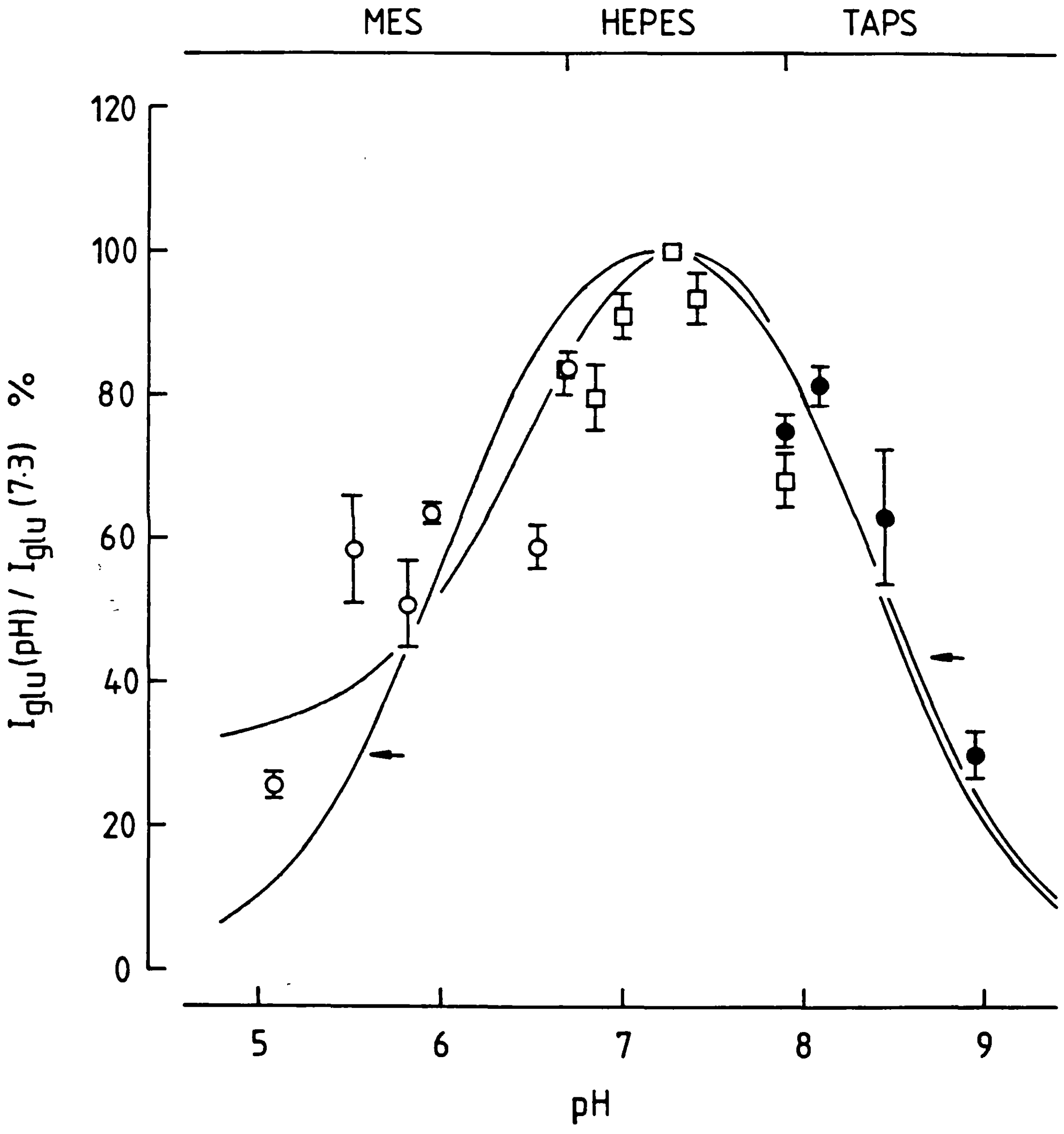
MES
HEPES
TAPS
120
100
80
60
40
20
0
$I_{glu}(pH) / I_{glu}(7{\cdot}3)$ %
5
6
7
8
9
pH

Chapter 4

Modulation of glutamate uptake

It is not known what mechanisms regulate the activity of the glutamate uptake carrier. This chapter describes experiments in which a number of second messenger systems were manipulated, and the effects on the uptake current observed, in order to identify potential regulatory mechanisms of glutamate uptake.

4.1 Dependence on internal calcium

Whether glutamate uptake is modulated by the internal calcium concentration was tested by buffering pipette $[Ca^{2+}]_i$ to different values with 20mM EGTA (solution O). The mean magnitudes of the currents (normalised by capacitance) evoked by 30μM glutamate at -44mV (external solution B), measured approximately 5 minutes after patch rupture, with internal calcium buffered to 10^{-8}, 10^{-7} and 10^{-6}M were 0.63 ± 0.14, 0.58 ± 0.14 and 0.64 ± 0.10 pA/pF (± SEM, n = 6, 7 and 6) respectively. None of these values is significantly different from the others ($P > 0.4$), so it is concluded that variations of internal calcium do not affect glutamate uptake.

4.2 Effect of cGMP

In order to investigate whether the uptake carrier could be modulated by phosphorylation by cGMP-dependent protein kinase, the effects of including cGMP in the pipette-filling solution were tested. Two groups of 6 cells each were compared, one with a standard pipette-filling solution (Y) and the other with 100μM cGMP added to the same pipette-filling solution. The mean currents (normalised by capacitance) evoked by 30μM glutamate at

Table 4.1

I_{glu}/C ± SD (pA/pF), n = 6

t	1 min	5 min	10 min	15 min
0 cGMP	0.78 ± 0.04	0.72 ± 0.05	0.68 ± 0.04	0.68 ± 0.04
100μM cGMP	0.70 ± 0.10	0.70 ± 0.08	0.67 ± 0.06	0.65 ± 0.07
t-test	$P > 0.05$	$P > 0.6$	$P > 0.8$	$P > 0.3$

$\{I_{glu}(t)/C(t)\}/\{I_{glu}(1min)/C(1min)\}$ ± SD, n = 6

t	1 min	5 min	10 min	15 min
0 cGMP	1.00	0.92 ± 0.05	0.87 ± 0.04	0.86 ± 0.05
100μM cGMP	1.00	1.00 ± 0.06	0.97 ± 0.09	0.92 ± 0.08
t-test	-	$P < 0.02$	$P < 0.05$	$P > 0.1$

-43mV (external solution B) were compared at 1, 5, 10 and 15 minutes after patch rupture. The results are presented in table 4.1. The top panel shows the mean I_{glu}/C for each time, without and with cGMP in the pipette, and the P values from a Students t-test comparison of the averages at each time are also given. Inclusion of cGMP made no significant difference at any of the times tested.

The bottom panel is based on the same data, but, before averaging, the I_{glu}/C values for each cell were normalised to the value obtained at t = 1 minute. This procedure should reduce variation due to different uptake current densities in different cells. When analysed in this way, it appears that including cGMP in the pipette retards the slow decline of I_{glu}/C seen under control conditions. The difference is significant at t = 5 and 10 minutes ($P < 0.02$ and $P < 0.05$ respectively). However, the effect is small, the difference of the means reaching a maximum of 11%.

4.3 Effect of cAMP

Phosphorylation of the uptake carrier by cAMP-dependent protein kinase is one putative mechanism for regulation of glutamate uptake. In order to test this possibility, the effects of including cAMP in the pipette solution were investigated. Responses to 30μM glutamate at -43mV (external solution B) were compared between two groups of cells: a control group with pipette solution Y and the test group which had 100μM cAMP added to solution Y. The mean glutamate-evoked currents, normalised by capacitance and measured 5 minutes after patch rupture, were 0.70 ± 0.02 pA/pF (SEM, n = 9) for the control group and 0.74 ± 0.04 pA/pF (n = 10) for the test group; not significantly different ($P > 0.3$). The ratios of the response at 5 minutes to that at 1 minute after patch rupture were also compared. Over that time the mean response for the control cells declined to 86 ± 2 % (SEM,

Table 4.2

I_{glu}/C ± SD (pA/pF), number of cells in brackets

t	1 min	5 min	20 min
0 GTP-γ-S (n)	0.72 ± 0.19 (17)	0.77 ± 0.13 (12)	0.59 ± 0.18 (15)
100μM GTP-γ-S (n)	0.68 ± 0.18 (13)	0.72 ± 0.19 (9)	0.62 ± 0.19 (12)
t-test	P > 0.5	P > 0.5	P > 0.7

$\{I_{glu}(t)/C(t)\}$ / $\{I_{glu}(1min)/C(1min)\}$ ± SD, number of cells in brackets

t	1 min	5 min	20 min
0 GTP-γ-S (n)	1	0.96 ± 0.11 (12)	0.81 ± 0.10 (15)
100μM GTP-γ-S (n)	1	1.04 ± 0.22 (9)	0.88 ± 0.22 (11)
t-test	-	P > 0.2	P > 0.3

n = 9) of the response at 1 minute, while the test group mean declined to 94 ± 6% (n = 10). These two values are also not significantly different ($P > 0.2$), suggesting that raising cAMP has no effect on the uptake carrier.

4.4 Effect of GTP-γ-S

GTP-binding proteins are involved in signal transduction in a number of second messenger systems and have also been shown to directly modulate ion channels (Dolphin, 1990). Whether a G-protein is involved in the control of glutamate uptake was tested by including in the pipette solution 100μM GTP-γ-S, a non-hydrolysable analogue of GTP which irreversibly activates G-proteins. The GTP-γ-S was added to solution Y as a tetra-lithium salt. The pH of the test solution was readjusted to 7.0 with a negligible amount of NaOH and the appropriate amount of LiCl (400μM) was added to the control solution. The results shown in table 4.2 demonstrate that inclusion of GTP-γ-S in the pipette solution had no detectable effect on the glutamate-evoked current (30μM glutamate; holding potential -43mV; external solution B). The top panel shows the mean magnitude of the glutamate-evoked current (normalised by capacitance) at different times (t) after patch rupture. For the bottom panel, the I_{glu}/C values for each cell were normalised to the value at t = 1 minute before averaging.

4.5 Effect of phorbol ester

The possibility that phosphorylation of the glutamate uptake carrier by protein kinase C (PKC) might modulate the carrier properties was tested by applying a phorbol ester. Phorbol 12-myristate 13-acetate (TPA) has been shown to activate PKC in many preparations. A 4.5 minute application of 100nM TPA (0.005% DMSO in test and control external solution, B) had almost no effect on the magnitude of the current evoked by 30μM glutamate at -43mV (Fig. 4.3A). Over the 4.5 minutes of TPA application, the uptake current (normalised by capacitance) declined by only 5.5 ± 1% (SEM, n = 5).

These data are from an experiment in which the pipette solution (Y) had the usual calcium concentration of $1.2x10^{-7}M$. Because the degree of activation of PKC by phorbol ester is calcium-dependent (Sekiguchi et al, 1988), the effects of phorbol ester were also tested with the pipette calcium concentration buffered to $10^{-6}M$ (solution Y, but with 3.5mM added $CaCl_2$). In this case I_{glu}/C declined by only 1 ± 5% (SEM, n = 4) over 4 minutes. A small decline of I_{glu}/C would normally be expected to occur even in the absence of drug, so it is concluded that the phorbol ester has a negligible effect, if any, on glutamate uptake under these conditions.

4.6 Effects of arachidonic acid

Arachidonic acid metabolites such as the prostaglandins and leukotrienes have many biological actions and it has been suggested that these metabolites (or arachidonic acid itself) may act as intercellular messengers in the CNS (Piomelli et al, 1987). The action of glutamate (or NMDA) on cultured neurones leads to a release of arachidonic acid (Dumuis et al, 1988; Lazarewicz et al, 1988), so a release of arachidonic acid is likely to occur at glutamatergic synapses. Arachidonic acid at high concentrations has been shown to reduce glutamate uptake in cell and synaptosome suspensions (Chan et al, 1983; Yu et al 1986, 1987), but its mechanism of action is unknown. Given the limitations of the radiotracing techniques, the inhibition of uptake might be mediated by inhibition of the sodium pump by arachidonic acid (Chan et al, 1983; Swann, 1984) and a subsequent rise of $[Na]_i$, or by depolarisation of the cell, which would also inhibit uptake (Brew & Attwell, 1987).

Fig. 4.1 Arachidonic acid induces a progressive inhibition of the uptake current. **A-C** Uptake current assessed by repeated applications of 30μM glutamate at -43mV (external solution B; pipette solution Y). Arachidonic acid applied for 2 minutes at concentrations of 1μM (A), 10μM (B) and 30μM (C). **D** Dose-response curve for arachidonic acid. Plot of the percentage inhibition (mean ± SEM, figures in brackets by each point = n) of the uptake current (normalised by capacitance) produced by a 2 minute application of arachidonic acid, as a function of the concentration of arachidonic acid applied.

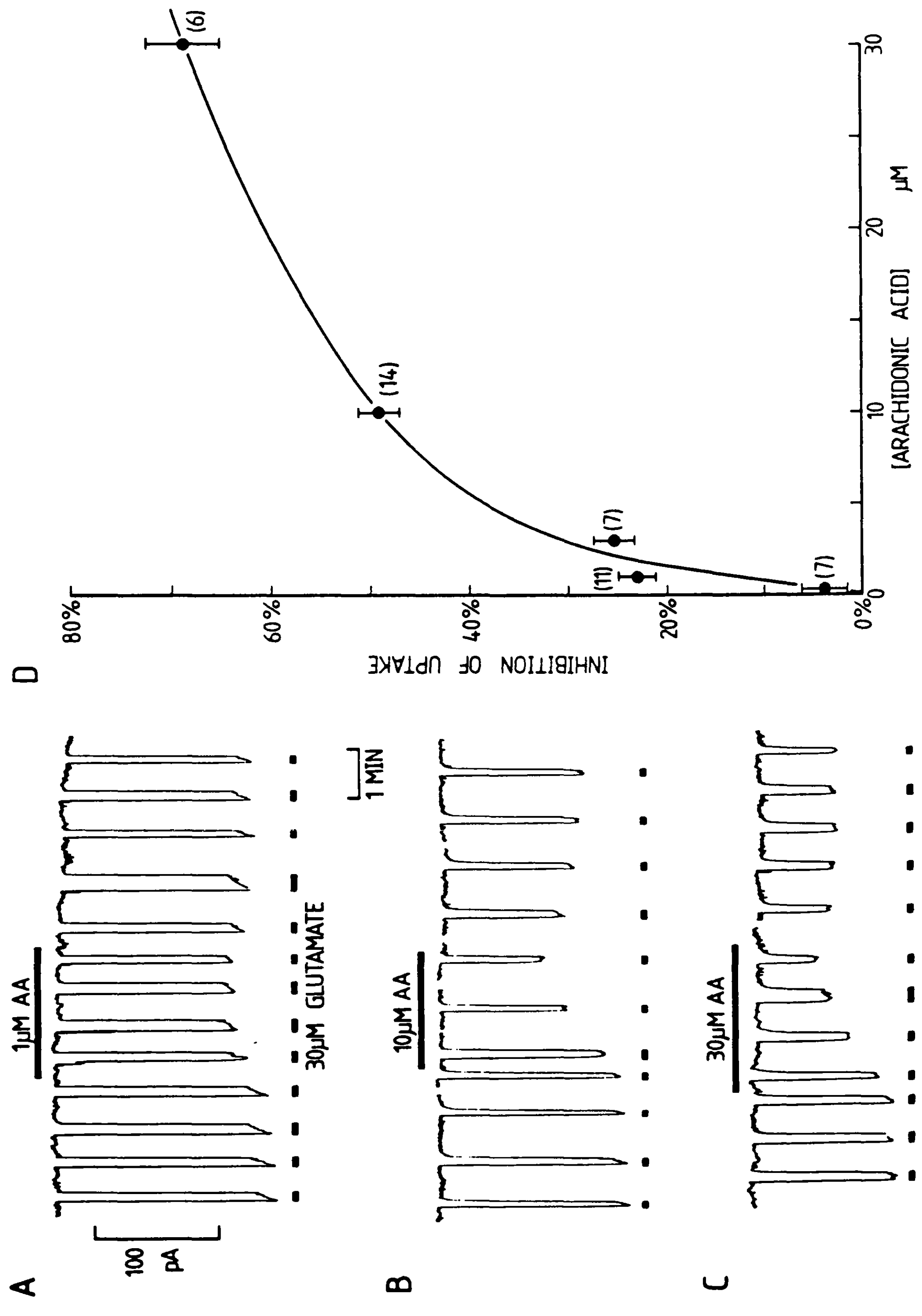
A
100 pA
1µM AA
30µM GLUTAMATE
1 MIN
B
10µM AA
C
30µM AA
D
INHIBITION OF UPTAKE
80%
60%
40%
20%
0%
(11)
(7)
(7)
(14)
(6)
0
10
20
30
[ARACHIDONIC ACID] µM

In order to test whether arachidonic acid has a direct action on glutamate uptake, the effects of arachidonic acid on the uptake current in Müller cells were investigated. Fig. 4.1A-D shows that application of micromolar arachidonic acid induces a progressive decline of the magnitude of the current evoked by 30μM glutamate; there is a partial recovery following washout of arachidonic acid (holding potential -43mV; external solution B). A two minute application of 10μM arachidonic acid produces a roughly 50% inhibition of the uptake current (Fig. 4.1B) while 1μM has a smaller, but significant effect (Fig. 4.1A). A dose-response relation is shown in Fig. 4.1D, where the inhibition of the uptake current (normalised by cell capacitance) produced after two minutes of arachidonic acid application is plotted as a function of the arachidonic acid concentration. On average, 10μM arachidonic acid causes a 49 ± 2% (SEM, n = 14) inhibition after 2 minutes and 1μM causes a reduction of 23 ± 2% (SEM, n = 11).

4.7 Possible mechanisms of action of arachidonic acid

The mechanism of action of arachidonic acid was investigated pharmacologically. Ouabain (10^{-4}M) did not prevent the inhibition produced by 10μM arachidonic acid (Fig. 4.2A), the mean inhibition after 2 minutes being 58 ± 2% (SEM, n = 3), similar to that seen in the absence of ouabain. The inhibitory action of arachidonic acid was therefore not an indirect result of intracellular sodium accumulation following inhibition of the sodium pump. Such depletion of the sodium gradient is, in any case, unlikely to occur to any great degree in the whole-cell patch-clamp mode, and indeed the application of ouabain only produced a small inhibition (7 ± 1%, SEM; n = 3).

Fig. 4.2 Ouabain and inhibitors of arachidonic acid metabolism do not prevent the inhibition produced by arachidonic acid. **A** In the presence of 10^{-4}M ouabain, 10μM arachidonic acid produces a similar inhibition of the glutamate evoked current to that produced in the absence of ouabain (see Fig. 4.1). **B** 5μM indomethacin, a cyclo-oxygenase inhibitor, applied for 20-30 minutes, does not affect the inhibition of the uptake current produced by 10μM arachidonic acid. **C** Nordihydroguaiaretic acid (NDGA, 10μM), a lipoxygenase inhibitor, itself inhibits the uptake current, but does not prevent the inhibition produced by arachidonic acid. All panels: 30μM glutamate, 10μM arachidonic acid, external solution B, pipette solution Y, holding potential -43mV.

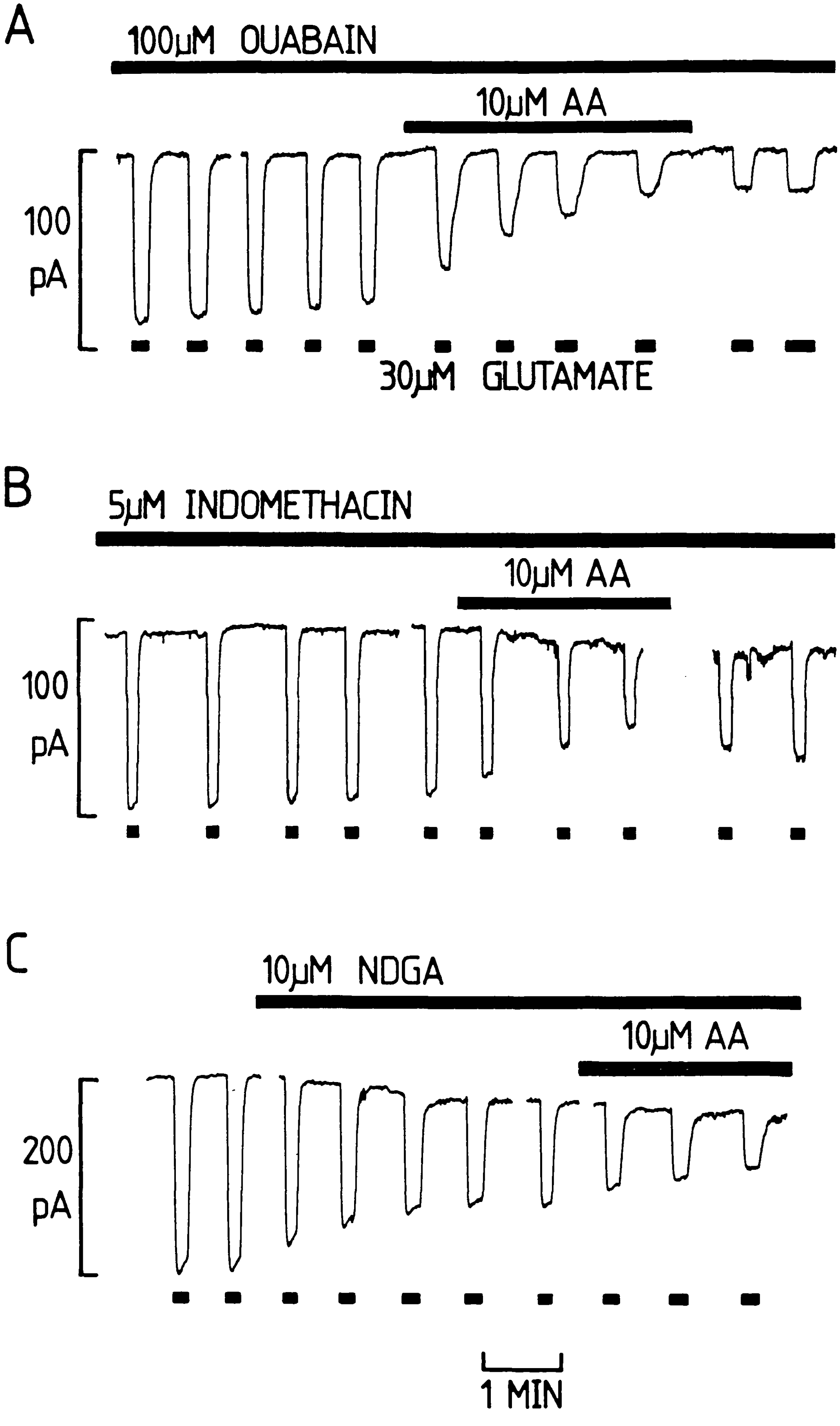
A
100µM OUABAIN
10µM AA
100
pA
30µM GLUTAMATE
B
5µM INDOMETHACIN
10µM AA
100
pA
C
10µM NDGA
10µM AA
200
pA
1 MIN

Arachidonic acid is metabolised by two main pathways, catalysed by the enzymes cyclo-oxygenase (generating prostaglandins) and lipoxygenase (generating HETEs, HPETEs and leukotrienes). In order to test whether arachidonic acid was acting via one of its metabolites, it was applied in the presence of inhibitors of its metabolism. In the presence of 5μM indomethacin (applied for 20-30 min), a cyclo-oxygenase inhibitor, 10μM arachidonic acid still inhibited the uptake current (Fig. 4.2B). The mean reduction was 48 ± 5% (SEM, n = 3) over 2 minutes, similar to the reduction seen in the absence of indomethacin. Nordihydroguaiaretic acid (NDGA, 10μM, Fig. 4.2C), a lipoxygenase inhibitor, itself reduced the uptake current (by 53 ± 2% after 8 minutes; SEM, n = 9), but subsequent application of 10μM arachidonic acid further reduced the uptake current by 45 ± 5% (after 2 minutes; n = 10), again similar to the reduction seen in the absence of NDGA.

The lack of effect of blockers of arachidonic acid metabolism on the action of arachidonic acid suggests that it does not inhibit uptake via a metabolite. The concentrations of the inhibitors used are expected to substantially inhibit cyclo-oxygenase and lipoxygenase: 6μM indomethacin inhibits cyclo-oxygenase by > 90% in toad bladder (Wong et al, 1972) and in the rat the IC_{50} is about 0.4μM (Ford-Hutchinson et al, 1979), while the estimated IC_{50} for block of lipoxygenase by NDGA is ~0.9μM in the rat (Ford-Hutchinson et al, 1979). However, as the block of the enzymes is certainly not complete, and knowing that arachidonic acid metabolites can be active at nanomolar concentrations, these results on their own do not completely exclude the possibility that it is an arachidonate derivative which inhibits glutamate uptake. Nevertheless, the observation (below) that unsaturated fatty acids unrelated to arachidonic acid have a similar inhibitory action is further evidence that the inhibition is not due metabolites of arachidonic acid.

Fig. 4.3 Arachidonic acid does not act via PKC on the glutamate uptake carrier. **A** 100nM phorbol 12-myristate 13-acetate (TPA) has a negligible effect on the current evoked by glutamate. **B** Inclusion of 340μM H-7, a protein kinase inhibitor, in the pipette filling solution (Y) does not prevent the inhibition of the uptake current produced by 10μM arachidonic acid application 10 minutes after patch rupture. **C** 10μM docosahexaenoic acid, an unsaturated fatty acid known not to activate PKC, produces a progressive inhibition of the uptake current. For all panels: 30μM glutamate, external solution B, pipette solution Y, holding potential -43mV.

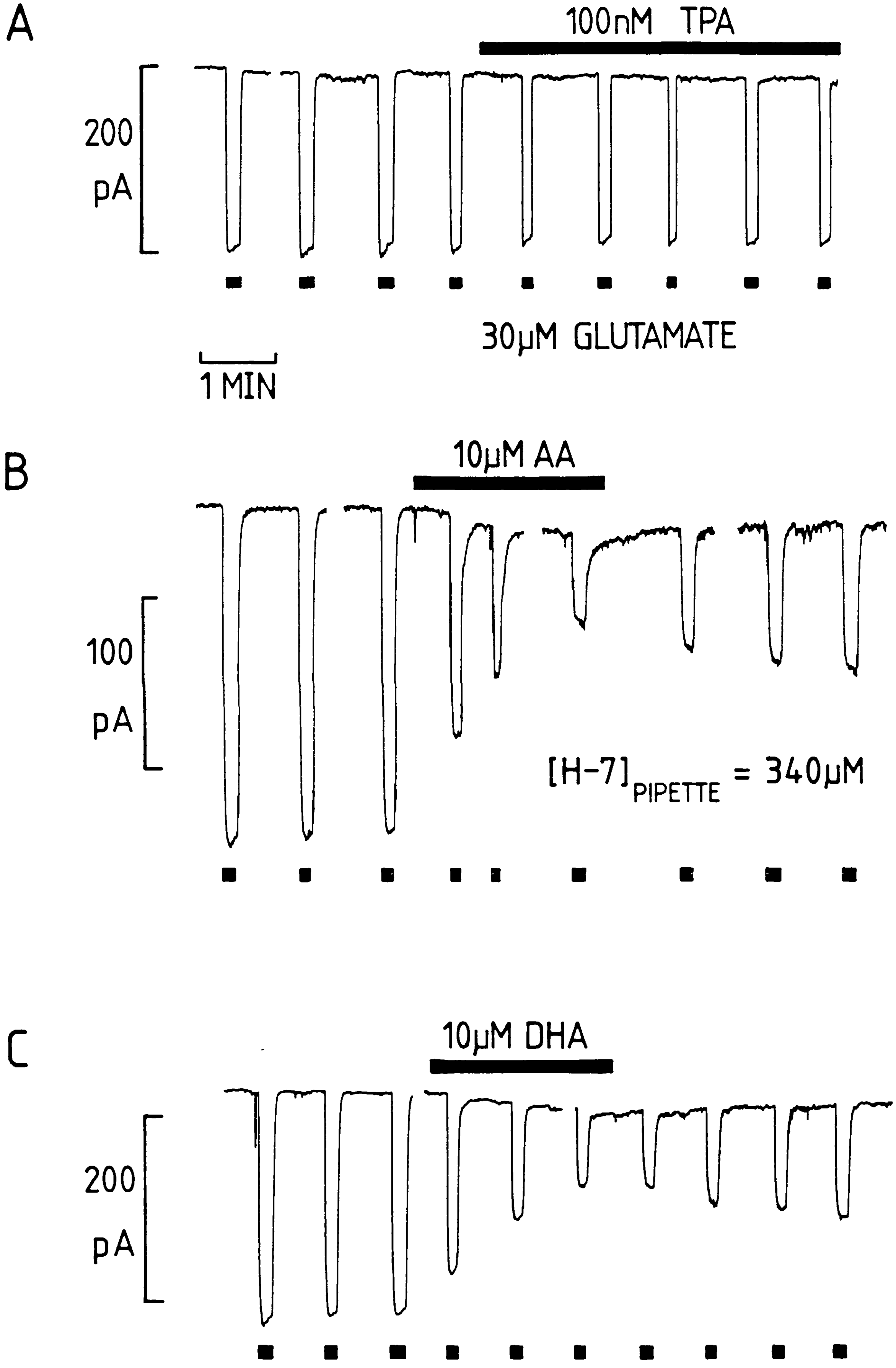
A
100nM TPA
200
pA
30µM GLUTAMATE
1 MIN
B
10µM AA
100
pA
[H-7]PIPETTE = 340µM
C
10µM DHA
200
pA

Arachidonic acid and a number of other unsaturated fatty acids, including oleic acid which below is shown to have a similar inhibitory action to arachidonic acid, activate protein kinase C (Sekiguchi et al, 1988). Thus, a possible mechanism for the action of arachidonate is that it activates protein kinase C which in turn inhibits glutamate uptake by phosphorylating the uptake carrier. At first sight this possibility seems to be ruled out by the demonstration that phorbol ester has no effect on glutamate uptake (section 4.5). However, Sekiguchi et al (1988) have shown that the various isozymes of PKC can be activated differently by arachidonic acid and phorbol ester. Also, Linden and Routtenberg (1989) have suggested that the proteins phosphorylated by protein kinase C differ, depending on whether phorbol ester or arachidonic acid is the activator. Thus, a lack of effect of phorbol ester may not rule out PKC regulating the uptake carrier.

The possible role of PKC was further tested by including in the patch-pipette a protein kinase inhibitor, H-7, at a concentration of 340μM. The K_i for inhibition of PKC by H-7 is 6μM, and this compound also blocks cGMP-dependent and cAMP-dependent kinases with similar potency (Hidaka et al, 1984). Fig. 4.3B shows that including H-7 in the pipette did not prevent the inhibition of uptake caused by 10μM arachidonic acid. The mean inhibition was 65 ± 3% (SEM, n = 5) over 2 minutes, compared with a mean inhibition of 61 ± 2% in 5 cells tested without H-7 in the pipette. There being no significant difference between these values ($P > 0.2$), it is concluded that the action of arachidonic acid does not involve PKC activation. This conclusion is supported by the result shown in Fig. 4.3C, in which another unsaturated fatty acid, docosahexaenoic acid (10μM), is shown to inhibit progressively the uptake current. Over 2 minutes a 59 ± 3% (SEM, n = 5) reduction was produced. This fatty acid has been shown, in vitro, not to activate PKC at all (Sekiguchi et al, 1988).

4.8 Effects of other fatty acids

Docosahexaenoic acid has a 22-carbon chain with 6 cis double bonds (22:cis 6). The observation that it produces a similar inhibition to arachidonic acid, which has a 20-carbon chain with 4 cis double bonds (20:cis 4) suggests that it may be the presence of the cis double bonds which leads to the inhibition of the uptake current.

This was tested by applying another cis unsaturated fatty acid, oleic acid (18:cis 1). Oleate (10μM) also inhibited the uptake current (Fig. 4.4C), although the mean inhibition of 29 ± 1% (SEM, n = 7; over 2 minutes) is somewhat less than that produced by arachidonic acid. Another prediction of the hypothesis that cis unsaturated fatty acids inhibit glutamate uptake is that saturated, or trans unsaturated fatty acids should not inhibit the uptake current. Application of 10μM arachidic acid, a saturated analogue of arachidonic acid (20:0), generated a small inhibition of the uptake current (Fig. 4.4B), the mean reduction over 2 minutes was 10 ± 1% (SEM, n = 8), only a fifth of that produced by arachidonic acid. Elaidic acid, a fatty acid with the same chemical structure as oleic acid, but with a trans (instead of a cis) double bond (18:trans 1), produced only a slight inhibition of the uptake current (Fig. 4.4D), 7 ± 2% (SEM, n = 9; 10μM elaidate applied for 2 minutes).

In summary, of the five fatty acids tested, the three with cis double bonds produced the most inhibition of the uptake current, while the trans unsaturated and saturated fatty acids produced less inhibition (Fig. 4.4E). Thus there is a correlation between the presence of cis double bonds and inhibition of the uptake current.

Fig. 4.4 Inhibition of the uptake current by fatty acids correlates with the presence of cis double bonds. All fatty acids applied at 10μM for 2 minutes. **A** Arachidonic acid (C20:cis 4). **B** Arachidic acid (C20:0), a saturated analogue of arachidonic acid. **C** Oleic acid (C18:cis 1). **D** Elaidic acid (C18:trans 1) has the same chemical structure as oleic acid, but a trans instead of cis double bond. **E** Histogram (mean ± SEM) of the reduction of the uptake current produced by 2 minute applications of each of the above fatty acids and docosahexaenoic acid (DHA) (Fig. 4.3). For DHA, arachidonic acid, oleic acid, arachidic acid and elaidic acid, 5, 14, 8, 7 and 9 cells were studied, respectively. The cis unsaturated fatty acids produced the greatest inhibition. External solution B; pipette solution Y; holding potential -43mV.

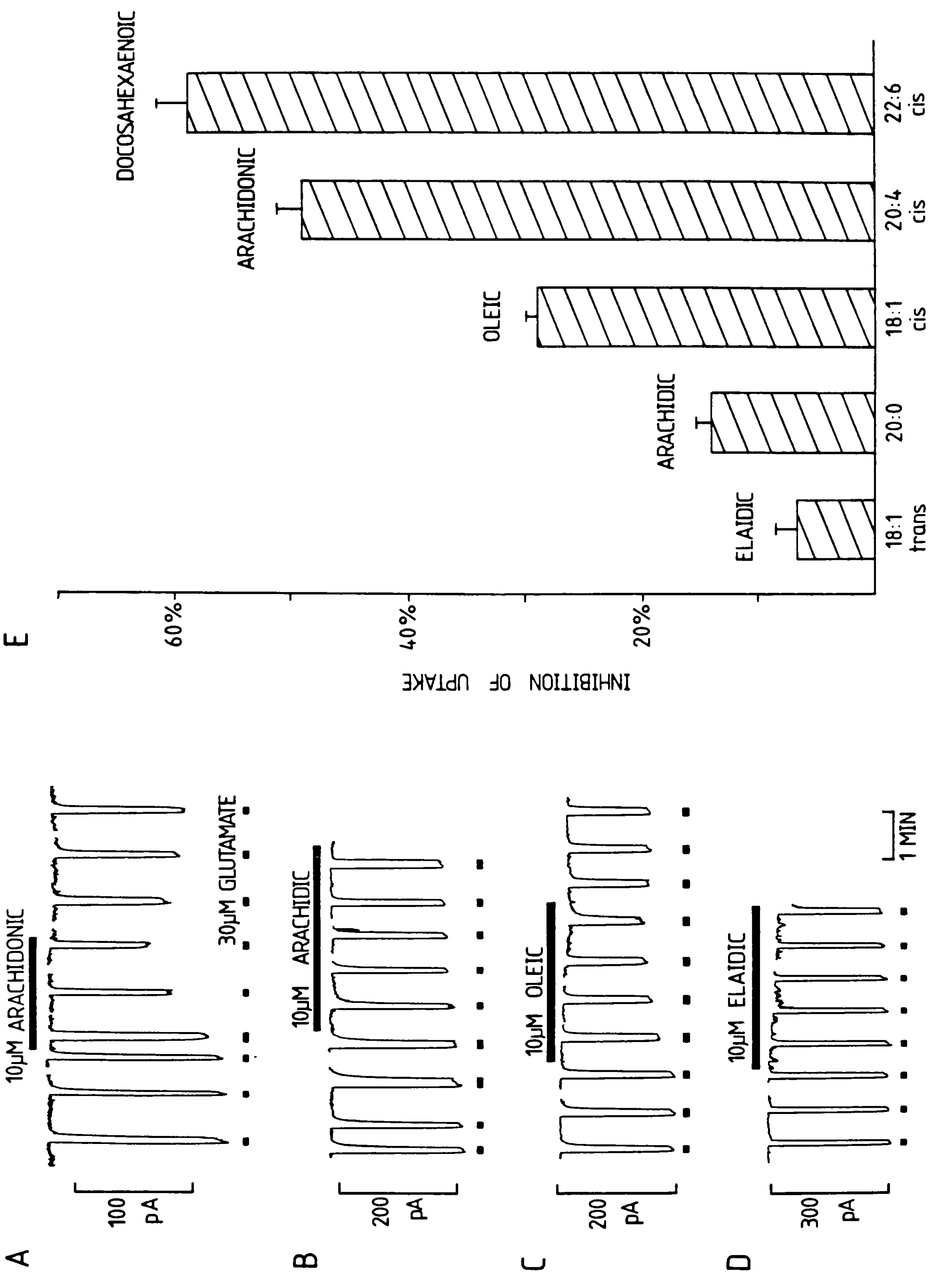
A
100 pA
10μM ARACHIDONIC
30μM GLUTAMATE
B
200 pA
10μM ARACHIDIC
C
200 pA
10μM OLEIC
D
300 pA
10μM ELAIDIC
1 MIN
E
INHIBITION OF UPTAKE
60%
40%
20%
ELAIDIC
18:1 trans
ARACHIDIC
20:0
OLEIC
18:1 cis
ARACHIDONIC
20:4 cis
DOCOSAHEXAENOIC
22:6 cis

4.9 Kinetics of inhibition by arachidonic acid

Evident in the specimen traces showing the inhibition produced by arachidonic acid is an apparently partial recovery following its washout. This was investigated quantitatively by comparing the mean time course of the uptake current in nine cells to which arachidonic acid was applied (10μM for 2 minutes) with the time course in 10 cells to which no arachidonic acid was applied (Fig. 4.5). Uptake currents were recorded for 40 minutes at 1 minute intervals and normalised by capacitance which was measured at least every 5 minutes. The time course for each cell was normalised to the magnitude of the uptake current (normalised by capacitance) at t = 7 minutes after patch rupture. The currents were normalised by cell capacitance because, even in the absence of arachidonic acid, there was a steady reduction of the glutamate-evoked current with time which was largely correlated with a decrease of cell capacitance. On average, the uptake current in the control group declined by 45% over 30 minutes recording time; normalisation by capacitance reduced this to 12%. Arachidonic acid was applied to the test group of cells between the 7th and 9th minutes following patch rupture, producing approximately 50% inhibition of uptake. After removal of arachidonic acid there was a rapid partial recovery followed by a sustained period in which the uptake current remained significantly depressed relative to the uptake current in the control group ($P < 0.01$, 0.05 and 0.1 at 10, 20 and 30 minutes after arachidonic acid removal).

Fig. 4.5 Arachidonic acid produces a prolonged inhibition of the uptake current. Graph shows the mean I_{glu}/C (± SEM) for two groups of cells as a function of time after patch rupture. The I_{glu}/C time course for each cell was normalised to the I_{glu}/C at $t = 7$ minutes before averaging. Control group (open symbols) to which 30μM glutamate was applied at 1 minute intervals for 40 minutes following patch rupture ($t = 0$). The same protocol was applied to the test group, but, in addition, 10μM arachidonic acid was applied between the 7th and 9th minutes. A t-test of the significance of the difference between the two groups gives $P < 0.01$, 0.05 and 0.1 at $t = 19$, 29 and 39 minutes. External solution B, pipette solution Y, holding potential -43mV. Cell capacitance for normalisation was measured at least every 5 minutes.

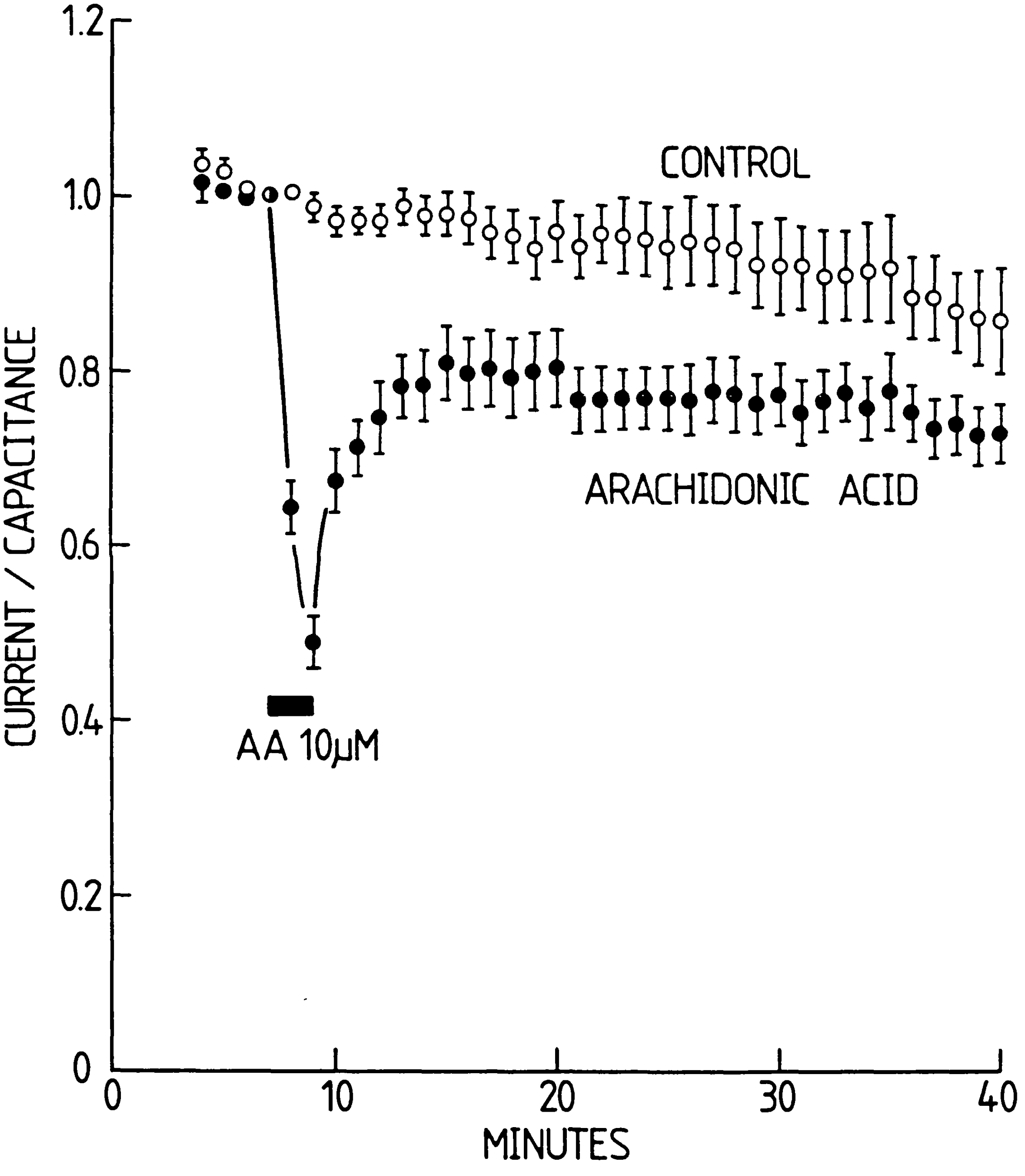
1.2
1.0
0.8
0.6
0.4
0.2
0
CURRENT / CAPACITANCE
0
10
20
30
40
MINUTES
CONTROL
ARACHIDONIC ACID
AA 10μM

Chapter 5.

A fluorescence assay for glutamate uptake

5.1 Introduction

High affinity, sodium-dependent glutamate uptake is not the only mechanism which transports glutamate into cells. In particular, 'chloride-dependent' (Pin et al, 1984) and 'low affinity' (Logan & Snyder, 1972) glutamate uptake systems have been described. The results in chapter 3 and in Brew and Attwell (1987) show that such systems do not contribute to the uptake current recorded in Müller cells. It is not known, however, whether these systems are electrogenic. If they were electroneutral, they would of course not be detected by the voltage-clamp method. Thus, in order to assess whether such systems operate in Müller cells, a different method of detecting glutamate uptake is necessary.

In Brew & Attwell (1987) and in chapter 3, variations of the magnitude of the glutamate-evoked current in Müller cells were interpreted as reflecting changes of the underlying rate of glutamate uptake. For example, the inhibition of the glutamate-evoked current induced by depolarisation was interpreted as showing that the rate of glutamate uptake is slower at positive holding potentials. Such conclusions assume that, under a variety of conditions, the ratio of glutamate transported to charge transported remains constant. The validity of this assumption has not been proven, and since there are a number of reports that the stoichiometry of uptake may change (Burckhardt et al, 1980; Murer et al, 1980; Nelson et al, 1983), it is necessary to test it. For this, a measure of glutamate uptake, independent of the uptake current, is required.

Thus to address both of the above problems, a technique was required for measuring glutamate uptake into isolated, voltage-clamped cells, other than by measuring the current that uptake produces. Such a method was developed by modifying a fluorescence assay for glutamate (Nicholls & Sihra, 1986; Nicholls et al, 1987). The basis of this assay is the reaction catalysed by glutamate dehydrogenase (GDH)

$$\text{glu} + \text{NAD(P)}^+ + H_2O \leftrightarrow \alpha\text{-ketoglutarate} + \text{NAD(P)H} + NH_4^+ + H^+$$

NADH and NADPH are fluorescent, allowing the progress of the reaction to be monitored using fluorescence measurements. Both compounds have similar excitation and emission spectra, with an absorption peak at 340nm and an emission peak at 455nm. Nicholls & Sihra (1986) assayed glutamate release from synaptosomes by including NAD and GDH in the incubation medium and measuring the NADH fluorescence.

In order to use this assay inside a Müller cell, it is necessary to supply only NAD in the patch pipette. It is not necessary to introduce GDH into the cell, because glial cells have an endogenous GDH activity (Hertz, 1979). GDH is localised in the mitochondria (Madl et al, 1988), so the GDH activity is not expected to be rapidly dialysed out of the cell during whole-cell recording. Clearly, glutamate which has been taken up into the cytoplasm must be transferred to the mitochondrion before metabolism by GDH. There are at least two mechanisms by which this could be achieved: glutamate/aspartate exchange or glutamate and proton co-transport (LaNoue & Schoolwerth, 1979).

To use this assay to measure glutamate influx, isolated Müller cells were whole-cell patch-clamped as before (methods, chapter 3), except that all the pipette filling solutions used contained the following additions: 5mM NAD, 100μM malonate and 20mM 2-deoxy-D-glucose. Malonate is a competitive inhibitor of the Kreb's cycle enzyme succinate dehydrogenase (K_i 18μM, Dervartanian & Veeger, 1964) and 2-deoxy-D-glucose is metabolised to

2-deoxyglucose-6-phosphate which competitively inhibits the glycolytic enzyme phosphoglucose isomerase (Wick et al, 1957; Horton et al, 1973). These compounds were included in an attempt to lower the basal NADH concentration. The fluorescence of the isolated cell was monitored using a photomultiplier (see Methods).

The aims of these fluorescence experiments were threefold. Firstly, to investigate the mechanism(s) by which Müller cells take up glutamate; whether 'chloride-dependent' or electroneutral uptake processes contribute (see section 6.2). Secondly, to confirm qualitatively that manipulations which alter the magnitude of the glutamate-evoked current also reduce the uptake, as measured by this fluorescence method. Thirdly, to attempt to test quantitatively the assumption that glutamate uptake operates with a fixed glutamate:charge transport ratio under a variety of conditions. This was investigated under the conditions of changed glutamate concentration, altered holding potential, lowered internal potassium concentration and raised external potassium concentration.

In all experiments, except those in which potassium concentrations were varied, pipettes contained solution R (see table 2.7) and the extracellular solution was B (see table 2.1). Before analysis, current records were filtered at 30Hz and fluorescence records at 5Hz, except for the fluorescence trace in Fig. 5.1 where the fluorescence was filtered at 2Hz. Absolute current and fluorescence baseline levels have not been reproduced in the figures.

5.2 The glutamate-evoked fluorescence response

Figure 5.1 shows a typical record from an experiment in which glutamate uptake into an isolated Müller cell was monitored by simultaneous electrical and fluorescence measurements. As before, application of 30μM L-glutamate to a whole-cell patch-clamped Müller cell at -83mV evokes an inward current (upper trace) reflecting electrogenic

Fig. 5.1. The glutamate-evoked fluorescence change is sodium-dependent. Upper trace: membrane current. Lower trace: single cell fluorescence. 30μM glutamate applied to an isolated Müller cell whole-cell patch-clamped at -83mV with solution R in the pipette and extracellular solution B (107mM $[Na]_o$). Replacement of the external sodium with choline (changing to solution C with x=0) reversibly abolishes both the glutamate-evoked current and the glutamate-evoked fluorescence response.

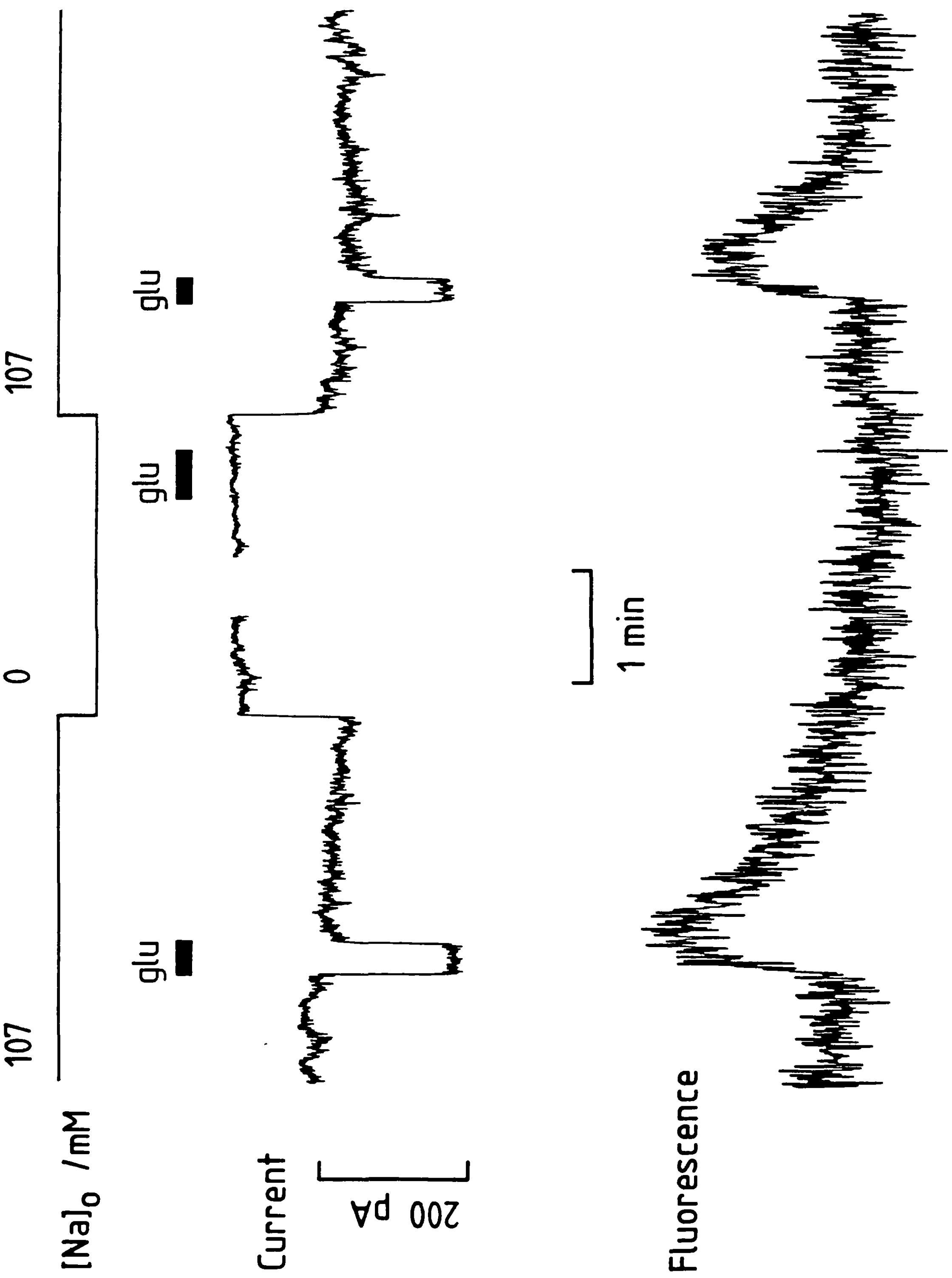
[Na]o /mM
107
0
107
glu
glu
glu
Current
200 pA
1 min
Fluorescence

glutamate uptake (Brew & Attwell, 1987).

After patch rupture and illumination of the cell, the single cell fluorescence declined, reaching a steady level after about 7 minutes. This was typical; an example of part of this decline can be seen in Fig. 5.2. The cause of this decline was not investigated, but is presumed to represent a mixture of two processes. Firstly, there is probably a decrease of cell NADH concentration due to the actions of malonate, 2-deoxyglucose and dialysis of the cell interior by the pipette solution. Secondly, some form of photochemical reaction or bleaching may also contribute, because a decline of fluorescence was also observed in illuminated cells which were not whole-cell patch-clamped. The traces in Fig. 5.1 were obtained after the fluorescence had reached a steady level. The application of glutamate evoked a sharp rise of fluorescence which peaked before the glutamate was washed off and recovered slowly after removal of the glutamate.

5.3 Sodium-dependence of the fluorescence response

Although this fluorescence increase is consistent with activation of glutamate uptake, and metabolism of accumulated glutamate by GDH increasing the concentration of NADH, the fluorescence might, in principle, be due to other actions of glutamate. Müller cells do not appear to express glutamate-gated channels (Brew & Attwell, 1987), so activation of channels can be excluded as a cause of the fluorescence response. Glutamate may, however, be acting at a receptor which mobilises calcium from intracellular stores, such as has been recently described in cultured astrocytes (Cornell-Bell et al, 1990). A rise of intracellular calcium might then alter the redox state of the cell. Another possibility is that glutamate enters the cell as a weak acid or by a 'chloride-dependent' glutamate uptake system (Pin et al, 1984; Waniewski & Martin, 1984; Zaczek et al, 1987).

Fig. 5.2. Aspartate does not evoke a fluorescence response. 30μM L-glutamate applied at -3mV evokes a small current and a marked fluorescence response. 30μM L-, and D-aspartate applied at -83mV evoke large inward currents, but no fluorescence responses. Pipette solution R. Extracellular solution B.

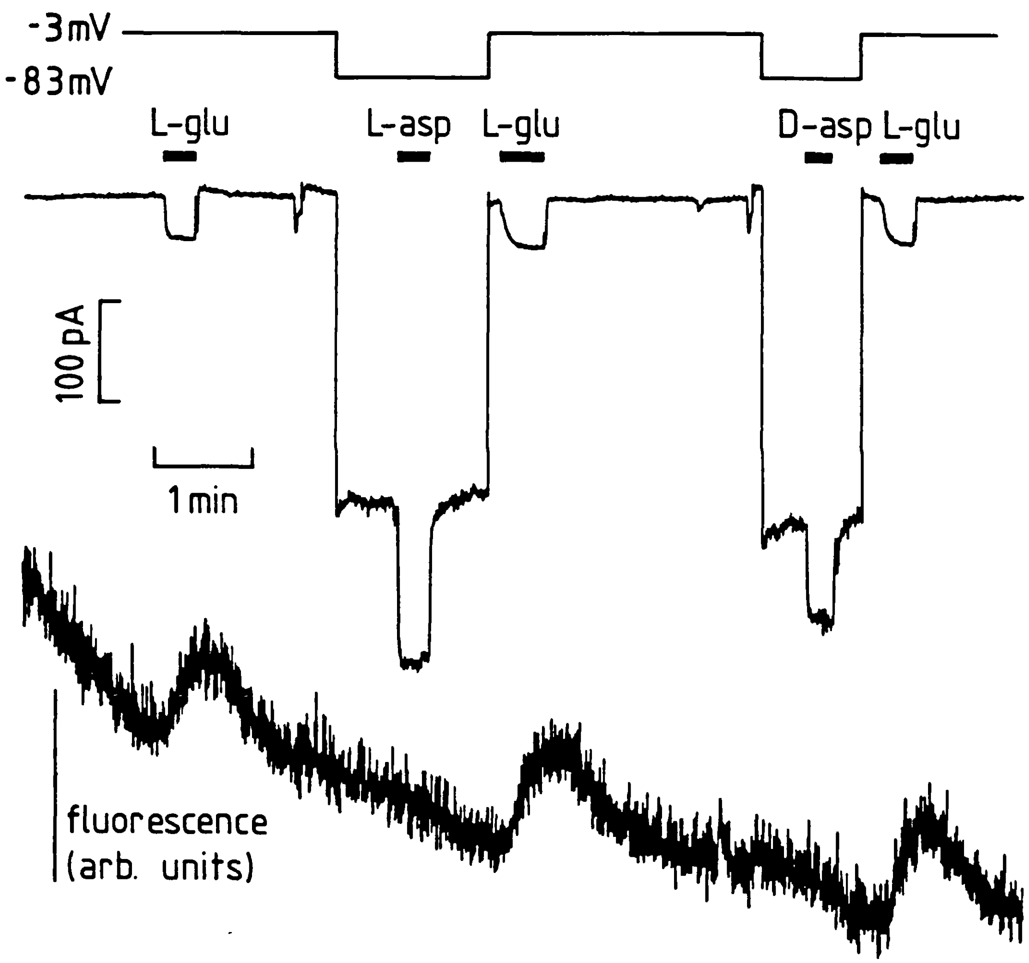
-3mV
-83mV
L-glu
L-asp
L-glu
D-asp
L-glu
100 pA
1 min
fluorescence
(arb. units)

The result shown in Fig. 5.1 is evidence which strongly supports the hypothesis that the fluorescence response depends upon the activation of sodium-dependent glutamate uptake. It shows that complete replacement of the 107mM extracellular sodium with choline (changing from solution B to solution C, with x=0; see table 2.1) reversibly abolishes the glutamate-evoked fluorescence response, as well as the glutamate-evoked current. Similar results were obtained in 3 cells and in 3 other cells in which $[Na]_o$ was reduced to 2mM rather than zero.

This rules out glutamate entry as a weak acid, or by the chloride-dependent uptake system, as neither route is sodium-dependent (Pin et al, 1984; Waniewski & Martin, 1984; Zaczek et al, 1987). It also shows that glutamate is not acting at a receptor linked to the mobilisation of intracellular calcium, because this action of glutamate is independent of extracellular sodium (Cornell-Bell et al, 1990).

5.4 Specificity for glutamate

The complete sodium-dependence of the glutamate-evoked fluorescence response indicates that activation of sodium-dependent uptake is necessary for its generation, but does not prove that it is specifically the influx of glutamate and its subsequent metabolism which gives rise to the fluorescence. Glutamate uptake has a complex stoichiometry and the uptake of glutamate will be accompanied by an influx of sodium (Stallcup et al, 1979; Baetge et al, 1979) and possibly of protons (Nelson et al, 1983). There is probably also an efflux of potassium ions, as it is likely that the carrier counter-transports glutamate and potassium (Kanner & Sharon, 1978a & b; section 6.4). It is necessary to exclude the possibility that it is the accompanying fluxes of inorganic ions, rather than the glutamate influx, which cause the rise of fluorescence.

Evidence which rules out this possibility is shown in

Fig. 5.2, where the effects of L-glutamate are compared with those of L-, and D-aspartate. Both L, and D-aspartate are taken up by the same carrier as L-glutamate (Balcar & Johnson, 1972) and are therefore likely to generate the same ion fluxes as glutamate. Neither L-, nor D-aspartate, however, is a substrate for glutamate dehydrogenase (Euler et al, 1938) and thus should not evoke a fluorescence change after being taken up. In Fig. 5.2 applications of D- and L-aspartate (30μM) both evoked an inward current, consistent with electrogenic uptake, but neither evoked a detectable fluorescence change. In contrast, the interleaved control applications of glutamate generated both an inward current and a fluorescence rise.

The cell was depolarised to -3mV for the applications of glutamate to ensure that the current, and presumably the accompanying ion fluxes, evoked by glutamate were smaller than those evoked by aspartate. At -83mV, glutamate would have evoked a larger uptake current than aspartate (Fig. 3.6 shows a comparison of the current magnitudes for D-asp and L-glu at the same potential). Changes of holding potential did not influence the background fluorescence in this or any other of the cells recorded from.

These results (seen in 3 cells) indicate that the fluorescence rise is caused by glutamate influx and its subsequent metabolism, probably by glutamate dehydrogenase.

5.5 Quantitation of the glutamate-evoked fluorescence response

With the fluorescence response characterised as described above, it could be used to monitor glutamate uptake in a qualitative manner. For example, the abolition of the glutamate-evoked fluorescence response by sodium removal confirms the sodium-dependence of glutamate uptake (ignoring the circular logic). However, if fluorescence measurements are to be used to assess different rates of glutamate uptake and to compare these to the glutamate-evoked current, it is necessary to quantify the fluorescence response and then relate it to the rate of glutamate influx into the Müller cell.

Figure 5.3 shows how this was done for a specimen glutamate-evoked current and the accompanying fluorescence response. As before, the current was assessed by measuring the magnitude of the peak inward current (Brew & Attwell, 1987; chapter 3). The peak inward current is reached when the change to glutamate containing solution is complete. The inward current then declines slowly from the peak (possibly due to Na^+ and glutamate accumulation within the cell).

An objective measure is required to quantitate the fluorescence response. In principle, it would be desirable to measure the initial rate of rise of the response, because this would depend on the rate of glutamate influx, but should not be influenced by substrate depletion and product build up. However, the initial rate of rise of fluorescence would not be a very useful measure to compare with the peak glutamate-evoked current (the ultimate aim). This is because the time-to-peak of the current, which is limited by the speed of solution change around the cell, can be up to 3 seconds. So the initial rate of rise of fluorescence would refer to a time at which the peak current had not yet been reached. Clearly, if the fluorescence and current measures are to be compared, the fluorescence measure must correspond to a time after the solution change has been completed.

It was therefore decided to measure the fluorescence rise over the first 6 seconds following the onset of the inward current (or the best estimate of the time at which glutamate reached the cell if no current was detectable). The graphical method used to do this is illustrated in figure 5.3. In cases where the fluorescence was changing before the application of glutamate, this rate of change was subtracted from the rate of change of the response onset. Measuring the fluorescence rise over 6 seconds

Fig. 5.3. Quantification of the fluorescence response. A graphical method was used to measure the rise of fluorescence over 6s from the origin of the current response. Sometimes the fluorescence baseline was not flat before a response. In these cases the rise of the fluorescence was measured from an extrapolation of the baseline. The straight lines were fitted to the fluorescence trace by eye.

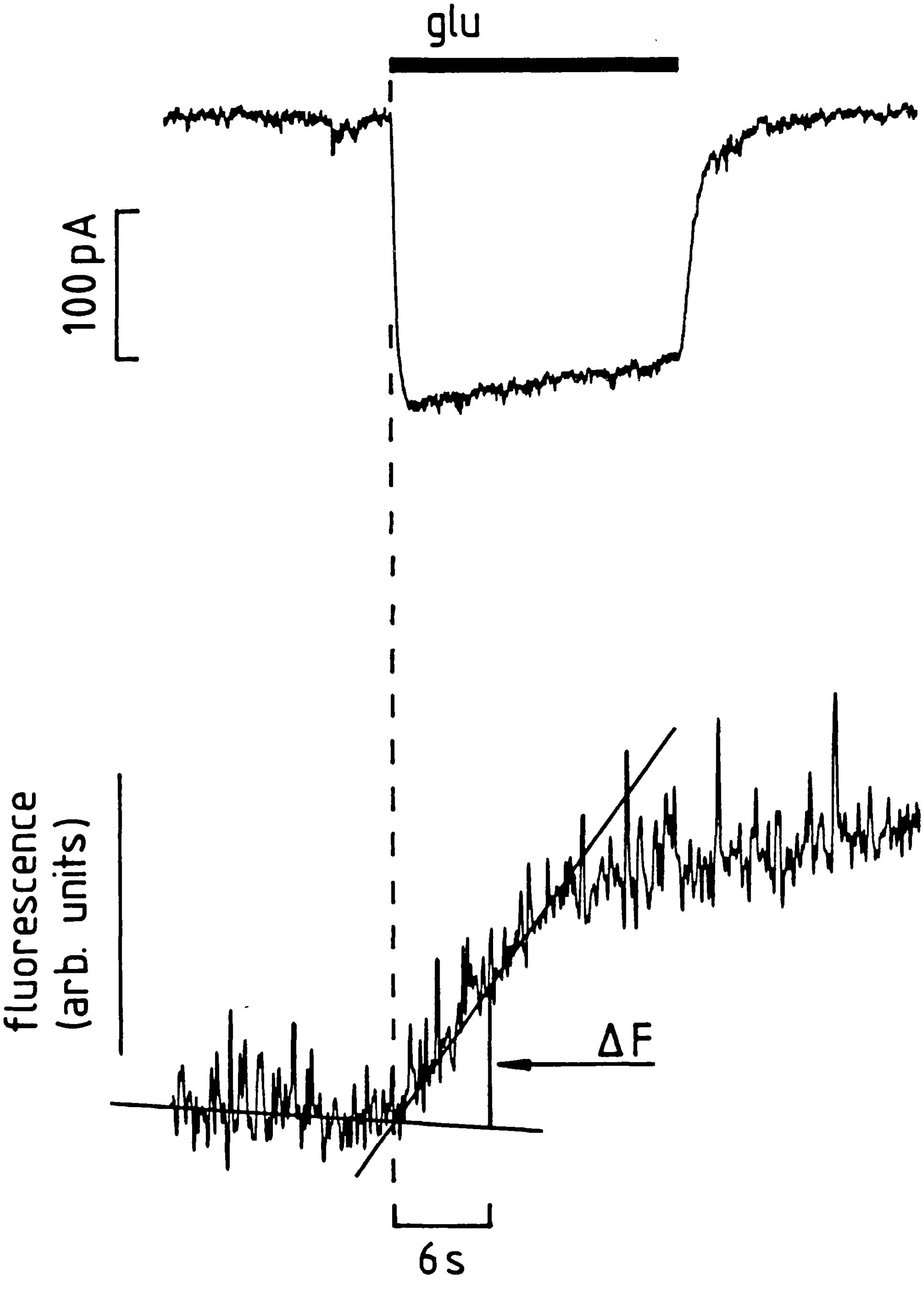
glu
100 pA
fluorescence
(arb. units)
ΔF
6 s

represents a compromise: the measure refers to a time after the solution change is complete, but still gives values similar to the initial rate of rise, because the fluorescence happens to rise linearly for at least 6 seconds in most cells. In some cells this method of measurement gave values which were lower than would have been obtained by estimating the initial slope; in a few cells it led to a greater value.

The size and rate of rise of the fluorescence response varied considerably between cells and with time in a single cell. For this reason the fluorescence response under test conditions (eg. altered holding potential) was compared with two control responses which bracketed it. The control responses for all experiments, except those in which the external potassium concentration was varied, were obtained by applying 30μM glutamate at -83mV.

After an application of glutamate a period of time had to elapse before a second application would evoke a similar fluorescence response. Glutamate applications were therefore separated by intervals of approximately 4 minutes. For all of the responses included for analysis in the following experiments, the fluorescence had returned to baseline before the succeeding application of glutamate. For 6 pairs of fluorescence responses to 30μM glutamate at -83mV separated by 4 minutes, the fluorescence measure (rise over 6s) of the second response was 93 ± 8% (mean ± SEM) of that of the first, while the mean glutamate-evoked current was reduced to 94 ± 4%.

5.6 Variation of the glutamate-evoked current and fluorescence with glutamate concentration

Using the above method of quantifying the fluorescence response, experiments were performed to determine the dependence of the glutamate-evoked current and fluorescence on the glutamate concentration. Traces from a typical experiment are shown in Fig. 5.4.

Fig. 5.4. The glutamate-evoked fluorescence response varies with glutamate concentration. 3μM glutamate evoked a smaller current and a slower rising fluorescence response than the control applications of 30μM glutamate. The 3μM current was 20% of the mean of the 30μM controls. The 3μM fluorescence measure was 50% of the mean of the 30μM controls. Holding potential -83mV. Pipette solution R. Extracellular solution B.

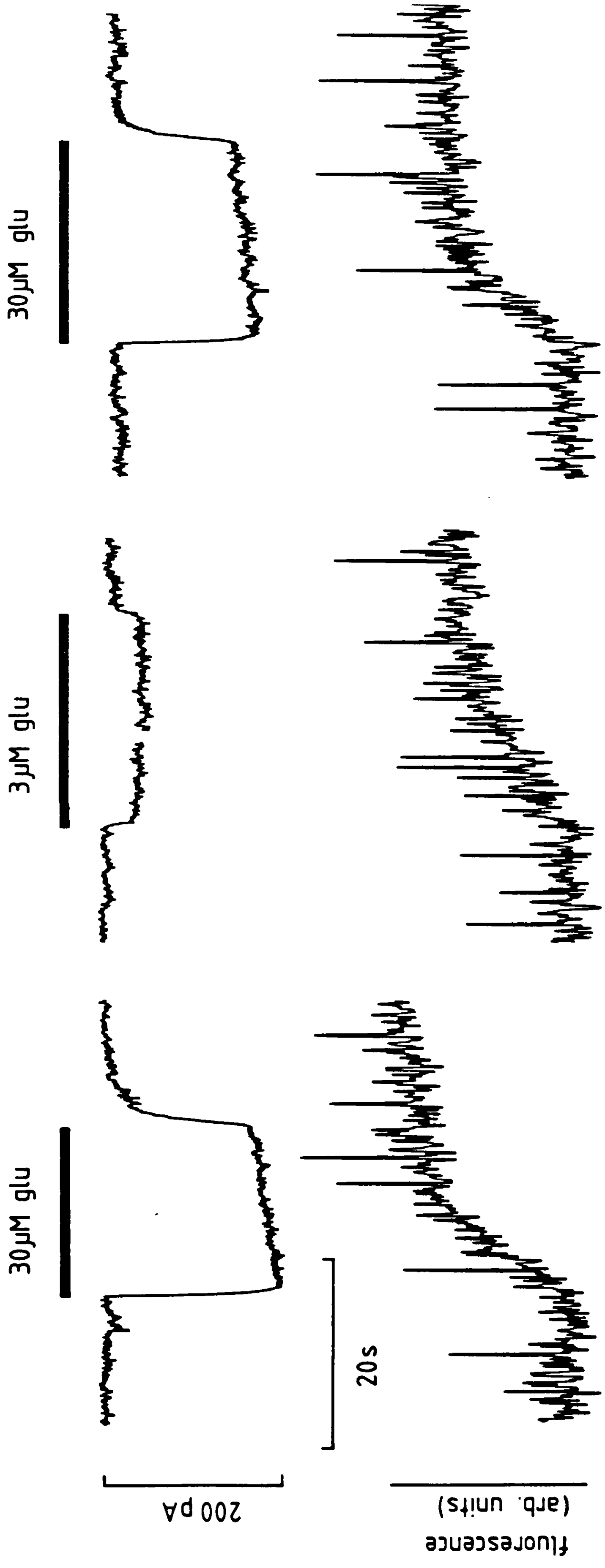
30μM glu
3μM glu
30μM glu
20s
200 pA
fluorescence
(arb. units)

A test application of 3µM glutamate is shown between preceding and subsequent control applications of 30µM glutamate. The reduced glutamate concentration evokes a smaller current, about 20% of control, and a slower rising fluorescence response (about 50% slower than control), consistent with a slower rate of uptake.

The graph in Fig. 5.5 shows the pooled results from several such experiments. It is a plot of the mean current and fluorescence responses, normalised to their values for 30µM glutamate (ie. 2 x test / {pre-test control + post-test control}), as a function of the test concentration of glutamate. As previously described, the dose-response data for the glutamate-evoked current (filled symbols) are well fitted by a Michaelis-Menten curve (Brew & Attwell, 1987). The apparent K_m here is 21µM ($I_{max}/I_{30\mu M\ [glu]}$ = 1.71, obtained from an Eadie-Hofstee plot). The fluorescence data (open symbols) are also approximately fitted by a Michaelis-Menten curve with an apparent K_m of 2.8µM ($F_{max}/F_{30\mu M\ [glu]}$ = 1.09; from an Eadie-Hofstee plot).

This dependence of the fluorescence response on glutamate concentration shows that it is a more sensitive way of detecting glutamate uptake than measuring the glutamate-evoked current. For instance, as shown in Fig. 5.10, 1µM glutamate evokes a current that is at the limit of detection (given the noise levels in these experiments), but it still gives a marked fluorescence rise (the mean fluorescence measure for 1µM glutamate is 35% of that produced by 30µM glutamate).

Fig. 5.5. Dose-response curves for the glutamate-evoked current and fluorescence response. Individual data obtained as in Fig. 5.4: control 1, test, control 2, where the controls were responses to 30μM glutamate. The graph shows the mean normalised (ie. 2 x test response / {control 1 + control 2}) current (filled circles) and fluorescence response (open circles) as a function of the test glutamate concentration. Error bars are ± 1 SEM. The figure by each point represents the number of cells recorded. Currents were too small to measure accurately below 3μM glutamate. Both sets of data are fitted with Michaelis-Menten curves. For the current: K_I = 21μM, $I_{max}/I_{30\mu M\ [glu]}$ = 1.71. For the fluorescence: K_F = 2.8μM, $F_{max}/F_{30\mu M\ [glu]}$ = 1.09. All experiments carried out at -83mV. Pipette solution R. Extracellular solution B.

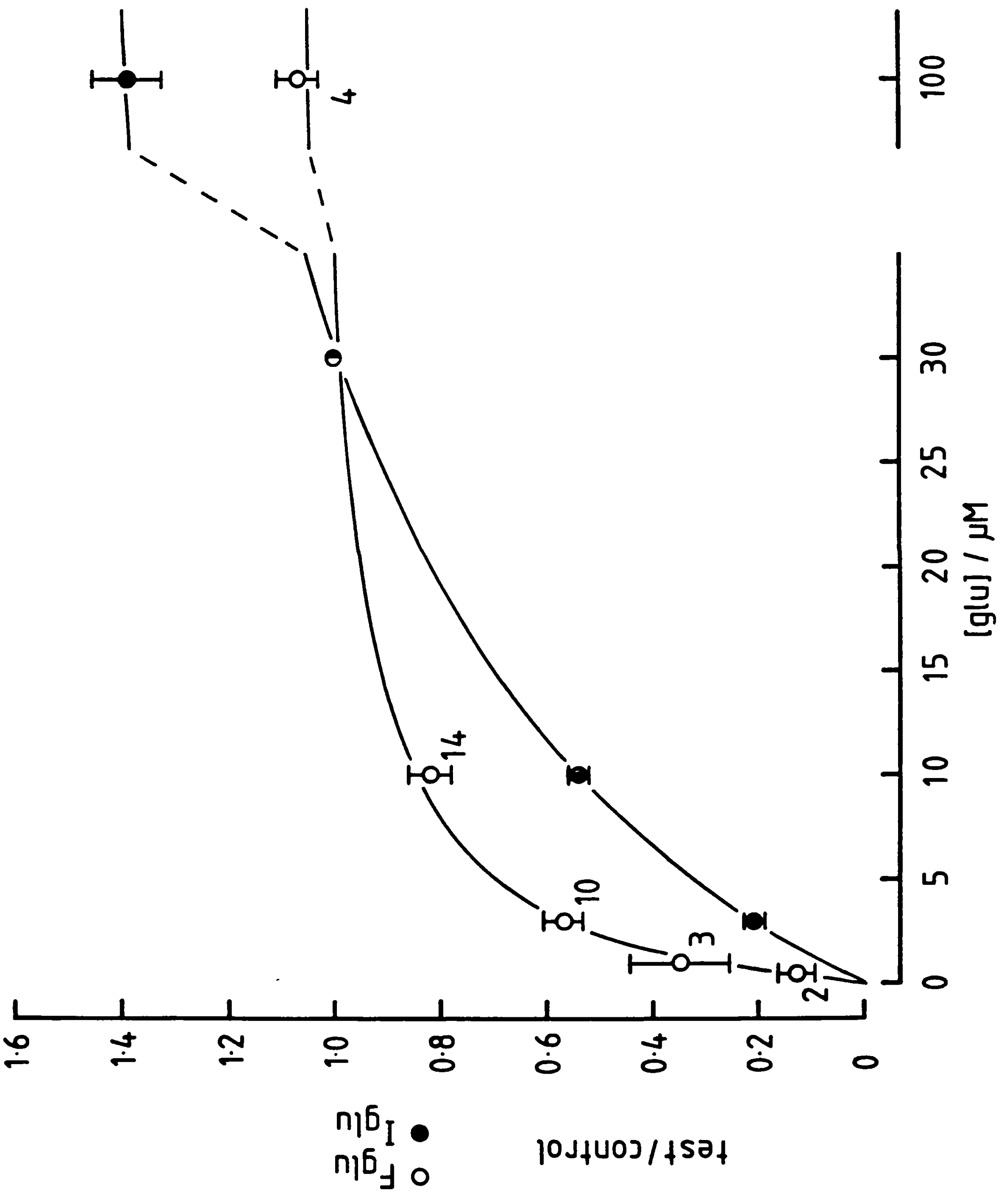
○ Fglu
● Iglu
test / control
0
0·2
0·4
0·6
0·8
1·0
1·2
1·4
1·6
0
5
10
15
20
25
30
100
[glu] / μM
2
3
10
14
4

5.7 Relation of the fluorescence response to glutamate uptake

The results shown in Fig. 5.5 can be used to obtain a relation between the fluorescence response and glutamate uptake, if it is assumed that the magnitude of the glutamate-evoked current at different glutamate concentrations is proportional to the underlying rate of glutamate uptake. For this to be true, changes of glutamate concentration must not alter the stoichiometric ratio of charge transported per glutamate taken up. Consistent with this assumption is the fact that both the uptake current (in salamander and rabbit Müller cells) and the amount of glutamate uptake (in a variety of preparations, including rabbit Müller cells) depend on the glutamate concentration in a Michaelis-Menten manner (White & Neal, 1976; Hertz, 1979; Erecinska, 1987; Lerner, 1987; Sarantis & Attwell, 1990).

Having made this assumption, the dependence of the fluorescence response on the rate of uptake is obtained by plotting the fluorescence response as a function of the glutamate-evoked current. Fig. 5.6 shows the data from Fig. 5.5 replotted to show the form of the relation between the fluorescence response and the glutamate uptake current. The fluorescence response depends on the uptake rate (=current) according to a Michaelis-Menten relation: eqn (5.3) below, with $K'_F = 0.26$ and $F'_{max} = 1.25$. The curve was fitted using a Eadie-Hofstee plot of the four glutamate concentrations for which reliable current values were obtained. The two leftmost points had current values assigned to them, calculated from the known Michaelis-Menten dependence of the current on glutamate concentration (see Fig. 5.5).

Given that both the current and fluorescence responses depend on the glutamate concentration in approximately Michaelis-Menten fashion (Fig. 5.5), it can be shown that the fluorescence response also depends on the glutamate-evoked current according to a Michaelis-Menten relation.

Fig. 5.6. Fluorescence-current relation for the dose-response data. Data from Fig. 5.5 have been replotted with the fluorescence as a function of the current. Error bars are ± 1 SEM. The figure by each point is the number of cells recorded. The Michaelis-Menten curve has the parameters: $K_F = 0.26$ and $F_{max} = 1.25$. The two leftmost points, corresponding to 0.5 and 1μM glutamate, are plotted at predicted current values (0.04 and 0.08 respectively), calculated from the observed Michaelis-Menten dependence of the current on the glutamate concentration.

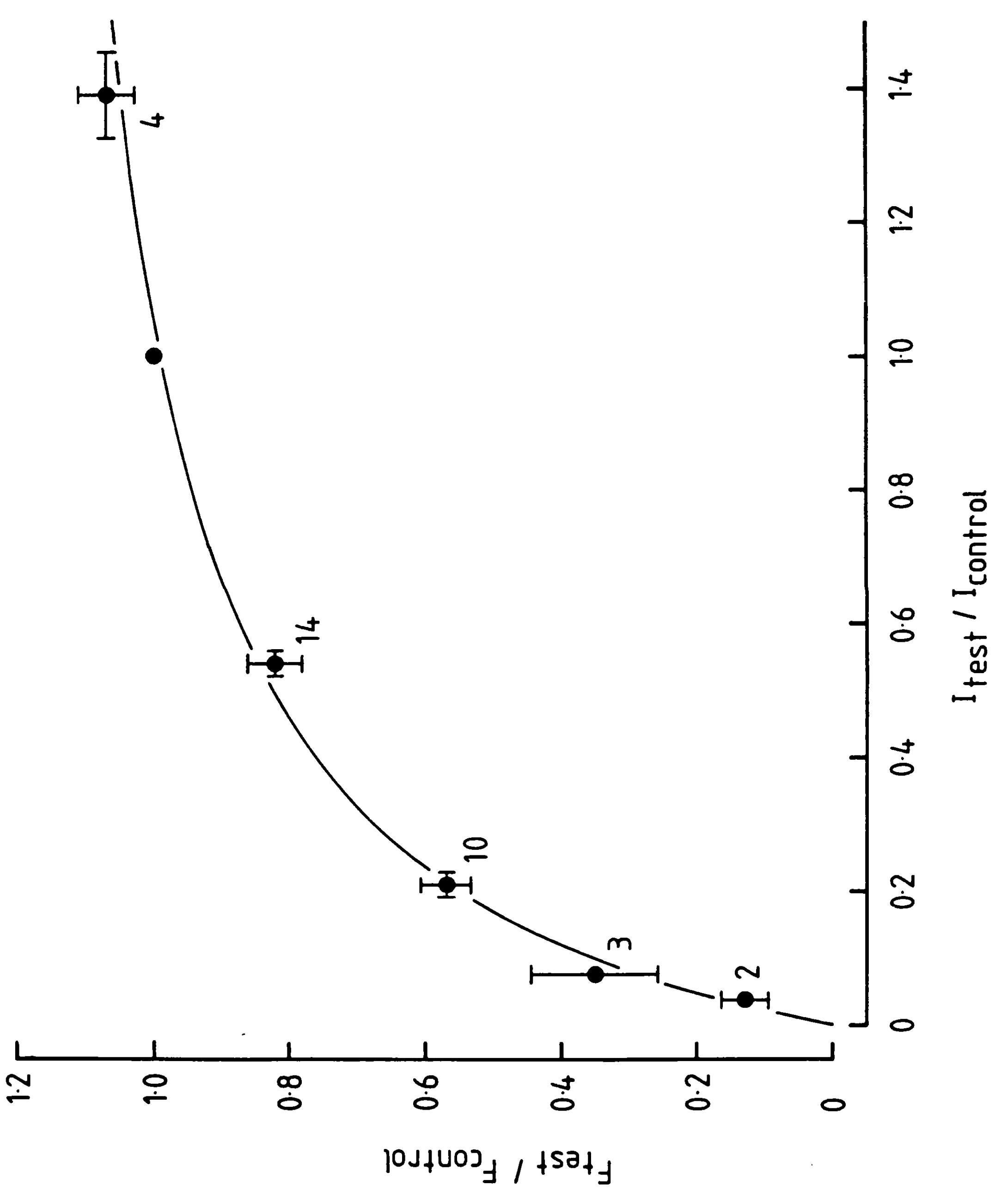
F_test / F_control
0
0·2
0·4
0·6
0·8
1·0
1·2
I_test / I_control
0
0·2
0·4
0·6
0·8
1·0
1·2
1·4
2
3
10
14
4

Let K_I, I_{max}, K_F and F_{max} be the Michaelis-Menten parameters for the current and fluorescence curves in Fig. 5.5, respectively, such that

$$I = I_{max} \frac{[glu]}{[glu] + K_I} \tag{5.1}$$

$$F = F_{max} \frac{[glu]}{[glu] + K_F} \tag{5.2}$$

Then by eliminating the substrate concentration, [glu], it can be seen that the relation between fluorescence and current also has a Michaelis-Menten form

$$F = \frac{F'_{max}\, I}{I + K'_F} \tag{5.3}$$

where $F'_{max} = \frac{K_I\, F_{max}}{(K_I - K_F)}$ and $K'_F = \frac{K_F\, I_{max}}{(K_I - K_F)}$.

Substitution of the parameters from Fig. 5.5 into this equation gives predicted values of $K'_F = 0.25$ and $F'_{max} = 1.25$ which agree very closely with those (0.26 and 1.25) obtained by fitting the curve directly. The precise reasons for the form of the relation between the fluorescence response and uptake rate are not known, but saturation of the system carrying glutamate into the mitochondrion, or saturation of the enzyme GDH itself, could both account for the observed saturation of the fluorescence response at large uptake rates.

The fluorescence-current relation in Fig. 5.6 shows that the fluorescence response varies in an approximately Michaelis-Menten fashion with the rate of glutamate uptake (subject to the validity of the assumption that changes of [glu] do not change the ratio of charge and glutamate transported). This 'calibration curve' can now be used to assess quantitatively changes of the fluorescence response obtained by manipulating the magnitude of the glutamate-evoked current in other ways: by changing the holding potential, or varying the internal potassium concentration, for example. If, under such conditions, the glutamate: charge transport ratio is unchanged, then the fluorescence and current responses should fall on the 'calibration' fluorescence-current relation shown in Fig. 5.6. Conversely, if depolarisation or lowered $[K]_i$ reduced the uptake current by decreasing the charge transported with each glutamate ion (and not by reducing the rate of uptake with a fixed stoichiometry), then these manipulations would result in points falling above the calibration curve at low current values (ie. there would be more uptake per current).

5.8 Voltage-dependence of the glutamate-evoked current and fluorescence change

An important result from measurements of the glutamate-evoked current was a quantitative determination of the voltage-dependence of the uptake current (Brew & Attwell, 1987). It is of importance to test whether the voltage-dependence of the current reflects a similar voltage-dependence of uptake, because inhibition of uptake by depolarisation would contribute to glutamate neurotoxicity. There is a suggestion that glutamate uptake can be electroneutral, at least under certain conditions (Murer et al, 1980). Any electroneutral uptake would, of course, be undetectable using current measurements.

The voltage-dependence of the glutamate-evoked fluorescence response was investigated by performing a series of experiments very similar to those shown in Figs. 5.4, 5.5, & 5.6, the only difference being the test application of glutamate. Instead of applying a different concentration of glutamate, 30μM glutamate was applied at a different holding potential. A specimen trace from these experiments is shown in Fig. 5.7.

Fig. 5.7. Depolarisation reduces the glutamate-evoked fluorescence response. 30μM glutamate applied at -83mV, -3mV and -83mV. The glutamate-evoked current at -3mV was 13% of its value at -83mV, while the fluorescence measure was 53% of its value at -83mV. Pipette solution R. Extracellular solution B.

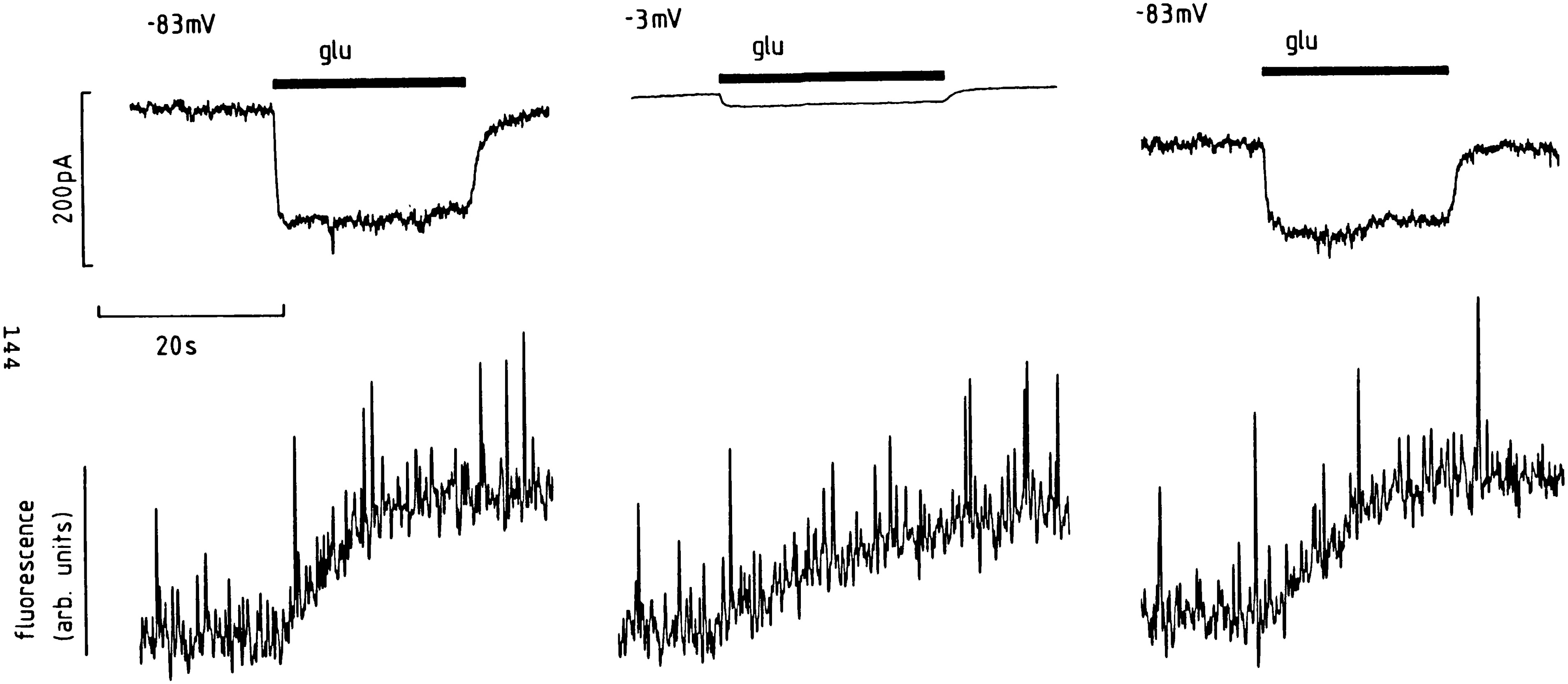
-83mV
glu
-3mV
glu
-83mV
glu
200pA
20s
fluorescence
(arb. units)

Fig. 5.8. Voltage-dependence of the glutamate-evoked fluorescence response. Graph of the mean normalised current (filled circles) and fluorescence (open circles) responses to 30μM glutamate as a function of holding potential. Data obtained as in Fig. 5.7, normalisation procedure as before (Fig. 5.5 legend). Control applications were 30μM glutamate at -83mV. Error bars are ± 1 SEM. The figure by each point is the number of cells recorded. All points are plotted below the horizontal because the glutamate-evoked current is inward. Curves fitted by eye.

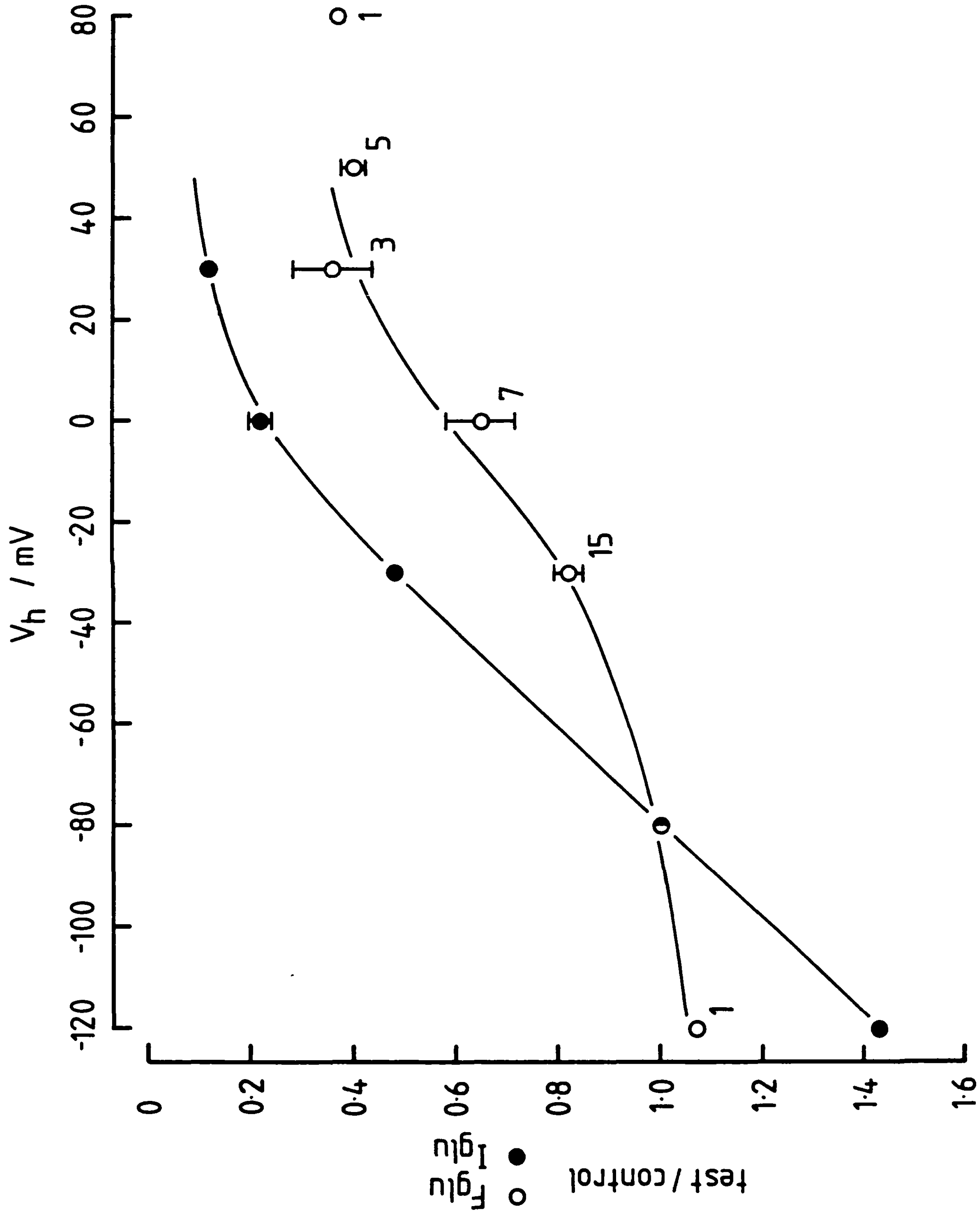
V_h / mV
-120
-100
-80
-60
-40
-20
0
20
40
60
80
0
0·2
0·4
0·6
0·8
1·0
1·2
1·4
1·6
test / control
○ F_{glu}
● I_{glu}
1
15
7
3
5
1

Fig. 5.9. Fluorescence-current relation for the voltage data. The data from Fig. 5.8 are replotted with the mean normalised fluorescence response a function of the mean normalised current response (filled circles). Error bars are ± 1 SEM and the figure by each point represents the number of cells recorded. Data obtained at +47mV and +77mV are omitted because no glutamate-evoked current was resolvable. The smooth curve was not fitted to these data, but is the calibration curve of the fluorescence-current relation from the dose-response data in Fig. 5.6.

The open square shows the mean normalised fluorescence response and the mean normalised current for experiments in which responses with 0 $[K]_i$ and 90mM $[K]_i$ were compared. The mean 0 $[K]_i$ responses were normalised to the mean 90mM $[K]_i$ responses. Error bars are ± 1 SD. Data from 5 test cells and 5 control cells.

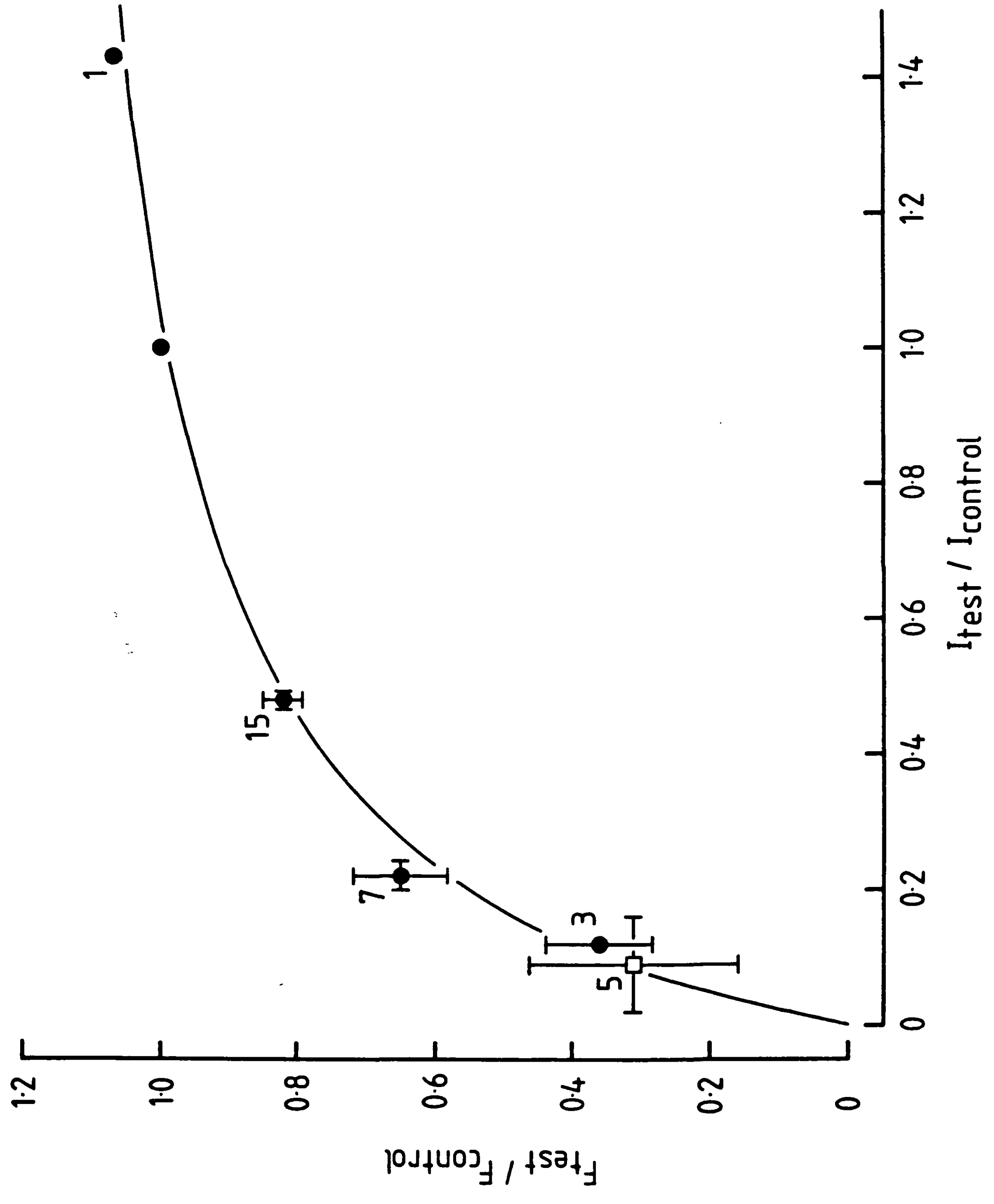

$F_{test} / F_{control}$
0
0·2
0·4
0·6
0·8
1·0
1·2
$I_{test} / I_{control}$
0
0·2
0·4
0·6
0·8
1·0
1·2
1·4
1
15
7
3
5

Depolarisation of the cell from -83mV to -3mV reduced the glutamate-evoked current to 13% of control and slowed the rise of fluorescence to 53% of control, consistent with a decreased rate of glutamate uptake at this depolarised potential. The mean results from these experiments are shown in Fig. 5.8, where normalised current and fluorescence responses are plotted as a function of holding potential. The points are plotted below the horizontal axis, because the glutamate-evoked current is inward.

The decrease of both current and fluorescence responses with depolarisation in Fig. 5.8 confirms qualitatively that depolarisation reduces the rate of glutamate uptake. In order to quantify this relation, the results from Fig. 5.8 are replotted in Fig. 5.9, showing normalised fluorescence as a function of the normalised current (filled circles). The smooth curve through the points is the 'calibration curve' obtained from the dose-response data in Fig. 5.6. The data points from the voltage experiments all fall very close to the curve. This demonstrates that a single relation holds between the glutamate-evoked fluorescence and current, irrespective of whether the uptake current is varied by changes of potential or of glutamate concentration. Thus, provided that the carrier's stoichiometry is not altered by changes of [glu] (see section 5.7) then these data show that the ratio of charge transported to glutamate taken up is also constant when the membrane potential is varied.

At very depolarised potentials (+47mV, +77mV) the glutamate-evoked current becomes undetectable, but the fluorescence response remains about 35-40% of its control value at -83mV. This slow fluorescence response is comparable to that evoked by 1-2μM glutamate at -83mV (see Fig. 5.5). This can also be seen in Fig. 5.10 which shows responses to 1μM glutamate at -83mV and 30μM glutamate at +47mV in the same cell.

Fig. 5.10. The fluorescence response is reduced to a similar extent by depolarisation to +47mV or by reduction of the glutamate concentration to 1μM. Responses from one cell to 30μM glutamate (at -83mV), then to 1μM (-83mV), 30μM (+47mV) and 30μM (-83mV). 1μM glutamate evoked an 8pA current (9% of the mean value with 30μM glutamate at -83mV). No glutamate-evoked current could be resolved at +47mV. The fluorescence responses were 52% (1μM) and 39% (+47mV) of the mean value with 30μM glutamate at -83mV. Pipette solution R. Extracellular solution B.

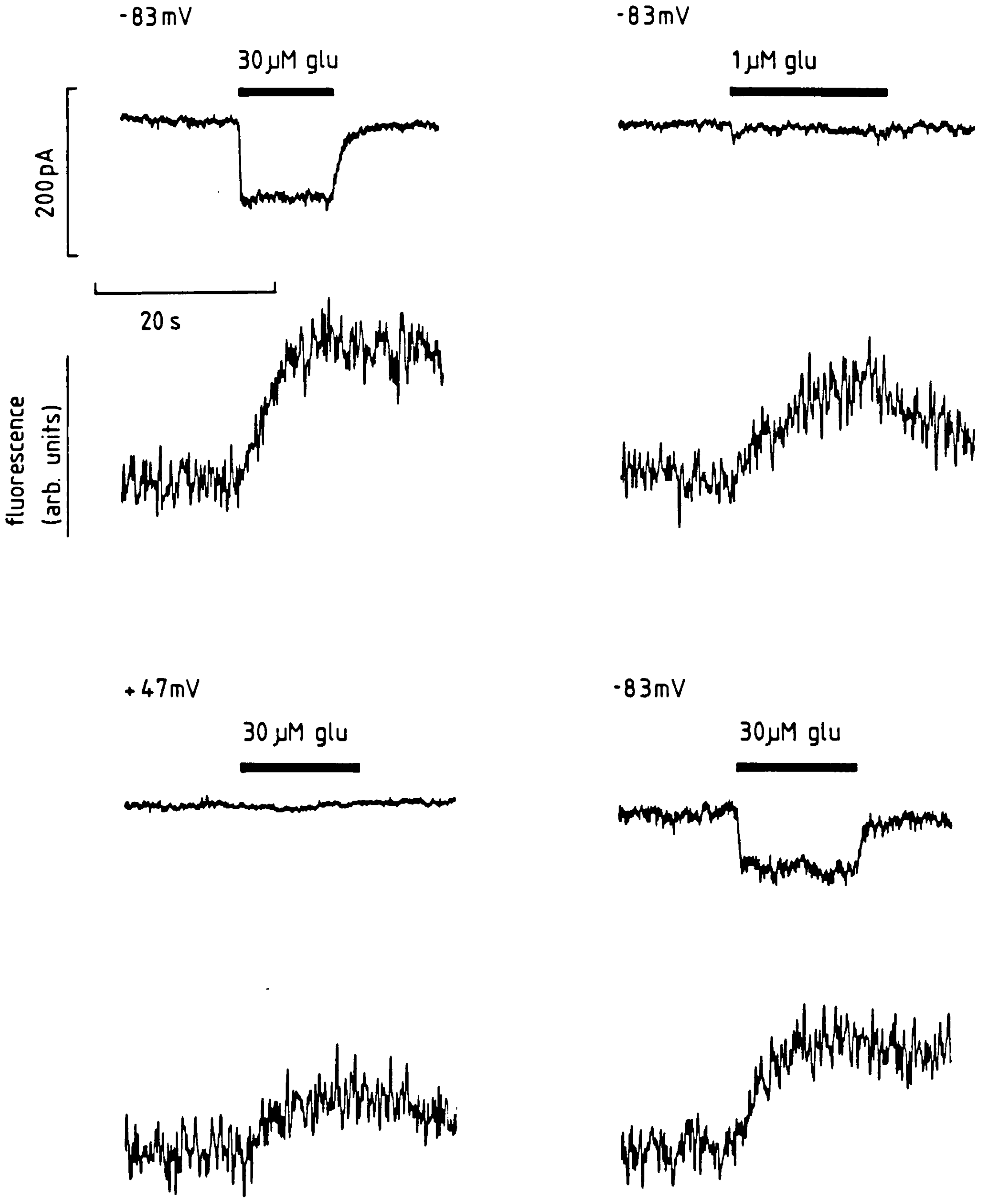
-83mV
30 µM glu
200pA
20 s
fluorescence
(arb. units)
-83mV
1 µM glu
+47mV
30 µM glu
-83mV
30µM glu

Continuing this argument, the mean fluorescence response to 30μM glutamate at +47mV in 5 cells was 40% of that at -83mV. From Fig. 5.6 it can be seen that a 40% fluorescence response is associated with an uptake current 12% of the control (30μM glutamate, -83mV). This information allows an upper bound to be placed on the rate of any voltage-insensitive uptake (ie. electroneutral uptake). Even if all of the fluorescence response at +47mV were generated by electroneutral uptake, its rate would be only 12% of the rate of uptake at -83mV. In fact, given the rather flat voltage-dependence of the glutamate-evoked current at positive potentials, it is possible that electrogenic uptake (with a current too small to resolve) could account completely for the residual fluorescence response in this voltage range.

5.9 Potassium-dependence of the glutamate-evoked fluorescence response

In experiments on the glutamate-evoked current (chapter 3), reduction of the internal, or increase of the external potassium concentration inhibited the uptake current. Probably the uptake carrier counter-transports potassium out of the cell as glutamate is taken up. It is necessary to show that potassium changes have similar effects on the glutamate-evoked fluorescence for two reasons. Firstly, whatever its mechanism, inhibition of uptake by external potassium would contribute to glutamate neurotoxicity (see section 6.9). Secondly, there are reports of sodium-dependent glutamate uptake proceeding, albeit more slowly, in the absence of potassium (Burckhardt et al, 1980; Nelson et al, 1983; but cf Kanner & Sharon, 1978a & b). This presumably occurs with a changed stoichiometry, and may be electroneutral (Murer et al, 1980). The effects of changes of the intra- and extracellular [K] on the glutamate-evoked fluorescence response are described in the next two sections.

5.10 Removal of intracellular potassium

The effects on the glutamate-evoked fluorescence response of replacing intracellular potassium with choline were investigated. Two groups of cells were whole-cell patch-clamped with pipettes containing either, for the control group, solution Q (see table 2.7) which contained 90mM potassium, or, for the test group, solution P which contained no potassium. The experiments were carried out in extracellular solution C (see table 2.1) which also contained no potassium. 30μM glutamate was applied at -81mV, 4.5 minutes after patch rupture, by which time the fluorescence decline was levelling out, and the intracellular potassium concentration was expected to be approaching equilibrium with the potassium concentration inside the pipette (see section 3.6).

Fig. 5.11 shows typical results from these experiments (data from three different cells). With 90mM potassium in the pipette glutamate evoked a large inward current and a fast-rising fluorescence response. With zero potassium in the pipette, glutamate evoked only a very small inward current (if detectable) and a smaller, slower rising fluorescence response, consistent with a reduced rate of glutamate uptake under these conditions. (Two responses with zero internal potassium are shown in Fig. 5.11, to indicate the range of response magnitude).

The control group and the test group contained 5 cells each. These cells were recorded from in strict, alternating sequence: control, test, control etc. There was no significant difference between the groups in terms of mean capacitance or of series resistance, measured shortly before the glutamate application at 4.5 minutes after patch rupture. The mean capacitances were 189 ± 6pF (SEM, control group) and 207 ± 21pF (test group) ($P > 0.4$). The mean series resistances were identical, 2.7 ± 0.2MΩ (SEM, control) and 2.7 ± 0.4MΩ (test group). For analysis, the glutamate-evoked currents were normalised by capacitance.

Fig. 5.11. Removal of intracellular potassium reduces the glutamate-evoked fluorescence response. One control response to 30μM glutamate with 90mM $[K]_i$ (pipette solution Q) and two test responses with 0 $[K]_i$ (pipette solution P) are shown. Data from 3 different cells. All experiments carried out at -81mV with an extracellular solution (D) which contained no potassium. From the left, the currents were 210pA, 20pA and 10pA (the last was an assigned value, see text). The fluorescence measures were in the ratio 1: 0.44: 0.21.

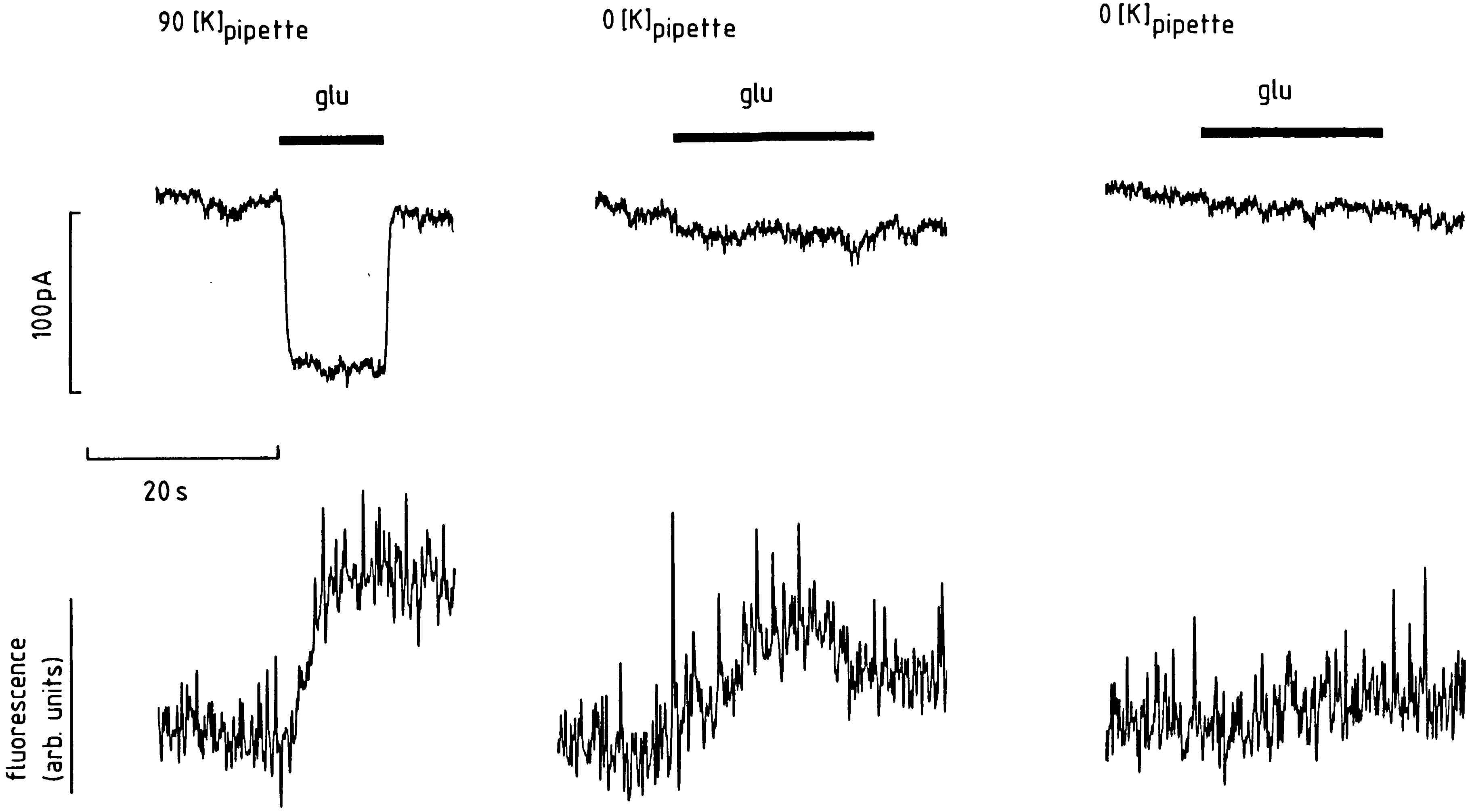
90 [K]pipette
0 [K]pipette
0 [K]pipette
glu
glu
glu
100pA
20 s
fluorescence (arb. units)

In 2 cells in the test group, there was no detectable glutamate-evoked current. These cells were assigned current values of 10pA, half the smallest response that could reasonably have been resolved above the noise in these experiments. Including these values, the mean current evoked by 30μM glutamate at -81mV was 0.11 ± 0.04 pA/pF (SEM) for the test group, while the control group value was 1.21 ± 0.17 pA/pF (SEM), giving a test/control ratio of 9.0 ± 7.1% (SD).

In the absence of internal potassium, the fluorescence response associated with the residual glutamate-evoked current suggests that the current reflects electrogenic glutamate uptake. If glutamate uptake depended absolutely on internal potassium, this result would imply that there was a small amount of potassium remaining in the cell. The alternative is that the current represents electrogenic uptake in the absence of potassium.

The mean fluorescence rise (over 6s) for the test group was 32 ± 15% (SD) of the control value with potassium in the pipette. The fluorescence measure was thus significantly reduced under the test condition ($P < 0.01$). These test/control ratios of current and fluorescence have been plotted on the normalised fluorescence vs. normalised current graph in Fig. 5.9 (open square). The data point falls almost exactly on the calibration curve which was replotted from Fig. 5.6. The close agreement of the experimental data with the calibration curve implies that the ratio of charge to glutamate transported is not altered when uptake is inhibited by lowering $[K]_i$.

What is the rate of glutamate uptake with nominally zero potassium in the cell? From the calibration curve of Fig. 5.6, it can be calculated that a normalised fluorescence response of 32% (the average with 0 $[K]_{pipette}$) is associated with an uptake rate 9% of control. This shows, subject to the validity of the assumption in section 5.7, that removal of internal potassium substantially inhibits glutamate influx.

These conclusions are sensitive to the method used to quantify the fluorescence response. In 2 out of the 5 cells in the test group, the fluorescence response was not linear over 6 seconds, but initially rose rapidly and peaked within 1-2 seconds. Thus, if the initial rate of rise is used to measure the fluorescence response, the reduction of the fluorescence response with 0 $[K]_i$ is not significant ($P<0.2$). See section 5.5 for a justification of the method used to quantify the fluorescence response.

5.11 Raising the extracellular potassium concentration

From the results in section 3.8, it can be seen that raising the extracellular potassium concentration from 0 to 57mM inhibits the glutamate-evoked current by about 40%. Given the form of the relation between fluorescence and current in Fig. 5.6, a 40% decrease in current from control might be expected to reduce the fluorescence response by only about 15%. Such a small change would be difficult to demonstrate clearly. In order to maximise the expected fluorescence change, the control conditions were altered to make the control currents smaller (by holding all the cells at -33mV). This should reduce all of the uptake rates to a range where, according to Fig. 5.6, the fluorescence response is more sensitive to changes of uptake rate.

The specimen trace in Fig. 5.12 shows the protocol of these experiments. 30μM glutamate was applied at -33mV to cells recorded with solution R filling the pipette. The control extracellular solution (E with y=0, see table 2.1) contained no potassium, and the test solution (E with y=57) contained 57mM potassium. The test application of glutamate in raised potassium evokes a smaller current and a slower rising fluorescence response. In four cells in which reliable current values were obtained for all glutamate applications, the mean glutamate-evoked current in 57mM potassium was 45 ± 3% (SEM, n=4) of its control value in zero $[K]_o$.

Fig. 5.12. The glutamate-evoked fluorescence response is inhibited by raising the external potassium concentration. Current and fluorescence responses to 30μM glutamate with (from left) 0, 57mM and 0 $[K]_o$ (extracellular solution E with y = 0, 57 & 0). All at -33mV with pipette solution R. The test current was 41% of control and the test fluorescence response (measured over 10s - see text) was 46% of control.

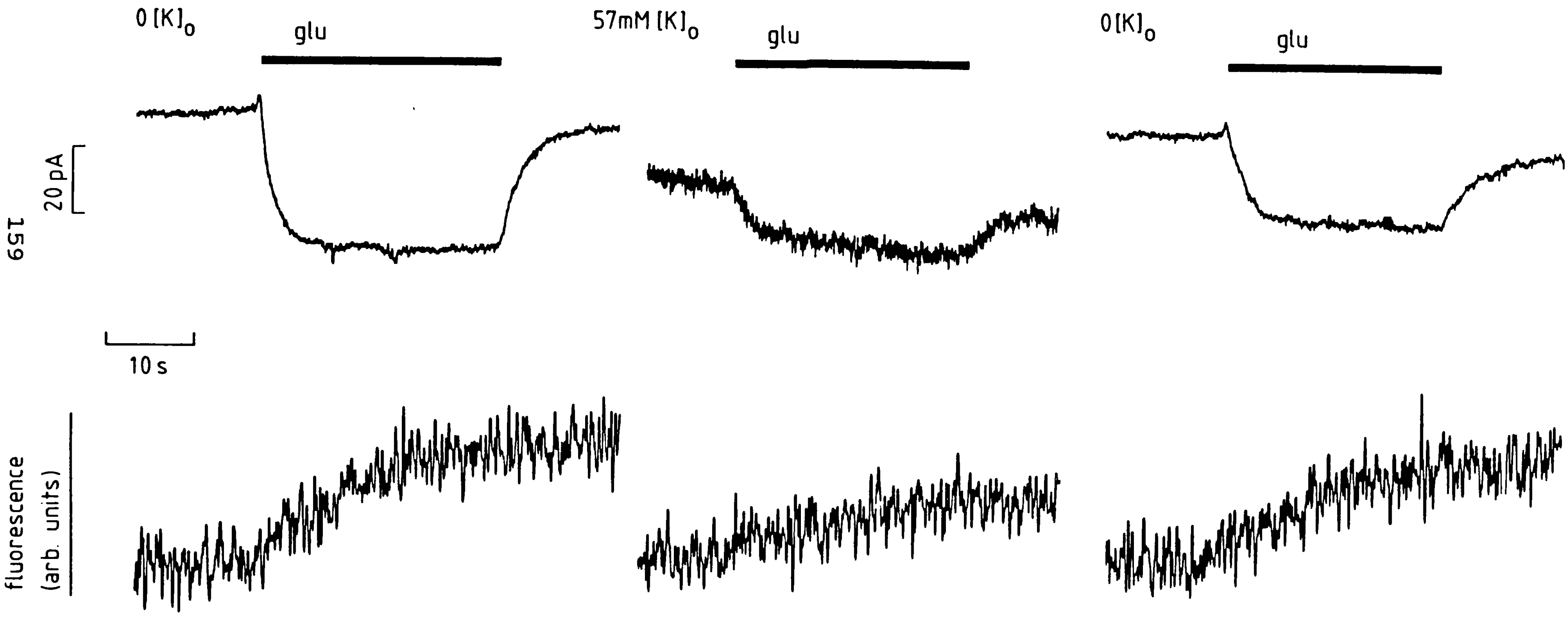
0 [K]$_o$
glu
57mM [K]$_o$
glu
0 [K]$_o$
glu
20 pA
10 s
fluorescence
(arb. units)

The fluorescence rise was measured over 10 seconds in these experiments, for two reasons. Firstly, because the time-to-peak of the current was, in some cells, longer than 3 seconds (the maximum for all the other experiments in this chapter) due to a slower rate of perfusion. Secondly, because application of glutamate sometimes evoked a rapid fluorescence transient, or spike, apparently superimposed on the normally observed steadily rising response. An example is shown in Fig. 5.13 (right-hand fluorescence trace). The mechanism of this phenomenon is unknown: its sodium-dependence was not tested. These spikes occurred in 4 out of 7 cells, sometimes only appearing when glutamate was applied in 57mM $[K]_0$. To avoid contamination of the fluorescence measurements by these spikes, which may be unconnected with glutamate uptake, the fluorescence rise was measured over 10 seconds. Measured in this way, the mean fluorescence response in 7 cells in 57mM $[K]_0$ was 64 ± 11% (SEM) of control. This is a significant ($P < 0.02$) reduction, suggesting that glutamate uptake is indeed inhibited under these conditions. The conclusion is provisional, however, because the mechanism of the fluorescence spikes is not understood.

Fig. 5.13. A glutamate-evoked fluorescence 'spike'. Left-hand traces: with 0 $[K]_o$ (solution E with y=0), 30μM glutamate evoked a steadily rising fluorescence response. Right-hand traces: with 57mM $[K]_o$ (solution E with y=57), application of glutamate to the same cell evoked a biphasic fluorescence response. Holding potential -33mV. Pipette solution R.

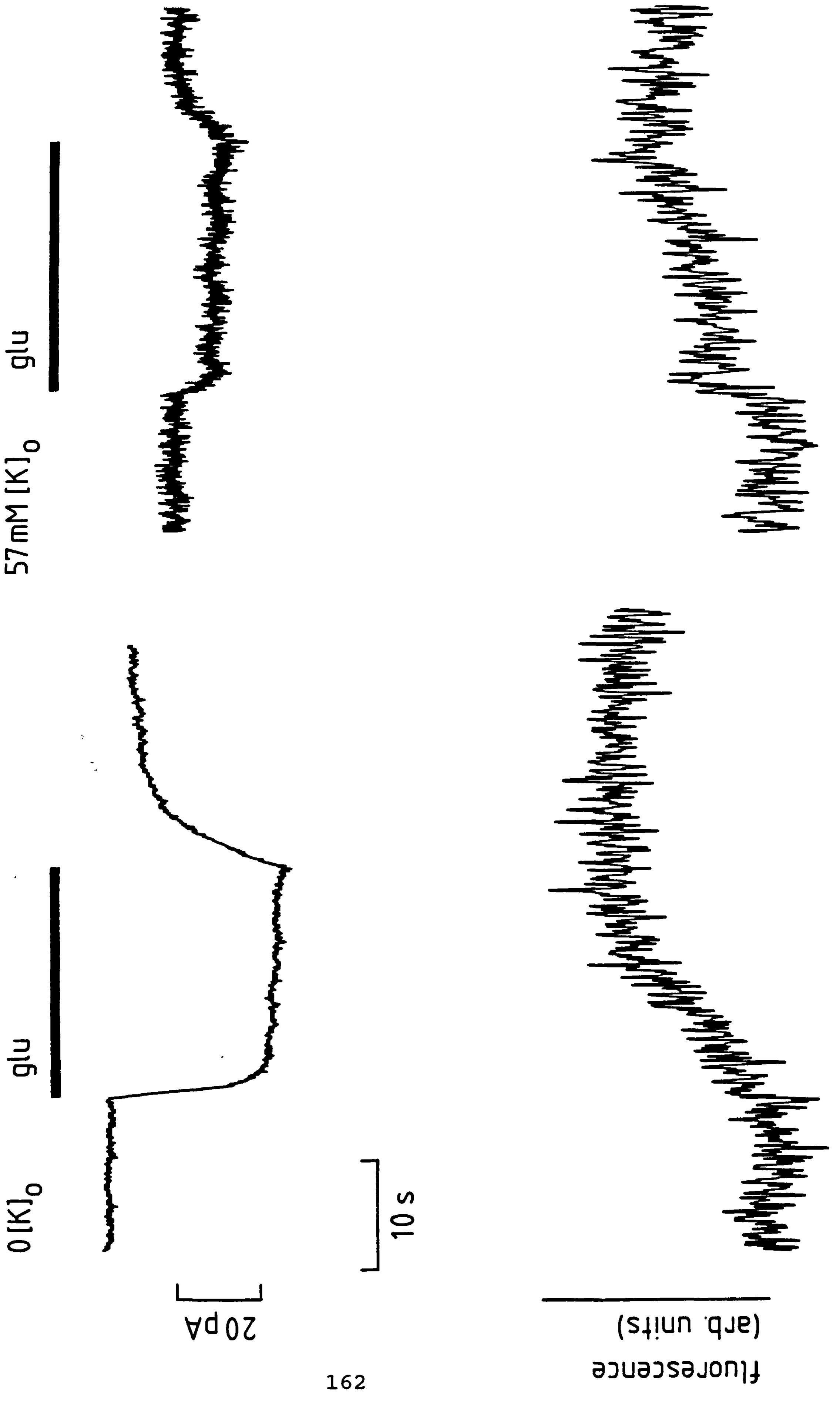
0[K]o
glu
57mM [K]o
glu
10 s
20 pA
fluorescence
(arb. units)

Discussion

6.1 Uptake current or channel?

It is necessary to establish that the glutamate-evoked current in Müller cells is due to electrogenic glutamate uptake and not glutamate-gated channels. Brew & Attwell (1987) showed that the pharmacology and voltage-dependence of the glutamate-evoked current were inconsistent with previously reported glutamate-gated channels (Watkins & Evans, 1981; Mayer & Westbrook, 1984; Usowicz, Gallo & Cull-Candy, 1989), but agreed well with the properties of glutamate uptake determined by radiotracing experiments (Balcar & Johnston, 1972; Johnston, Kennedy & Twitchin, 1979). In addition, the suppressive effect of removing internal potassium (section 3.6) is difficult to explain in terms of a channel permeable to Na and K ions.

The possibility remains, however, that the current is generated by a novel glutamate-gated channel, of unusual pharmacology, conducting ions other than sodium and potassium; chloride or calcium for example. All the evidence is against this. There is no detectable change in the current noise during activation of the glutamate-evoked current: a noise increase would be expected from increased channel openings. Most of the ions present in the experimental solutions have been eliminated as possible charge carriers through the putative channel. Variations of the concentrations of Ca_o, Mg_o, Ba_o (Brew & Attwell, 1987, and unpublished observations), Ca_i (section 4.1), Cl_i and Cl_o (section 3.9) have no effect on the glutamate-evoked current. Changing from a HEPES buffered to a CO_2/HCO_3^--buffered external solution also had no effect on the uptake current (Marek Szatkowski, personal communication). It is therefore unlikely that any of these ions could be carrying current through a glutamate-gated channel. The same evidence also shows that these ions are not involved in the uptake process.

There is positive evidence that the glutamate-evoked current reflects electrogenic glutamate uptake. Inclusion of glutamate in the patch pipette inhibits the current, and this inhibition depends on the internal sodium concentration (sections 3.4 & 3.5). This result is almost impossible to explain with a channel, but is easily accounted for by a carrier co-transporting glutamate and sodium (section 3.5). Finally, the fluorescence assay for glutamate uptake described in chapter 5 was used to show that the glutamate-evoked current is associated with glutamate influx into the cell and that the current and influx vary together under a variety of conditions. It is concluded that the glutamate-evoked current in Müller cells represents electrogenic glutamate uptake and that there is no detectable contamination by glutamate-gated channels.

6.2 Types of glutamate uptake

Mechanisms of glutamate uptake can be distinguished on the basis of their ionic dependence, pharmacological profile or by localisation to particular membranes (eg. plasmalemma, synaptic vesicles or mitochondria). For the purposes of this discussion I shall classify the uptake systems as follows: high-affinity, sodium-dependent uptake; low-affinity uptake (which may or may not be sodium-dependent); chloride-dependent uptake (all of which are expressed in the plasmalemma) and uptake into synaptic vesicles. I shall show that in salamander Müller cells only the high-affinity, sodium-dependent system operates at glutamate concentrations below 30μM (this was the concentration used in the experiments investigating the voltage-dependence of the glutamate-evoked fluorescence: these data are used below to place an upper limit on the rate of voltage-insensitive uptake of glutamate).

Brew & Attwell (1987) showed that glutamate activates the uptake current with 1st order Michaelis-Menten kinetics, with the apparent K_m in the range 8-22μM. This is typical for 'high-affinity' uptake (Hertz, 1979). Both the uptake current (section 3.2; Brew & Attwell, 1987) and the glutamate-evoked fluorescence (section 5.3) are completely abolished by removal of external sodium. This means that neither 'chloride-dependent' uptake, nor the system seen in synaptic vesicles, contributes to glutamate uptake into Müller cells, as both of these systems are sodium-independent (Pin et al, 1984; Naito & Ueda, 1985; Zaczek et al, 1987; Maycox et al, 1990). Furthermore, glutamate uptake by both of these sodium-independent systems is stimulated by external chloride whereas the uptake current in Müller cells is unaffected by complete replacement of external (or internal) chloride by gluconate ions (section 3.9).

There remains the possibility that, even with low ($<30\mu M$) glutamate concentrations, an electroneutral low-affinity uptake system could make a significant contribution. Below, after reviewing the properties of low-affinity uptake, I will argue that any such contribution is unlikely.

Kinetic characterisation of glutamate and aspartate uptake often reveals, in addition to high-affinity uptake, a second, low affinity component of uptake, with a wide range of apparent K_m values ($100\mu M$ to 5mM; cf $5-50\mu M$ for high-affinity uptake). There is not a consensus concerning its properties and importance. In cultured astrocytes (Hertz et al, 1978) and cultured cerebellar granule cells (Stallcup et al, 1979) the low-affinity component comprises at most 15% of the total uptake with 1mM [glu]. In most other studies the V_{max} of low-affinity uptake was 0.5-3x the V_{max} of the high-affinity system (in various brain slice preparations: Davies & Johnston, 1976; Balcar & Johnston, 1973 and in synaptosomal preparations: Logan & Snyder, 1972; Bennett, Logan & Snyder, 1973). Bennett et al (1973) and Stallcup et al (1979) report that low-affinity uptake is sodium-independent. The above studies suggest that at resting $[glu]_o$ values (a few μM, see section 6.5) and low extracellular glutamate concentrations (eg. <100μM), uptake via the high affinity system will be quantitatively more important than that via the low affinity system.

In contradiction, a study of glutamate uptake into the rat retina (White & Neal, 1976) found that the V_{max} of the low-affinity system (K_m = 630μM) was 25x that of the high-affinity system (K_m = 21μM). However, they report that the high- and low-affinity uptake systems appear to have otherwise identical properties: both are sodium-dependent, have similar pharmacological profiles and sensitivity to metabolic inhibitors. This suggests that the apparently dual nature of the uptake may be artefactual. A simple explanation of how this could arise is as follows.

Within intact brain tissue, glutamate uptake and restricted diffusion ensure that only a small fraction of exogenously applied glutamate actually reaches the interior of the tissue. This explains the many-fold potency difference (up to 1000-fold), for activation of ion channels, between glutamate applied to isolated cells and to intact retinae (Shiells et al, 1986) or brain slices (Garthwaite, 1985). Consider a simple model of the retina, with only high-affinity uptake carriers which are distributed into 2 compartments. One compartment, corresponding to carriers in superficial membranes, has good diffusive contact with the perfusate. The second compartment, containing the majority of the carriers (ie. 96%), corresponds to carriers in the interior of the retina. (This and the values below were chosen so as to mimic the results of White & Neal, 1976.) Making the reasonable assumption that the [glu] in the interior compartment is 1/30th of that exogenously applied, the following expression gives the total rate of uptake as

$$V = V_{max} \left\{ \frac{0.04[glu]}{[glu] + K_m} + \frac{0.96[glu]/30}{([glu]/30) + K_m} \right\} \qquad (6.1)$$

$$= k \left\{ \frac{[glu]}{[glu] + K_m} + \frac{24[glu]}{[glu] + 30K_m} \right\} \qquad (6.2)$$

where $k = V_{max}/25$. With the K_m for the high-affinity system being 20μM, equation (6.2) approximately predicts the kinetic behaviour observed by White & Neal (1976), with apparently distinct high-affinity (K_m = 20μM) and low-affinity (K_m about 600μM) uptake systems.

Similar considerations may also apply for some of the low-affinity uptake observed in brain slices, accounting for the large variability of the reported K_ms for the low-affinity components. To summarise, there is little evidence that low-affinity uptake is quantitatively important. Excluding White & Neal (1976), the consensus is that low-affinity uptake is sodium-independent (Bennett et al, 1973; Stallcup et al, 1979).

Whether or not low-affinity uptake is sodium-dependent, the data described in this thesis show that it makes a negligible contribution to uptake into Müller cells at glutamate concentrations below 30μM. If low-affinity uptake is assumed to be sodium-independent, then the absolute sodium-dependence of the glutamate-evoked current and fluorescence unequivocally excludes any role for low-affinity uptake. If low-affinity uptake is assumed to be sodium-dependent, the argument is more involved. The glutamate-evoked current obeys Michaelis-Menten kinetics with respect to the glutamate concentration (Brew & Attwell, 1987), saturating in the range at which low-affinity uptake would operate (> 100μM). Thus, any low-affinity uptake must be electroneutral and is therefore likely to be insensitive to changes of voltage. However, using the fluorescence assay for glutamate uptake, I have shown that any voltage-insensitive uptake contributes a maximum of 12% of the glutamate uptake occurring with 30μM [glu] at -83mV (section 5.8).

In conclusion, the only quantitatively significant glutamate uptake system operating in Müller cells for $[glu]_o$ < 30μM is high affinity, sodium-dependent uptake.

6.3 Mammalian and amphibian uptake systems are similar

In discussing the properties of glutamate uptake, I will often draw on evidence from the mammalian central nervous system and from the kidney. Also, much of the relevance of the results is discussed with respect to the mammalian CNS. I shall review briefly, therefore, the evidence that the properties of high-affinity, sodium-dependent glutamate uptake are the same in these preparations as in the salamander glial cells studied here. Sarantis & Attwell (1990) showed that the glutamate uptake current in rabbit Müller cells has an almost identical ionic dependence to that in salamander Müller cells (Brew & Attwell, 1987; this thesis). This includes the apparent affinity for glutamate, the sigmoid sodium dependence, the voltage-dependence and the modulation by internal and external potassium. There is also little apparent difference between the neuronal and glial uptake systems: the best radiotracing evidence for potassium counter-transport comes from mammalian synaptosomes (Kanner & Sharon, 1978a,b; Roskoski, 1979). Sensitivity to membrane potential (Murer et al, 1980) and to $[K]_i$ (Burckhardt et al, 1980) has also been demonstrated in the kidney.

The only reported differences between any of these preparations are: the different sodium-dependence of radio-labelled glutamate uptake between some neurones and glia (see next section) and the extent of potassium-independent (but still sodium-dependent) uptake in the kidney (Burckhardt et al, 1980) and CNS (Kanner & Sharon, 1978a,b).

6.4 Stoichiometry of uptake

In discussing the likely stoichiometry of the high-affinity, sodium-dependent glutamate uptake carrier I shall assume that its properties are the same in mammals and amphibia (see previous section). I will discuss the involvement of each ion in turn, but state the conclusion in advance: the uptake of each glutamate anion is linked to the influx of 2 or maybe 3 sodium ions, to the efflux of a potassium ion and maybe to the influx of a proton.

Glutamate

All studies of high-affinity glutamate uptake have shown it to obey 1st order Michaelis-Menten kinetics with apparent K_m values in the range 5-50μM (Hertz, 1979; Lerner, 1987; Erecinska, 1987) indicating that there is a single binding site for external glutamate.

Sodium

Given the external sodium-dependence of net glutamate uptake (Roskoski, 1978), the fact that glutamate stimulates sodium uptake (Stallcup et al, 1979; Baetge et al, 1979; Kimelberg et al, 1989) and the inhibition of uptake by internal sodium (section 3.3), it is certain that glutamate uptake is via a sodium co-transporting carrier. Direct measurements of sodium and glutamate fluxes suggest that 2 (Stallcup et al, 1979; Baetge et al, 1979) or maybe 3 (Kimelberg et al, 1989) sodium ions are transported with each glutamate molecule. A similar conclusion (2 Na ions per glutamate) was reached by Erecinska et al (1983; 1986) who investigated the sodium-dependence of the equilibrium $[\text{D-asp}]_i/[\text{D-asp}]_o$ distribution in synaptosomes and cultured glioma cells.

The sigmoid sodium-dependence of the uptake current in Müller cells (Brew & Attwell, 1987; this thesis, Fig. 3.1D; Schwartz & Tachibana, 1990) is also consistent with the transport of 2 or more sodium ions with each glutamate. A similar sigmoid sodium-dependence has been observed for radiotraced uptake into synaptosomes (Peterson & Raghupathy, 1972) and cultured granule cells (Drejer et al, 1982). A puzzling aspect is that a number of studies have found the sodium-dependence of glutamate uptake in cultured astrocytes to be well fitted by first order Michaelis-Menten kinetics (Drejer et al, 1982; Kimelberg et al, 1989 are the most convincing). It may be that these results indicate a genuine difference of affinity of a sodium binding site in these cells. Alternatively, as the cells were not voltage-clamped, it is conceivable that the astrocytes were depolarised in a sodium-dependent fashion by glutamate-gated channels and/or glutamate uptake (Bowman & Kimelberg, 1984). This would inhibit uptake when sodium was high and might alter a sigmoid dependence on $[Na]_o$ (at constant voltage) to be nearer to a Michaelis-Menten relation.

In summary, most of the available evidence indicates that the ratio of sodium and glutamate transported is 2:1.

Potassium

There are a number of reports investigating the influence of potassium on glutamate uptake. Kanner & Sharon (1978a & b), Burckhardt et al (1980) and Schneider & Sacktor (1980) showed that loading membrane vesicles (synaptosomes or vesicles derived from the renal brush border) with potassium, such that there was a $[K]_i > [K]_o$ gradient, stimulated glutamate uptake. In addition, raising $[K]_o$ inhibited uptake (Peterson & Raghupathy, 1972) and stimulated glutamate efflux (Kanner & Marva, 1982). These results have been interpreted as demonstrating that the glutamate uptake carrier exchanges glutamate and potassium ions (as well as co-transporting sodium ions).

The problem with this interpretation is that, as argued in the Introduction (section 1.5), there is an alternative explanation for the effects of potassium. In the preparations used, the manipulations of potassium are expected to change the membrane potential and thus modulate glutamate uptake by virtue of its voltage-dependence. For example, a raised $[K]_i$ will generate an inside negative membrane potential, stimulating uptake (Brew & Attwell, 1987).

Arguing against the hypothesis that the effects of potassium are solely due to changes of membrane potential is the following evidence. Roskoski (1979) showed that net aspartate uptake requires the presence of potassium ions (outside, but presumably they were also present inside); Kanner & Sharon (1978a & b) showed that glutamate uptake was almost completely dependent on internal potassium, even under conditions expected to generate an inside negative membrane potential.

Although it thus seemed likely that potassium ions were counter-transported by the uptake carrier, such radiotracing experiments were unable to quantify the respective effects of potassium transport and potassium-induced changes of membrane potential.

The experiments showing the dependence of the uptake current (section 3.6) and the glutamate-evoked fluorescence (section 5.10) on internal potassium demonstrate unequivocally that potassium has effects independent of its effects on the membrane potential. Furthermore, the simple Michaelis-Menten dependence on $[K]_i$ (Fig. 3.5) and the inhibitory effect of raising external $[K]_o$ (Fig. 3.10) suggest that potassium is transported out of the cell after binding to a single site at the internal face of the carrier.

The apparent contradiction between these results and those of Schwartz & Tachibana (1990), who show little change of the D-aspartate evoked current when $[K]_i$ was lowered from 90mM to 9mM, is partially resolved by the observation that D-aspartate uptake has a higher apparent affinity for $[K]_i$ than does the L-glutamate uptake current (Fig. 3.6). However, a reduction of $[K]_i$ to 9mM would still be expected to decrease the D-aspartate-evoked current by about 30% (according to Fig. 3.6), but Schwartz & Tachibana (1990) observe a less than 10% decrease (their Fig. 5). This may be due to their use of caesium ions in the external solution which could substitute for K^+_i (Fig. 3.7) after entering the cells either via potassium channels, or via the sodium pump (Rang & Ritchie, 1968) in the experiments in which sodium was included in the pipette filling solution.

Using changes of potassium to manipulate the membrane potential, Erecinska et al (1983; 1986) concluded that the potassium- (and hence voltage-) dependence of the equilibrium $[\text{D-asp}]_i/[\text{D-asp}]_o$ distribution in synaptosomes and glioma cells indicated that 2 positive charges entered the cell with each aspartate ion. In fact, their results are equally consistent with the counter-transport of one potassium ion and the net inward movement of a single positive charge, as occurs in the stoichiometries proposed below.

In conclusion, the glutamate uptake carrier is potassium-dependent: probably as each glutamate ion is taken up, a potassium ion is transported out of the cell.

Protons

There is some evidence that protons may be co-transported into the cell with glutamate. The best evidence comes from the kidney. Using membrane vesicles prepared from the renal brush border, Nelson et al (1983) showed that even in the absence of sodium and potassium gradients glutamate uptake is stimulated by an applied proton gradient ($pH_o < pH_i$). It was not possible, however, to check that the proton changes had no effect on the membrane potential, so an indirect effect of the proton gradient cannot be ruled out. Erecinska et al (1983) recorded an alkalinisation associated with aspartate uptake into synaptosomes, consistent with proton co-transport.

Against this is the evidence of Schwartz & Tachibana (1990) who loaded salamander Müller cells with the pH indicator BCECF. They showed that although addition of the weak acid acetate caused an intracellular acidification, the addition of D-aspartate (to activate uptake and the putative proton co-transport) did not generate a detectable pH change. They estimated that if protons were co-transported with D-aspartate (one proton per electronic charge) then ten times more protons should enter the cell than with the application of acetate. They concluded that glutamate is not co-transported with a proton. The only uncertainty with this result is that no control was performed to check whether the BCECF loading procedure (10μM BCECF-AM for 60min) had any effect on the uptake current.

The pH-dependence of the uptake current in section 3.10 is consistent with proton co-transport, but as explained, is equally consistent with titration of a group required for carrier operation.

Most likely stoichiometry

The first-order dependence of the uptake current on external glutamate and internal potassium implies that only one of each of these ions is transported per carrier cycle. Because glutamate evokes an inward current, the equivalent of at least three additional positive charges must move into the cell on each cycle. The simplest stoichiometry would be the co-transport of a glutamate anion with three sodium ions and counter-transport of a potassium ion. However, as most of the available evidence indicates that two sodium ions are co-transported with each glutamate ion, a better alternative would be the co-transport of two sodium ions and a proton (as shown in Fig. 1.2). The latter stoichiometry is consistent with the sodium- and potassium-dependence of the equilibrium $[asp]_i/[asp]_o$ ratio observed by Erecinska et al (1983; 1986). No other small ions appear to be transported, as wide variations of their concentrations do not affect the uptake current (this evidence was summarised in section 6.1). The possible involvement of larger ions such as ATP, EGTA and HEPES was not systematically tested.

6.5 Accumulative power of the carrier

A carrier with either of these stoichiometries would be capable of accumulating glutamate against a large concentration gradient. At equilibrium the Nernst potential for glutamate, E_{glu}, is given by the general formula

$$E_{glu} = (1-x-y+z)E_m + xE_{Na} + yE_H - zE_K \qquad (6.3)$$

where x and y are the numbers of sodium and hydrogen ions co-transported with each glutamate anion and z is the number of potassium ions counter-transported for each glutamate taken up. E_{Na}, E_H and E_K are the Nernst potentials for sodium, protons and potassium. E_m is the membrane potential. For the two proposed stoichiometries

$$E_{glu} = 3E_{Na} - E_K - E_m \qquad (6.4)$$

or

$$E_{glu} = 2E_{Na} + E_H - E_K - E_m \qquad (6.5)$$

for the 3Na,glu/K and 2Na,H,glu/K stoichiometries respectively. When E_{Na} = +50mV, E_K = -90mV, V_H = -10mV and V_m = -85mV, the predicted equilibrium $[glu]_i/[glu]_o$ ratios at 37°C are about 170,000 (3Na,glu/K) and 20,000 (2Na,H,glu/K). The Nernst potentials assumed here are estimates based on data given in: Hansen (1985); Ballanyi et al (1987) and Chesler & Kraig (1987).

Values for the cytoplasmic and extracellular glutamate concentrations in the brain are somewhat uncertain. An estimate of the average $[glu]_i$ based on glutamate content (Berger et al, 1977a & b) gave values of between 4.4 and 16.3mM for different brain regions. The glutamate contents of separately cultured glia and neurones are similar: 3.4

to 18.8mM for glia (Schousboe et al, 1975; Patel & Hunt, 1985; Yudkoff et al, 1986), 8.5 to 19.8mM for neurones (Kvamme et al, 1985; Patel & Hunt, 1985). However, use of antibodies against cross-linked glutamate reveals a denser staining of glutamatergic terminals than of glial processes and non-glutamatergic terminals (Somogyi et al, 1986; Montero & Wenthold, 1989), suggesting that $[glu]_i$ may be lower in glia than in neurones. Given the great difficulty of relating the staining density to glutamate concentration and the fact that the maximum difference of staining density observed was only 5-fold, it seems reasonable to conclude that $[glu]_i$ is of the order of 10mM in both glia and neurones.

A figure for the CNS extracellular glutamate concentration of about 3μM was obtained from micro-dialysis (Hamberger et al, 1983; Lehmann et al, 1983; Hagberg et al, 1985). This value may be an overestimate, because any damage associated with placement of the 'micro' dialysis tubing (0.3mm in diameter) will lead to a release of intracellular glutamate. If this were so, the in vivo $[glu]_i/[glu]_o$ ratio might approach tolerably close to the equilibrium ratio for the 2Na,H,glu/K stoichiometry: 10mM $[glu]_i$ predicts a $[glu]_o$ of about 0.5μM. A carrier with the 3Na,glu/K stoichiometry, for which the predicted $[glu]_o$ is 60nM, would be far from equilibrium in vivo.

6.6 Function of potassium counter-transport

Reported values for $[K]_i$ vary from 66mM to 170mM (Ballanyi et al, 1987; Hansen, 1985). At such levels a K^+-binding site with a K_m of 15mM will be quite saturated (about 85% occupied), so physiological variations of $[K]_i$ (a maximum rise of about 10mM: Ballanyi et al, 1987) would hardly affect the rate of glutamate uptake. The normal $[K]_o$ is about 3mM (Hansen, 1985) and physiological increases appear not to exceed 10mM (Heinemann & Lux, 1977). These will also have only small effects on the uptake rate, given the apparent affinity of the external binding site for potassium (about 100mM, section 3.8). (Pathological rises of potassium will, however, seriously disturb glutamate uptake; see section 6.9 on neurotoxicity.) The membrane potential (E_m) of glial cells is very close to the Nernst potential for potassium (E_K) (Kuffler et al, 1966; Ballanyi et al, 1987), so counter-transport of a potassium ion cannot provide much extra energy to drive glutamate uptake. (This would not, however, be the case in cells in which $E_m > E_K$, photoreceptors for example.) Thus, it appears that the function of the potassium counter-transport in glia is not regulatory and does not provide energy for uptake.

The benefit of potassium counter-transport, in glial cells at least, is therefore something of a mystery. The following are tentative suggestions. By reducing the net charge of part of the carrier, K^+-binding may facilitate movement of that part of the carrier through hydrophobic membrane regions. Potassium counter-transport will also reduce somewhat the osmotic load on the cell as glutamate and sodium are taken up.

6.7 Role of glutamate uptake at the synapse

All glutamate released into the synaptic cleft and extracellular space by neurones is ultimately taken up by neurones and glia. However, there is not enough information to assess whether glutamate uptake into neurones or glia is of sufficient velocity and appropriate location to influence the glutamate concentration transient at the synapse.

There is little evidence making it necessary to postulate this. A calculation based on the geometry of a typical CNS synapse (Eccles & Jaeger, 1958) suggests that glutamate would diffuse away from the synaptic cleft with a rough half-time of 0.1 - 0.2ms, so the glutamate transient would have largely subsided within 1ms. This would be fast enough to obviate the need for direct transmitter removal from the synaptic cleft. (This half-time is, however, an underestimate, because the calculation ignores restricted diffusion in the extrasynaptic space, assuming that transmitter leaving the cleft is instantly dissipated.) Furthermore, it seems likely that the time-course of the post-synaptic response can be accounted for by channel kinetics and desensitisation (Lester et al, 1990; Trussel & Fischbach, 1989).

Some slight support for the hypothesis that glutamate uptake can modulate the time course of the glutamate transient comes from an experiment on the effects of the uptake blocker dihydrokainate (DHK) on the synaptic currents in the hippocampus (Hestrin et al, 1990). Application of DHK potentiated the NMDA-receptor mediated component of the synaptic current. However, this effect of DHK could have been via alteration of the background level of glutamate rather than the glutamate transient. Control experiments to check whether DHK had any direct actions on the glutamate-gated channels were not performed.

Even if glutamate uptake has no direct influence on the time course of the glutamate transient at the synapse, it is nevertheless responsible for maintaining the low extracellular glutamate concentration that enables glutamate to diffuse away from the synapse. In addition to ensuring normal synaptic function, this homoeostatic function is vital because of the neurotoxicity of high glutamate concentrations (see section 6.9). The observation that a large fraction of exogenously applied glutamate is taken up by glial cells (Kennedy et al, 1974; McLennan, 1976; White & Neal, 1976; Ehinger, 1977) suggests that glial cell uptake is quantitatively more important than neuronal uptake in this respect.

6.8 Relevance of glutamate uptake to Long-Term Potentiation

Certain glutamatergic synapses exhibit activity-dependent and long-lasting changes of synaptic gain which are of interest as putative cellular models of learning and memory. The most studied of these phenomena is Long-Term Potentiation (LTP), a persistent increase of synaptic gain in the mammalian hippocampus. LTP can be induced either by high frequency stimulation of presynaptic fibres (Bliss & Lomo, 1973; Bliss & Gardner-Medwin, 1973) or by low frequency presynaptic stimulation 'paired' with depolarisation of the postsynaptic cell (Gustafsson & Wigström, 1986; Wigström et al, 1986). These induction conditions lead to glutamate release and depolarisation of the postsynaptic cell, events which together will activate NMDA channels (Nowak et al, 1984; Mayer et al, 1984). Activation of NMDA channels has been shown to be necessary for the induction of LTP (Collingridge et al, 1983). NMDA channels, as well as conducting sodium and potassium ions, are permeable to calcium (MacDermott et al, 1986). Experiments in which injection of EGTA into the postsynaptic cell prevented the induction of LTP (Lynch et al, 1983) led to the conclusion that a calcium influx through NMDA channels in the postsynaptic terminal is a necessary step in the induction of LTP.

One of the most controversial areas in the study of LTP has been the mechanism of the increased synaptic gain, the 'expression' of LTP. Much interest has centred on the proposal that an increased release of transmitter (glutamate) underlies the change of gain. Evidence in favour of this hypothesis is the increased efflux of glutamate from hippocampi in which LTP has been induced (Dolphin et al, 1982; Bliss et al, 1986). Interpretation of these results will be discussed below. A consequence of accepting this 'presynaptic' hypothesis is that it is then necessary to postulate the existence of a 'retrograde messenger' linking the postsynaptic induction site to the presynaptic expression site and instructing the increased release of transmitter.

A candidate for the retrograde messenger is arachidonic acid (Piomelli et al, 1987; Williams et al, 1989). It is released from neurones by the activation of NMDA receptors, the calcium influx through NMDA channels stimulating phospholipase A_2 which liberates arachidonic acid from phospholipids (Lazawrewicz et al, 1988; Dumuis et al, 1988). This suggests that arachidonic acid might be released from postsynaptic terminals during the induction of LTP.

The results in sections 4.6 - 4.9, showing that arachidonic acid inhibits glutamate uptake, suggested an alternative explanation for the increased glutamate release from hippocampi in which LTP had been induced. Namely, that arachidonic acid liberated from the postsynaptic terminal, instead of acting as a retrograde messenger, inhibits glutamate uptake in nearby neurones and glia. An inhibition of uptake would lead to increased release of glutamate into the perfusate. Experiments showing no difference of glutamate uptake into synaptosomes prepared from control and potentiated tissue (Lynch et al, 1985; Feasey et al, 1986; Bliss & Lynch, 1988) were inconclusive, because measurements were made after a 4-5 minute incubation with labelled glutamate. By this time the $[glu]_i/[glu]_o$ ratio is close to equilibrium (Erecinska et al, 1983, show a timecourse for D-aspartate accumulation into synaptosomes). This near-equilibrium ratio is determined by the electrochemical gradients of the transported ions and the membrane potential, but is quite insensitive to changes of the rate of uptake. A better measurement would have been the initial rate of uptake.

In the event, the presynaptic hypothesis has received strong support from a quantal analysis of hippocampal EPSCs before and after the induction of LTP (Malinow & Tsien, 1990; Bekkers & Stevens, 1990). It was concluded that most of the increase of synaptic gain was attributable to an increased probability of transmitter release. Arachidonic acid, however, is by no means established as the retrograde messenger.

The speculative suggestion that an inhibition of glutamate uptake by arachidonic acid might mediate the increased synaptic gain (by amplifying and prolonging the synaptic glutamate transient) is ruled out by the same data (Malinow & Tsien, 1990; Bekkers & Stevens, 1990) and also by the failure of arachidonic acid applied to a hippocampal slice to potentiate synaptic transmission (Williams et al, 1989).

6.9 Role of glutamate uptake in neurotoxicity

Interruption of the brain's blood supply, as occurs in stroke, deprives it of oxygen and nutrients. As the brain has only limited energy stores, these are rapidly depleted following the onset of ischaemia. This sets in motion a striking pattern of changes of the ionic composition of the extracellular fluid, the overall picture being one of a dramatic loss of ionic homoeostasis.

Following the onset of ischaemia, there is a slow rise of $[K]_o$ and an acidification of the extracellular space, but $[Na]_o$, $[Cl]_o$ and $[Ca]_o$ do not change (after Hansen, 1981, I shall refer to this as phase 1). After 1-2 minutes, when the $[K]_o$ has reached about 10mM, rapid, seemingly regenerative changes occur (phase 2): $[K]_o$ rises sharply to about 50mM, $[Na]_o$ falls to around 60mM, there is a fall of $[Cl]_o$ and, importantly, there is a sharp drop of $[Ca]_o$, typically from 1.2mM to 0.1mM (Hansen, 1981). Synchronous with these events there is a reduction of the extracellular volume. It is assumed that (except for the pH changes) the intracellular changes are the opposite of the extracellular changes. Thus, during phase 2 potassium leaves cells and sodium, chloride and calcium enter.

During ischaemia, there is a build up of glutamate (and aspartate) in the extracellular space, as measured by micro-dialysis (Benveniste et al, 1984; Hagberg et al, 1985; Graham et al, 1990). This observation is consistent with the theory that some of the cellular damage occurring in ischaemia is caused by the action of glutamate. Support for this idea comes from studies of the effects of glutamate on cultured neurones. Applying 100μM glutamate for 5 min leads to delayed neuronal death (Choi et al, 1987). This necrosis is largely prevented by NMDA antagonists (Choi et al, 1988) or by calcium removal (Choi, 1987), suggesting that a calcium influx through NMDA channels eventually leads to cell death (it is proposed that lethal calcium-dependent proteases and lipases are activated). In intact brain tissue, NMDA receptor antagonists can reduce ischaemic cell death (Gill et al, 1987; Ozyurt et al 1988).

Thus, a plausible mechanism for at least some of the damage following ischaemia is that glutamate is released into the extracellular space, activates NMDA channels and causes a lethal calcium influx into neurones. However, NMDA receptor antagonists appear to protect neurones well only in certain models of ischaemia, particularly focal ischaemia (Choi, 1990). As mentioned in the Introduction (section 1.3), it is likely that non-NMDA receptor-dependent processes also contribute to ischaemic damage in some situations (Garthwaite & Garthwaite, 1989; Sheardown et al, 1990). Of obvious therapeutic interest is the fact that in many ischaemia models (eg. Gill et al, 1987) the cellular degeneration takes 24 hours or more to develop and that NMDA and non-NMDA receptor antagonists protect against damage even when applied after a transient ischaemic episode (Steinberg et al, 1988; Garthwaite & Garthwaite, 1989; Sheardown et al, 1990).

The evidence reviewed above suggests that the rise of extracellular glutamate occurring during ischaemia is toxic to neurones. As the function of glutamate uptake is to maintain a low extracellular concentration of glutamate, an important question is why is glutamate uptake unable to prevent the toxic rise of glutamate?

The results described in this thesis and in Brew & Attwell (1987) show that many of the conditions prevailing in ischaemia are expected to inhibit glutamate uptake. There is a rise of $[K]_o$. In section 3.8 (and 5.11) I showed that this directly inhibits uptake as a consequence of potassium counter-transport by the carrier. For a rise of $[K]_o$ to 50mM (such as is achieved after phase 2) uptake would be reduced by 35% by this mechanism. Not only does $[K]_o$ directly inhibit uptake, but in vivo it will also depolarise cells. The depolarisation from -90 to -20mV expected from the above $[K]_o$ rise will inhibit uptake by 66% (Brew & Attwell, 1987). If the inhibitions due to potassium and depolarisation are assumed to be independent (ie. that the shape of the I-V relation is not altered by raising $[K]_o$, this is untested), the combined inhibition by these two processes is 78%. Clearly, glutamate uptake will be severely compromised, just at the time it is needed most. Interestingly, the $[K]_o$-sensitivity of uptake is greater in rabbit Müller cells (Sarantis & Attwell, 1990) and a similar $[K]_o$ rise there would reduce the rate of uptake by about 90%.

Arachidonic and oleic acid (sections 4.6 & 4.8) may further inhibit uptake during ischaemia: a marked increase of the brain content of free unsaturated fatty acids (particularly arachidonic and oleic acid) has been observed to occur during anoxia (Rehncrona et al, 1982), presumably as a result of the activation of calcium-dependent lipases (phospholipases A_2 and C for example). However, because the partition of these fatty acids between membranes and the extracellular fluid is not known, it is difficult relate the brain content values to the dose-response curve in section 4.6.

Some support for the notion that fatty acids inhibit uptake during anoxia comes from the following finding (Silverstein et al, 1986). Uptake into synaptosomes prepared from anoxic tissue is reduced for at least an hour compared to uptake into control synaptosomes. Uptake into the 'anoxic' synaptosomes is preferentially stimulated by the addition of BSA, which binds fatty acids and could, in principle, remove them from the synaptosome membrane. The fact that uptake remains inhibited for 1 hour at least (but less than 24 hours) is consistent with the persistent inhibition by arachidonic acid observed in section 4.9. This long-term effect of arachidonic acid may be of relevance to the delayed neurotoxic processes which continue after an initial ischaemic event in the brain.

An unresolved question concerns the origin of the extracellular glutamate which builds up during anoxia. The obvious suggestion is that it is due to synaptic release, but a number of results cast some doubt on this idea. The calcium-dependence of the glutamate rise in vivo is controversial (Drejer et al, 1985; Ikeda et al, 1989). Except for the beginning of phase 1, the EEG is silent (Hansen, 1981), suggesting a lack of neuronal activity (although it might not detect asynchronous firing). Furthermore, calcium-dependent release of glutamate from synaptosomes is inhibited when the ATP/ADP ratio falls in anoxia (cyanide) (Sanchez-Prieto & Gonzalez, 1988).

An alternative source of the extracellular glutamate would be through reversed glutamate uptake. The graph in Fig. 6.1 shows the equilibrium $[glu]_o$ as a function of the external potassium concentration for the two proposed stoichiometries of uptake (calculated using equations 6.4 & 6.5). The graph assumes a cytoplasmic [glu] of 10mM, that the cell depolarises ($E_m = E_K$) and that $[Na]_o$ falls by the same amount as $[K]_o$ rises. At 60mM $[K]_o$ the equilibrium $[glu]_o$ will be 75μM and 250μM for the 3Na,glu/K and 2Na,H,glu/K stoichiometries respectively. The uptake carrier will not be able to pump glutamate below these levels and, if $[glu]_o$ is initially below these levels, the carrier will actually release glutamate from the large cytoplasmic store until equilibrium is reached. These glutamate concentrations are sufficient to kill neurones in culture (Choi et al, 1987).

These new insights into the possible roles of glutamate uptake in the processes leading to ischaemic/anoxic damage do not suggest many simple therapeutic interventions. It seems very unlikely that carrier properties as basic as potassium counter-transport and voltage-sensitivity will be readily modified by drugs. The possible involvement of inhibition by unsaturated fatty acids such as arachidonic acid, however, could be tested and maybe prevented by drugs which inhibit phospholipase A_2.

Fig. 6.1. The minimum extracellular glutamate concentration that the glutamate uptake carrier can maintain rises when $[K^+]_o$ rises. For the two stoichiometries shown, the equilibrium $[glu]_o$ was calculated as a function of $[K^+]_o$ using equations (6.4) and (6.5), by assuming that $E_m = E_K$ and that $[Na^+]_o = 143mM - [K^+]_o$. For simplicity $[Na^+]_i$ and $[K^+]_i$ were assumed to remain constant. E_H was taken as zero. The value of $[glu]_i$ was set at 10mM; any other choice would simply scale the value of $[glu]_o$ proportionately.

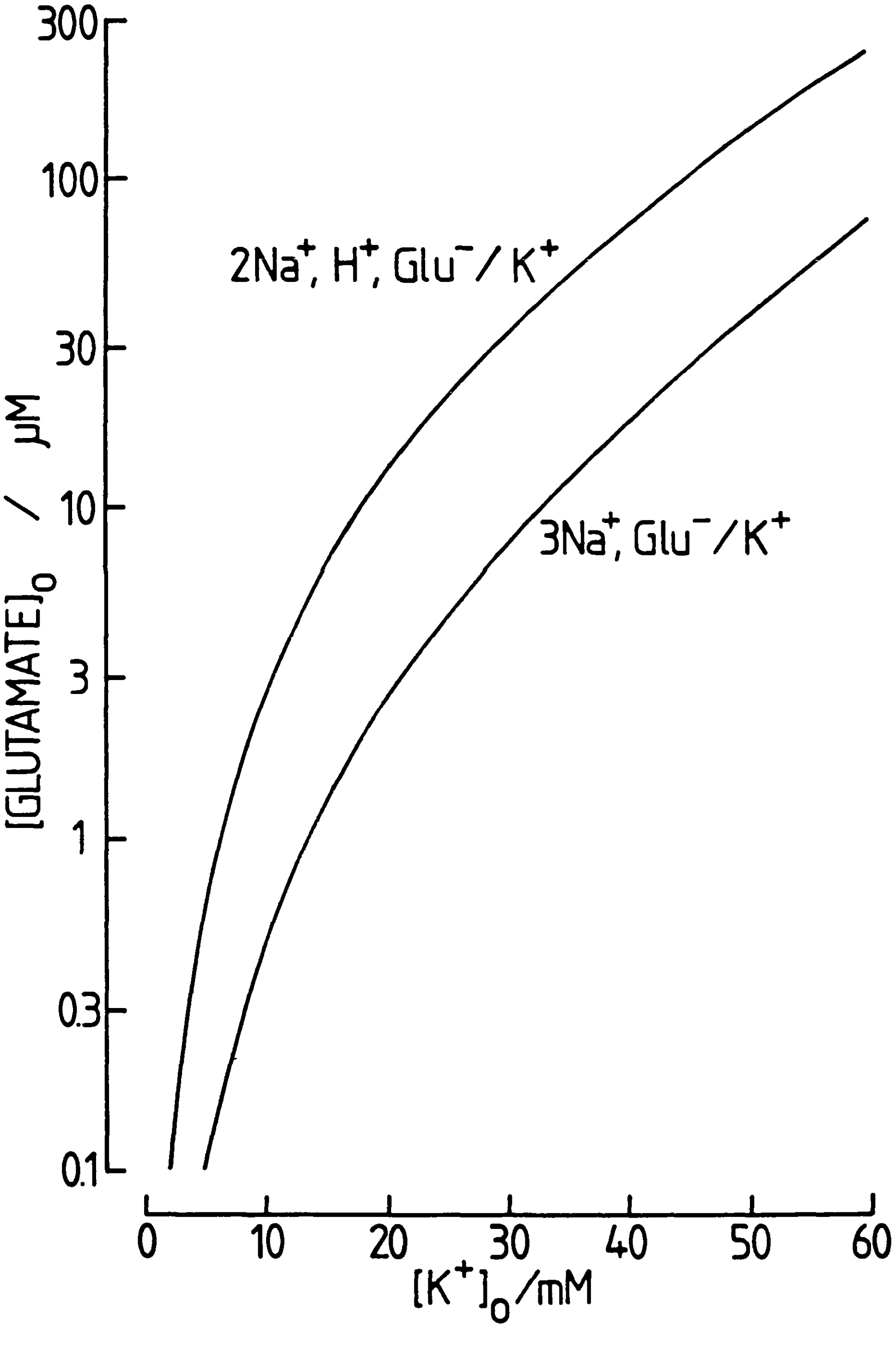
300
100
30
10
3
1
0.3
0.1
[GLUTAMATE]$_o$ / μM
2Na$^+$, H$^+$, Glu$^-$/ K$^+$
3Na$^+$, Glu$^-$/ K$^+$
0
10
20
30
40
50
60
[K$^+$]$_o$/mM

References

Agrawal, S.G. & Evans, R.H. (1986) The primary afferent depolarizing action of kainate in the rat. Br. J. Pharmac. 87: 345-355.

Attwell, D., Mobbs, P., Tessier-Lavigne, M. & Wilson, M. (1987) Neurotransmitter-induced currents in retinal bipolar cells of the axolotl, Ambystoma Mexicanum. J. Physiol. 387: 125-161.

Ayoub, G.S., Korenbrot, J.I. & Copenhagen, D.R. (1989) Release of endogenous glutamate from isolated cone photoreceptors of the lizard. Neurosci. Res. Suppl. 10: S47-S56.

Baetge, E.E., Bulloch, K. & Stallcup, W.B. (1979) A comparison of glutamate transport in cloned cell lines from the central nervous system. Brain Res. 167: 210-214.

Balcar, V.J. & Johnston, G.A.R. (1972) The structural specificity of the high affinity uptake of L-glutamate and L-aspartate by rat brain slices. J. Neurochem. 19: 2657-2666.

Balcar, V.J. & Johnston, G.A.R. (1973) High affinity uptake of transmitters: studies on the uptake of L-aspartate, GABA, L-glutamate and glycine in the cat spinal cord. J. Neurochem. 20: 529-539.

Ballanyi, K., Grafe, P. & Ten Bruggencate, G. (1987) Ion activities and potassium uptake mechanisms of glial cells in guinea-pig olfactory cortex slices. J. Physiol. 382: 159-174.

Bekkers, J.M. & Stevens, C.F. (1990) Presynaptic mechanism for long-term potentiation in the hippocampus. Nature 346: 724-729.

Bennett, Jr, J.P., Logan, W.J. & Snyder, S.H. (1973) Amino acids as central nervous transmitters: the influence of ions, amino acid analogues, and ontogeny on transport systems for L-glutamic and L-aspartic acids and glycine into central nervous synaptosomes of the rat. J. Neurochem. 21: 1533-1550.

Benveniste, H., Drejer, J., Schousboe, A. & Diemer, N.H. (1984) Elevation of the extracellular concentrations of glutamate and aspartate in rat hippocampus during transient cerebral ischaemia monitored by intracerebral microdialysis. J. Neurochem. 43: 1369-1374.

Berger, S.J., Carter, J.G. & Lowry, O.H. (1977) The distribution of glycine, GABA, glutamate and aspartate in rabbit spinal cord, cerebellum and hippocampus. J. Neurochem. 28: 149-158.

Berger, S.J., McDaniel, M.L., Carter, J.G. & Lowry, O.H. (1977) Distribution of four potential transmitter amino acids in monkey retina. J. Neurochem. 28: 159-163.

Bliss, T.V.P., Douglas, R.M., Errington, M.L. & Lynch, M.A. (1986) Correlation between long-term potentiation and release of endogenous amino acids from dentate gyrus of anaesthetized rats. J. Physiol. 377: 391-408.

Bliss, T.V.P. & Gardner-Medwin, A.R. (1973) Long-lasting potentiation of synaptic transmission in the dentate area of the unanaesthetized rabbit following stimulation of the perforant path. J. Physiol. 232: 357-374.

Bliss, T.V.P. & Lomo, T. (1973) Long-lasting potentiation of synaptic transmission in the dentate area of the anaesthetized rabbit following stimulation of the perforant path. J. Physiol. 232: 331-356.

Bliss, T.V.P & Lynch, M.A. (1988) Long-term potentiation of synaptic transmission in the hippocampus: properties and mechanisms. In 'Long-term potentiation: from biophysics to behaviour'. Eds. Landfield, P.W. & Deadwyler, S.A. Alan R. Liss, NY. pp 3-72.

Boulter, J., Hollmann, M., O'Shea-Greenfield, A., Hartley, M., Deneris, E., Maron, C. & Heinemann, S. (1990) Molecular cloning and functional expression of glutamate receptor subunit genes. Science 249: 1033-1037.

Bowman, C.L. & Kimelberg, H.K. (1984) Excitatory amino acids directly depolarize rat brain astrocytes in primary culture. Nature 311: 656-659.

Brew, H. & Attwell, D. (1987) Electrogenic glutamate uptake is a major current carrier in the membrane of axolotl retinal glial cells. Nature 327: 707-709.

Burckhardt, G., Kinne, R., Stange, G. & Murer, H. (1980) The effects of potassium and membrane potential on sodium-dependent glutamic acid uptake. BBA 599: 191-201.

Chan, P.H., Kerlan, R. & Fishman, R.A. (1983) Reductions of γ-aminobutyric acid and glutamate uptake and (Na^+ + K^+)-ATPase activity in brain slices and synaptosomes by arachidonic acid. J. Neurochem. 40: 309-316.

Chesler, M. & Kraig, R.P. (1987) Intracellular pH of astrocytes increases rapidly with cortical stimulation. Am. J. Physiol. 253: R666-R670.

Choi, D.W. (1987) Ionic dependence of glutamate neurotoxicity. J. Neurosci. 7: 369-379.

Choi, D.W. (1990) Cerebral hypoxia: some new approaches and unanswered questions. J. Neurosci. 10: 2493-2501.

Choi, D.W., Koh, J.-Y. & Peters, S. (1988) Pharmacology of glutamate neurotoxicity in cortical cell culture: attenuation by NMDA antagonists. J. Neurosci. 8: 185-196.

Choi, D.W., Maulucci-Gedde, M. & Kriegstein, A.R. (1987) Glutamate neurotoxicity in cortical cell culture. J. Neurosci. 7: 357-368.

Collingridge, G.L., Kehl, S.J. & McLennan, H. (1983) Excitatory amino acids in synaptic transmission in the Schaffer collateral-commissural pathway of the rat hippocampus. J. Physiol. 334: 33-46.

Cornell-Bell, A.H., Finkbeiner, S.M., Cooper, M.S. & Smith, S.J. (1990) Glutamate induces calcium waves in cultured astrocytes: long-range glial signalling. Science 247: 470-473.

Cotman, C.W., Flatman, J.A., Ganong, A.H. & Perkins, M.N. (1986) Effects of excitatory amino acid antagonists on evoked and spontaneous excitatory potentials in guinea-pig hippocampus. J. Physiol. 378: 403-415.

Cox, D.W.G., Headley, M.H. & Watkins, J.C. (1977) Actions of L- and D-homocysteate in rat CNS: a correlation between low-affinity uptake and the time courses of excitation by microelectrophoretically applied L-glutamate analogues. J. Neurochem. 29: 579-588.

Cull-Candy, S.G. (1976) Two types of extrajunctional L-glutamate receptors in locust muscle fibres. J. Physiol. 255: 449-464.

Davies, S.N. & Collingridge, G.L. (1989) Role of excitatory amino acid receptors in synaptic transmission in area CA1 of rat hippocampus. Proc. R. Soc. Lond. B236: 373-384.

Davies, L.P. & Johnston, G.A.R. (1976) Uptake and release of D- and L-aspartate by rat brain slices. J. Neurochem. 26: 1007-1014.

Dervartanian, D.V. & Veeger, C. (1964) Studies on succinate dehydrogenase. I. Spectral properties of the purified enzyme and formation of enzyme-competitive inhibitor complexes. BBA 92: 233-247.

Do, K.Q., Mattenberger, M., Streit, P. & Cuenód, M. (1986) In vitro release of endogenous excitatory sulfur-containing amino acids from various rat brain regions. J. Neurochem. 46: 779-786.

Dolphin, A.C. (1990) G protein modulation of calcium currents in neurones. Annu. Rev. Physiol. 52: 243-255.

Dolphin, A.C., Errington, M.L. & Bliss, T.V.P. (1982) Long-term potentiation of the perforant path in vivo is associated with increased glutamate release. Nature 297: 496-498.

Drejer, J., Benveniste, H., Diemer, N.H. & Schousboe, A. (1985) Cellular origin of ischaemia-induced glutamate release from brain tissue in vivo and in vitro. J. Neurochem. 45: 145-151.

Drejer, J., Larsson, O.M. & Schousboe, A. (1982) Characterization of L-glutamate uptake into and release from astrocytes and neurons cultured from different brain regions. Exp. Brain Res. 47: 259-269.

Dumuis, A., Sebben, M., Haynes, L. Pin, J.-P. & Bockaert, J. (1988) NMDA receptors activate the arachidonic acid cascade system in striatal neurons. Nature 336: 68-70.

Eccles, J.C. & Jaeger, J.C. (1958) The relationship between the mode of operation and the dimensions of the junctional regions at synapses and motor end-organs. Proc. R. Soc. B 148: 38-56.

Ehinger, B. (1977) Glial and neuronal uptake of GABA, glutamic acid, glutamine and glutathione in the rabbit retina. Exp. Eye Res. 25: 221-234.

Erecinska, M. (1987) The neurotransmitter amino acid transport systems. Biochemical Pharmacology 36: 3547-3555.

Erecinska, M., Troeger, M.B., Wilson, D.F. & Silver, I.A. (1986) The role of glial cells in regulation of neurotransmitter amino acids in the external environment. II. Mechanism of aspartate transport. Brain Res. 369: 203-214.

Erecinska, M., Wantorsky, D. & Wilson, D.F. (1983) Aspartate transport in synaptosomes from rat brain. J. Biol. Chem. 258: 9069-9077.

Euler, H.v., Adler, E., Günther, G. & Das, N.B. (1938) Über den enzymatischen abbau und aufbau der glutaminesäure. II. In tierischen geweben. Hoppe-Seyler's Zeitschrift f. Physiologische Chemie. 254: 61-103.

Falk, G. (1989) Signal transmission from rods to bipolar and horizontal cells: a synthesis. Prog. Retinal Research 8: 255-279.

Feasey, K.J., Lynch, M.A. & Bliss, T.V.P. (1986) Long-term potentiation is associated with an increase in calcium-dependent, potassium-stimulated release of [^{14}C]glutamate from hippocampal slices: an ex vivo study in the rat. Brain Res. 364: 39-44.

Fenwick, E.M., Marty, A. & Neher, E. (1982) A patch-clamp study of bovine chromaffin cells and of their sensitivity to acetylcholine. J. Physiol. 331: 577-598.

ffrench-Mullen, J.M.H., Koller, K., Zaczek, R., Coyle, J.T., Hori, N. & Carpenter, D.O. (1985) N-acetylaspartylglutamate: possible role as the neurotransmitter of the lateral olfactory tract. Proc. Natl. Acad. Sci. USA 82: 3897-3900.

Ford-Hutchinson, A.W., Bray, M.A. & Smith, M.J.H. (1979) The aggregation of rat neutrophils by arachidonic acid: a possible bioassay for lipoxygenase activity. J. Pharm. Pharmacol. 31: 868-869.

Forsythe, I.D. & Clements, J.D. (1990) Presynaptic glutamate receptors depress excitatory monosynaptic transmission between mouse hippocampal neurons. J. Physiol. 429: 1-16.

Garthwaite, J. (1985) Cellular uptake disguises the action of L-glutamate on N-methyl-D-aspartate receptors. With an appendix: diffusion of transported amino acids into brain slices. Br. J. Pharmac. 85: 297-307.

Garthwaite, G. & Garthwaite, J. (1989) Quisqualate neurotoxicity: a delayed, CNQX-sensitive process triggered by a CNQX-insensitive mechanism in young rat hippocampal slices. Neurosci. Lett. 99: 113-118.

Gill, R., Foster, A.C. & Woodruff, G.N. (1987) Systemic administration of MK-801 protects against ischaemia-induced hippocampal neurodegeneration in the gerbil. J. Neurosci. 7: 3343-3349.

Graham, S.H., Shiraishi, K., Panter, S.S., Simon, R.P. & Faden, A.I. (1990) Changes in extracellular amino acid neurotransmitters produced by focal cerebral ischaemia. Neurosci. Letts. 110: 124-130.

Gustafsson, B. & Wigström, H. (1986) Hippocampal long-lasting potentiation produced by pairing single volleys and brief conditioning tetani evoked in separate afferents. J. Neurosci. 6: 1575-1582.

Hablitz, J.J. & Langmoen, I.A. (1982) Excitation of hippocampal pyramidal cells by glutamate in the guinea-pig and rat. J. Physiol. 325: 317-331.

Hagberg, H., Lehmann, A., Sandberg, M., Nystrom, B., Jacobson, I. & Hamberger, A. (1985) Ischaemia-induced shift of inhibitory and excitatory amino acids from intra- to extracellular compartments. J. Cereb. Blood Flow Metab. 5: 413-419.

Hamberger, A., Berthold, C.-H., Karlsson, B., Lehmann, A. & Nystrom, B. (1983) Extracellular GABA, glutamate and glutamine in vivo - perfusion-dialysis of the rabbit hippocampus. In 'Glutamine, glutamate and GABA in the central nervous system'. Eds. Hertz, L., Kvamme, E., McGeer, E.G. & Schousboe, A. Alan R. Liss, NY. pp 473-492.

Hamill, O.P., Marty, A., Neher, E., Sakmann, B. & Sigworth, F.J. (1981) Improved patch-clamp techniques for high-resolution current recording from cells and cell-free membrane patches. Pflügers Arhchiv. 391: 85-100.

Hansen, A.J. (1981) Extracellular ion concentrations in cerebral ischaemia. In 'The application of ion-selective microelectrodes'. Ed. Zeuthen, T. Elsevier. pp 239-254.

Hansen, A.J. (1985) Effect of anoxia on ion distribution in the brain. Physiological Reviews 65: 101-148.

Heinemann, U. & Lux, H.D. (1977) Ceiling of stimulus induced rises in extracellular potassium concentration in the cerebral cortex of cat. Brain Res. 120: 231-249.

Hertz, L. (1979) Functional interactions between neurons and astrocytes I. Turnover and metabolism of putative amino acid transmitters. Prog. Neurobiol. 13: 277-323.

Hertz, L., Schousboe, A., Boechler, N., Mukerji, S. & Federoff, S. (1978) Kinetic characteristics of the glutamate uptake into normal astrocytes in cultures. Neurochem. Res. 3: 1-14.

Hestrin, S., Sah, P. & Nicoll, R.A. (1990) Mechanisms generating the time course of dual component excitatory synaptic currents recorded in hippocampal slices. Neuron 5: 247-253.

Heuttner, J.E. (1990) Glutamate receptor channels in rat DRG neurons: activation by kainate and quisqualate and blockade of desensitization by Con A. Neuron 5: 255-266.

Hidaka, H., Inagaki, M., Kawamoto, S. & Sasaki, Y. (1984) Isoquinolinesulfonamides, novel and potent inhibitors of cyclic nucleotide dependent protein kinase and protein kinase C. Biochemistry 23: 5036-5041.

Hollmann, M., O'Shea-Greenfield, A., Rogers, S.W. & Heinemann, S. (1989) Cloning by functional expression of a member of the glutamate receptor family. Nature 342: 643-648.

Honoré, T., Davies, S.N., Drejer, J., Fletcher, E.J., Jacobsen, P., Lodge, D. & Nielsen, F.E. (1988) Quinoxalinediones: potent competitive non-NMDA glutamate receptor antagonists. Science 241: 701-703.

Horton, R.W., Meldrum, B.S. & Bachelard, H.S. (1973) Enzymic and cerebral metabolic effects of 2-deoxy-D-glucose. J. Neurochem. 21: 507-520.

Ikeda, M., Nakazawa, T., Abe, K., Kaneko, T. & Yamatsu, K. (1989) Extracellular accumulation of glutamate in the hippocampus induced by ischaemia is not calcium dependent - in vitro and in vivo evidence. Neurosci. Letts. 96: 202-206.

Johnson, J.W. & Ascher, P. (1987) Glycine potentiates the NMDA response in cultured mouse brain neurons. Nature 325: 529-531.

Johnston, G.A.R, Kennedy, S.M.E. & Twitchin, B. (1979) Action of the neurotoxin kainic acid on high affinity uptake of L-glutamic acid in rat brain slices. J. Neurochem. 32: 121-127.

Jones, K.A. & Baughman, R.W. (1988) NMDA- and non-NMDA-receptor components of excitatory synaptic potentials recorded from cells in layer V of rat visual cortex. J. Neurosci. 8: 3522-3534.

Kanner, B.I. & Marva, E. (1982) Efflux of L-glutamate by synaptic plasma membrane vesicles isolated from rat brain. Biochemistry 21: 3143-3147.

Kanner, B.I. & Schuldiner, S. (1987) Mechanism of transport and storage of transmitters. CRC Crit. Rev. Biochem. 22: 1-38.

Kanner, B.I. & Sharon, I. (1978a) Active transport of L-glutamate by membrane vesicles isolated from the rat brain. Biochemistry 17: 3949-3953.

Kanner, B.I. & Sharon, I. (1978b) Solubilization and reconstitution of the L-glutamic acid transporter from rat brain. FEBS Lett. 94: 245-248

Keinänen, K., Wisden, W., Sommer, B., Werner, P., Herb, A., Verdoorn, T.A., Sakmann, B. & Seeburg, P.H. (1990) A family of AMPA-selective glutamate receptors. Science 249: 556-560.

Kennedy, A.J., Voaden, M.J. & Marshall, J. (1974) Glutamate metabolism in the frog retina. Nature 252: 51-52
Kimelberg, H.K., Pang, S. & Treble, D.H. (1989) Excitatory amino acid-stimulated uptake of $^{22}Na^{+}$ in primary astrocyte cultures. J. Neurosci. 9: 1141-1149.

Koerner, J.F. & Cotman, C.W. (1981) Micromolar L-2-amino-4-phosphonobutyric acid selectively inhibits perforant path synapses from lateral entorhinal cortex. Brain Res. 216: 192-198.

Kuffler, S.W., Nicholls J.G., & Orkand, R.K. (1966) Physiological properties of glial cells in the central nervous system of amphibia. J. Neurophysiol. 29: 768-787.

Kvamme, E., Schousboe, A., Hertz, L., Torgner, I.A. & Svenneby, G. (1985) Developmental change of endogenous glutamate and gamma-glutamyl transferase in cultured cerebral cortical interneurons and cerebellar granule cells, and in mouse cerebral cortex and cerebellum in vivo. Neurochem. Res. 10: 993-1008.

LaNoue, K.J. & Schoolwerth, A.C. (1979) Metabolite transport in mitochondria. Ann. Rev. Biochem. 48: 871-922.

Lazawrewicz, J.W., Wroblewski, J.T., Palmer, M.E. & Costa, E. (1988) Activation of N-methyl-D-aspartate-sensitive glutamate receptors stimulates arachidonic acid release in primary cultures of cerebellar granule cells. Neuropharmacology 27: 765-769.

Lehmann, A., Isacsson, H. & Hamberger, A. (1983) Effects of in vivo administration of kainic acid on the extracellular amino acid pool in the rabbit hippocampus. J. Neurochem 40: 1314-1320.

Lerner, J. (1987) Acidic amino acid transport in animal cells and tissues. Comp. Biochem. Physiol. 87B: 443-457.

Lester, R.A.J., Clements, J.D., Westbrook, G.L. & Jahr, C.E. (1990) Channel kinetics determine the time course of NMDA receptor-mediated synaptic currents. Nature 346: 565-567.

Linden, D.J. & Routtenberg, A. (1989) Cis-fatty acids, which activate protein kinase C, attenuate Na^+ and Ca^{2+} currents in mouse neuroblastoma cells. J. Physiol. 419: 95-119.

Lodge, D. & Johnson, K.M. (1990) Noncompetitive excitatory amino acid receptor antagonists. TIPS 11: 81-86.

Logan, W.J. & Snyder, S.H. (1972) High affinity uptake systems for glycine, glutamic and aspartic acids in synaptosomes of rat central nervous tissues. Brain Res. 42: 413-431.

Lynch, G., Larson, J., Kelso, S., Barrionuevo, G. & Schottler, F. (1983) Intracellular injections of EGTA block induction of hippocampal long-term potentiation. Nature 305: 719-721.

Lynch, M.A., Errington, M.L. & Bliss, T.V.P. (1985) Long-term potentiation of synaptic transmission in the dentate gyrus: increased release of [^{14}C]glutamate without increase in receptor binding. Neurosci. Letts. 62: 123-129.

MacDermott, A.B., Mayer, M.L., Westbrook, G.L., Smith, S.J. & Barker, J.L. (1986) NMDA-receptor activation increases cytoplasmic calcium concentration in cultured spinal cord neurones. Nature 321: 519-522.

Madl, J.E., Clements, J.R., Beitz, A.J., Wenthold, R.J. & Larson, A.A. (1988) Immunocytochemical localization of glutamate dehydrogenase in mitochondria of the cerebellum: an ultrastructural study using a monoclonal antibody. Brain Res. 452: 396-402.

Malinow, R. & Tsien, R.W. (1990) Presynaptic enhancement shown by whole-cell recordings of long-term potentiation in hippocampal slices. Nature 346: 177-180.

Martell, A.E. & Smith, R.M. (1974) Critical stability constants, volume 1: amino acids. Plenum.

Maycox, P.R., Deckwerth, T., Hell, J.W. & Jahn, R. (1988) Glutamate uptake by brain synaptic vesicles. J. Biol. Chem. 263: 15423-15428.

Maycox, P.R., Hell, J.W. & Jahn, R. (1990) Amino acid neurotransmitters: spotlight on synaptic vesicles. TINS 13: 83-87.

Mayer, M.L. & Westbrook, G.L. (1984) Mixed-agonist action of excitatory amino acids on mouse spinal cord neurones under voltage clamp. J. Physiol. 354: 29-53.

Mayer, M.L., Westbrook, G.L. & Guthrie, P.B. (1984) Voltage-dependent block by Mg^{2+} of NMDA responses in spinal cord neurones. Nature 309: 261-263.

McLennan, H. (1976) The autoradiographic localization of L-[^{3}H]glutamate in rat brain tissue. Brain Res. 115: 139-144.

Meldrum, B. & Garthwaite, J. (1990) Excitatory amino acid neurotoxicity and neurodegenerative disease. TIPS 11: 379-387.

Mewett, K.N., Oakes, D.J., Olverman, H.J., Smith, D.A.S. & Watkins, J.C. (1983) Pharmacology of the excitatory actions of sulphonic and sulphinic amino acids. In 'CNS receptors - from molecular pharmacology to behaviour'. Eds. DeFeudis, F.V. & Mandel, P. Raven Press, NY.

Miller, A. & Schwartz, E.A. (1983) Evidence for the identification of synaptic transmitters released by photoreceptors of the toad retina. J. Physiol. 334: 325-349.

Monaghan, D.T., Bridges, R.J. & Cotman, C.W. (1989) The excitatory amino acid receptors: their classes, pharmacology, and distinct properties in the function of the central nervous system. Annu. Rev. Pharmacol. Toxicol. 29: 365-402.

Montero, V.M. & Wenthold, R.J. (1989) Quantitative immunogold analysis reveals high glutamate levels in retinal and cortical synaptic terminals in the lateral geniculate nucleus of the macaque. Neurosci. 31: 639-647.

Murer, H., Leopolder, A., Kinne, R. & Burckhardt, G. (1980) Recent observations on the proximal tubular transport of acidic and basic amino acids by rat renal proximal tubular brush border vesicles. Int. J. Biochem. 12: 223-228.

Nadler, J.V., White, W.F., Vaca, K.W., Redburn, D.A. & Cotman, C.W. (1977) Characterization of putative amino acid transmitter release from slices of rat dentate gyrus. J. Neurochem. 29: 279-290.

Naito, S. & Ueda, T. (1985) Characterization of glutamate uptake into synaptic vesicles. J. Neurochem. 44: 99-109.

Nawy, S. & Jahr, C.E. (1990) Suppression by glutamate of cGMP-activated conductance in retinal bipolar cells. Nature 346: 269-271.

Nelson, P.J., Dean, G.E., Aronson, P.S. & Rudnick, G. (1983) Hydrogen ion cotransport by the renal brush border glutamate transporter. Biochemistry 22: 5459-5463.

Newman, E.A. (1984) Regional specialization of retinal glial cell membrane. Nature 309: 155-157.

Newman, E.A. (1985) Voltage-dependent calcium and potassium channels in retinal glial cells. Nature 317: 809-811.

Nicholls, D.J. & Sihra, T.S. (1986) Synaptosomes possess an excocytotic pool of glutamate. Nature 321: 772-773.

Nicholls, D.G., Sihra, T.G. & Sanchez-Prieto, J. (1987) Calcium-dependent and -independent release of glutamate from synaptosomes monitored by continuous fluorometry. J. Neurochem. 49: 50-57.

Nowak, L., Bregetovski, P., Ascher, P., Herbet, A. & Prochiantz, A. (1984) Magnesium gates glutamate-activated channels in mouse central neurones. Nature 307: 462-465.

Ozyurt, E., Graham, D.I., Woodruff, G.N. & McCulloch, J. (1988) Protective effect of the glutamate antagonist, MK-801 in focal cerebral ischaemia in the cat. J. Cereb. Blood Flow Metab. 8: 138-143.

Patel, A.J. & Hunt, A. (1985) Concentration of free amino acids in primary cultures of neurones and astrocytes. J. Neurochem. 44: 1816-1821.

Patneau, D.K. & Mayer, M.L. (1990) Structure-activity relationships for amino acid transmitter candidates acting at N-methyl-D-aspartate and quisqualate receptors. J. Neurosci. 10: 2385-2399.

Peterson, N.A. & Raghupathy, E. (1972) Characteristics of amino acid accumulation by synaptosomal particles isolated from rat brain. J. Neurochem. 19: 1423-1438.

Pin, J.-P., Bockaert, J. & Recasens, M. (1984) The Ca^{2+}/Cl$^-$ dependent L-[^{3}H]glutamate binding: a new receptor or a particular transport process? FEBS Lett. 175: 31-36.

Piomelli, D., Volterra, A., Dale, N., Siegelbaum, S.A., Kandel, E.R., Schwartz, J.H. & Belardetti, F. (1987) Lipoxygenase metabolites of arachidonic acid as second messengers for presynaptic inhibition of Aplysia sensory cells. Nature 328: 38-43.

Pittaluga, A., Barbeito, L., Serval, V., Godeheu, G., Artaud, F., Glowinski, J. & Chéramy, A. (1988) Depolarization-evoked release of N-acetyl-L-aspartyl-L-glutamate from rat brain synaptosomes. Eur. J. Pharmacol. 158: 263-266.

Rang, H.P. & Ritchie, J.M. (1968) On the electrogenic sodium pump in mammalian non-myelinated nerve fibres and its activation by various external cations. J. Physiol. 196: 183-221.

Rehncrona, S., Westerberg, E., Akesson, B. & Siesjo, B.K. (1982) Brain cortical fatty acids and phospholipids during and following complete and severe incomplete ischaemia. J. Neurochem. 38: 84-93.

Robinson, M.B., Blakely, R.D., Couto, R. & Coyle, J.T. (1987) Hydrolysis of the brain dipeptide N-acetyl-L-aspartyl-L-glutamate. J. Biol. Chem. 262: 14498-14506.

Roskoski, R. (1978) Net uptake of L-glutamate and GABA by high affinity synaptosomal transport systems. J. Neurochem. 31: 493-498.

Roskoski, R. (1979) Net uptake of aspartate by a high-affinity rat cortical synaptosomal transport system. Brain Res. 160: 85-93.

Sanchez-Prieto, J. & Gonzalez, P. (1988) Occurrence of a large Ca^{2+}-independent release of glutamate during anoxia in isolated nerve terminals (synaptosomes). J. Neurochem. 50: 1322-1324.

Sarantis, M. & Attwell, D. (1990) Glutamate uptake in mammalian retinal glia is voltage- and potassium-dependent. 516: 322-325.

Sarantis, M., Everett, K. & Attwell, D. (1988) A presynaptic action of glutamate at the cone output synapse. Nature 332: 451-453.

Schneider, E.G. & Sacktor, B. (1980) Sodium gradient-dependent L-glutamate transport in renal brush border membrane vesicles. Effect of an intravesicular > extravesicular potassium gradient. J. Biol. Chem. 255: 7645-7649.

Schousboe, A., Fosmark, H. & Hertz, L. (1975) High content of glutamate and of ATP in astrocytes cultured from rat brain hemispheres: effect of serum withdrawal and of cyclic AMP. J. Neurochem. 25: 909-911.

Schwartz, E.A. (1986) Synaptic transmission in amphibian retinae during conditions unfavourable for calcium entry into presynaptic terminals. J. Physiol. 376: 411-428.

Schwartz, E.A. & Tachibana, M. (1990) Electrophysiology of glutamate and sodium co-transport in a glial cell of the salamander retina. J. Physiol. 426: 43-80.

Sekiguchi, K., Tsukuda, M., Ase, K., Kikkawa, U. & Nishizuka, Y. (1988) Mode of activation and kinetic properties of three distinct forms of protein kinase C from rat brain. J. Biochem. 103: 759-765.

Sheardown, M.J., Nielsen, E.O., Hansen, A.J., Jacobsen, P. & Honoré, T. (1990) 2,3-dihydroxy-6-nitro-7-sulfamoyl-benzo(F)quinoxaline: a neuroprotectant for cerebral ischaemia. Science 247: 571-574.

Shiells, R.A., Falk, G. & Naghshineh, S. (1986) Iontophoretic study of the action of excitatory amino acids on rod horizontal cells of the dogfish retina. Proc. R. Soc. Lond. B 227: 121-135.

Silverstein, F.S., Buchanan, K. & Johnston, M.V. (1986) Perinatal hypoxia-ischaemia disrupts striatal high-affinity [^{3}H]glutamate uptake into synaptosomes. J.Neurochem. 47: 1614-1619.

Slaughter, M.M. & Miller, R.F. (1981) 2-amino-4-phosphonobutyric acid: a new pharmacological tool for retina research. Science 211: 182-185.

Slaughter, M.M. & Miller, R.F. (1983) The role of excitatory amino acid transmitters in the mudpuppy retina: an analysis with kainic acid and N-methyl-D-aspartate. J. Neurosci. 3: 1701-1711.

Sloviter, R.S. & Dempster, D.W. (1985) "Epileptic" brain damage is replicated qualitatively in the rat hippocampus by central injection of glutamate or aspartate but not by GABA or acetylcholine. Brain Res. Bull. 15: 39-60.

Sommer, B., Kainänen, K., Verdoorn, T.A., Wisden, W., Burnashev, N., Herb, A., Köhler, M., Takagi, T., Sakmann, B. & Seeburg, P.H. (1990) Flip and flop: a cell-specific functional switch in glutamate-operated channels in the CNS. Science 249: 1580-1585.

Somogyi, P., Halasy, K., Somogyi, J. Storm-Mathisen, J. & Ottersen, O.P. (1986) Quantification of immunogold labelling reveals enrichment of glutamate in mossy and parallel fibre terminals in cat cerebellum. Neurosci. 19: 1045-1050.

Stallcup, W.B., Bulloch, K. & Baetge, E.E. (1979) Coupled transport of glutamate and sodium in a cerebellar nerve cell line. J. Neurochem. 32: 57-65.

Steinberg, G.K., Saleh, J. & Kunis, D. (1988) Delayed treatment with dextromethorphan and dextrorphan reduces cerebral damage after transient focal ischaemia. Neurosci. Letts. 89: 193-197.

Stone, T.W. & Burton, N.R. (1988) NMDA receptors and ligands in the vertebrate CNS. Prog. Neurobiol. 30: 333-368.

Sugiyama, H., Ito, I. & Hirono, C. (1987) A new type of glutamate receptor linked to inositol phospholipid metabolism. Nature 325: 531-533.

Swann, A.C. (1984) Free fatty acids and (Na^+, K^+)-ATPase: effects on cation regulation, enzyme conformation, and interactions with ethanol. Archives of Biochemistry & Biophysics. 233: 354-361.

Szczepaniak, A.C. & Cottrell, G.A. (1973) Biphasic action of glutamic acid and synaptic inhibition in an identified serotonin-containing neurone. Nature New Biology 241: 62-64.

Trussel, L.O. & Fischbach, G.D. (1989) Glutamate receptor desensitization and its role in synaptic transmission. Neuron 3: 209-218.

Usowicz, M.M., Gallo, V. & Cull-Candy, S.G.(1989) Multiple conductance channels in type-2 cerebellar astrocytes activated by excitatory amino acids. Nature 339: 380-383.

Waniewski, R.A. & Martin, D.L. (1984) Characterization of L-glutamic acid transport by glioma cells in culture: evidence for sodium-independent, chloride-dependent high affinity influx. J. Neurosci. 4: 2237-2246.

Watkins, J.C. & Evans, R.H. (1981) Excitatory amino acid transmitters. Ann. Rev. Pharmacol. Toxicol. 21: 165-204.

Watkins, J.C., Krogsgaard-Larson, P. & Honoré, T. (1990) Structure-activity relationships in the development of excitatory amino acid receptor agonists and competitive antagonists. TIPS 11: 25-33.

Westbrook, G.L., Mayer, M.L., Namboodiri, M.A.A. & Neale, J.H. (1986) High concentrations of N-acetylaspartylglutamate (NAAG) selectively activate NMDA receptors on mouse spinal cord neurons in cell culture. J. Neurosci. 6: 3385-3392.

White, W.F., Nadler, J.V., Hamberger, A., Cotman, C.W. & Cummins, J.T. (1977) Glutamate as transmitter of hippocampal perforant path. Nature 270: 356-357.

White, R.D. & Neal, M.J. (1976) The uptake of L-glutamate by the retina. Brain Res. 111: 79-93.

Whittemore, E.R. & Koerner, J.F. (1989) An explanation for the purported excitation of piriform cortical neurons by N-acetyl-L-aspartyl-L-glutamic acid (NAAG). Proc. Natl. Acad. Sci. USA 86: 9602-9605.

Wick, A., Drury, D.R., Nakada, H.I. & Wolfe, J.B. (1957) Localization of the primary metabolic block produced by 2-deoxyglucose. J. Biol. Chem. 224: 963-969.

Wigström, H., Gustafsson, B., Huang Y.-Y. & Abraham, W.C. (1986) Hippocampal long-term potentiation is induced by pairing single afferent volleys with intracellularly injected depolarizing current pulses. Acta Physiol. Scand. 126: 317-319.

Williams, J.H., Errington, M.L., Lynch, M.A. & Bliss, T.V.P. (1989) Arachidonic acid induces a long-term activity-dependent enhancement of synaptic transmission in the hippocampus. Nature 341: 739-742.

Wilson, D.F. & Pastuszko, A. (1986) Transport of cysteate by synaptosomes isolated from rat brain: evidence that it utilizes the same transporter as aspartate, glutamate, and cysteine sulfinate. J. Neurochem. 47: 1091-1097.

Wong, P.Y.D., Bedwani, J.R. & Cuthbert, A.W. (1972) Hormone action and the levels of cyclic AMP and prostaglandins in the toad bladder. Nature New Biology 238: 27-31.

Yu, A.C.H., Chan, P.H. & Fishman, R.A. (1986) Effects of arachidonic acid on glutamate and -aminobutyric acid uptake in primary cultures of rat cerebral cortical astrocytes and neurons. J. Neurochem. 47: 1181-1189.

Yu, A.C.H, Chan, P.H. & Fishman, R.A. (1987) Arachidonic acid inhibits uptake of glutamate and glutamine but not of GABA in cultured cerebellar granule cells. J. Neurosci. Res. 17: 424-427.

Yudkoff, M., Nissim, I., Hummeler, K., Medow, M. & Pleasure, D. (1986) Utilization of [^{15}N]glutamate by cultured astrocytes. Biochem. J. 234: 185-192.

Zaczek, R., Balm, M., Arlis, S., Drucker, H. & Coyle, J.T. (1987) Quisqualate-sensitive, chloride-dependent transport of glutamate into rat brain synaptosomes. J. Neurosci. Res. 18: 425-431.